The Role of Transcription Factor EB in the Coordination of Cellular Endocytosis, mTORC1 Signaling, and Autophagy

by

Israel Chukwudi Nnah

A Dissertation submitted to the Rutgers-Newark Graduate School, The State University of New Jersey

Federated Department of Biological Sciences

In partial fulfillment of the requirements for the degree of

Doctor of Philosophy

In

Cell & Molecular Biology

Written under the supervision of

Dr. Radek Dobrowolski, PhD

and approved by

_____

_____

_____

_____

Newark, New Jersey

January, 2018

Copyright page:

ABSTRACT OF THE THESIS DISSERTATION

The Role of Transcription Factor EB in the Coordination of Cellular Endocytosis, mTORC1 Signaling, and Autophagy

By Israel Chukwudi Nnah

Dissertation Advisor: Radek Dobrowolski, Ph.D.

Over the last few years, extensive studies have linked the activity of the transcription factor EB (TFEB) to lysosomal function. These observations proposed an intriguing integration of cellular catabolism, sustained by lysosomes, with anabolic processes largely controlled by the mechanistic target of rapamycin complex 1 (mTORC1) signaling. Interestingly, lysosomal function directly affects mTORC1 activity and is regulated by TFEB, a transcription factor and direct substrate of mTORC1. Thus, the lysosomal-mTOR signaling complex represents a hub of cellular energy metabolism, and its dysregulation underlies the onset of several multifaceted disorders including neurodegeneration, cancer and Type 2 diabetes.

Recent evidence has suggested that under nutrient-deficient conditions TFEB controls mTORC1 reactivation and induction of anabolic processes upon nutrient replenishment by modulating the transcriptional levels of small GTPases to re-tether mTORC1 to lysosomal membranes. Although very significant, these studies did not address the subsequent intracellular mechanisms that lead to the stimulation of mTORC1 kinase activity and autophagy during starvation.

Here, I demonstrated that TFEB promotes assembly of a mTORC1-containing nutrient sensing complex through the formation of endosomes carrying activated phosphoinositide-dependent kinase 1 (p-PDK1), its activated substrate,

protein kinase B (p-AKT), and the mTORC1-tethering factor RagD. Therefore, TFEB-induced signaling endosomes en route to lysosomes are required to dissociate lysosomal-mTORC1 inhibitor, Tuberous Sclerosis complex (TSC), and re-tether mTORC1 to endolysosomal membranes. Chromatin immunoprecipitation assays identified 623 endocytic genes regulated by TFEB, of which 46 were core endocytic genes including Clathrin, Caveolin, early and the late endosomal markers, Rab5 and Rab7, respectively. Validation of expression of these endocytic proteins in blots and endocytosis assays using Dextran-Rhodamine and EGF-Rhodamine showed that TFEB stimulates endocytosis. Pharmacological and genetic inhibition of endocytosis or retrograde trafficking abolished mTORC1 activity without affecting total levels of pT308-Akt and despite the presence of active TFEB in the nucleus. These TFEB-induced endosomes are required to assemble the so-called lysosomal nutrient sensing complex (LYNUS), composed of vATPase, Ragulator and the small GTPases RagA/B and C/D. LYNUS tethers mTORC1 to lysosomal membranes. I show that during starvation, TFEB-triggered endocytosis reactivates mTORC1 and is required for autophagy. I found that TFEB-triggered endocytosis is required for delivery of mTORC1 activators, lysosome biogenesis and autophagy flux. This study identifies TFEB-mediated endocytosis as a critical process driving lysosome biogenesis and mTORC1 activation, and emphasizes the role of endolysosomal system in molecular clearance.

ACKNOWLEDGEMENTS

I thank my mentor, Dr. Radek Dobrowolski, for his never-ending support and encouragement throughout the duration of my PhD studies at Rutgers-Newark. I am grateful for his dedication and keen interest in my career development, and for constantly challenging my knowledge and skills in order to make me a better scientist.

I thank my thesis committee members, Dr. Gregory Weber, Dr. Nan Gao and Dr. Steven Levison, for their thoughtful and invaluable advice, all of which enabled me to achieve this success in a timely fashion. I also acknowledge the generosity and support of fellow members of the Dobrowolski lab: Dr. Chaitali Saqcena, Dr. Kavya Reddy, Dr. Biao Wang, Dr. Khoosheh Khayati and members of the Ballabio lab: Dr. Dustin Bagley, Dr. Rossella De Cegli, Dr. Gennaro Napolitano, Dr. Diego Medina and Dr. Andrea Ballabio. I also recognize Dr. Edward Bonder and the Department of Biological Sciences at Rutgers-Newark for the incredible support they gave to me during my studies.

Finally, I acknowledge and dedicate this work to my family for their unconditional love, support and unending words of encouragement throughout this experience. Above all, I give thanks to God almighty whose blessings, grace, and strength remained constant in my life during this journey.

Table of Contents

List of Illustrations

Chapter One

Chapter Three

List of Tables

Specific Aims

I hypothesized that cellular endocytosis and accompanying molecular trafficking controls mTORC1 signaling, and in nutrient-deprived conditionsTFEB-driven endocytosis directs the reactivation of mTORC1. To test this hypotheses, three specific aims were explored:

Aim 1: To determine whether TFEB controls cellular endocytosis. Endocytosis and intracellular signal transduction are tightly intertwined processes (Dobrowolski and De Robertis, 2012; Sorkin and von Zastrow, 2009). Endocytosis controls the generation or attenuation of intracellular signals by driving the internalization of ligand-activated receptors, formation of signaling platforms on endosomes or sequestration of inhibitory signaling molecules (Dobrowolski and De Robertis, 2012). These endocytosis-mediated processes have been described for many cellular signaling pathways including Wnt and TGFβ but not for the mTORC1-TFEB pathway. It is widely accepted that TFEB-dependent processes such as lysosomal biogenesis and autophagy rely on cellular endocytosis. However, an association between TFEB signaling and modulation of the endocytic pathway is yet to be studied.

To see whether TFEB signaling controls endocytosis, I sought to investigate whether TFEB induces the formation of signaling endosomes carrying mTORC1-activating proteins such as active Akt, and its impact on cellular endocytic rates under nutrient-deprived conditions. I found that amino acid-starvation induced endocytosis in a TFEB-dependent manner, increased TFEB signaling stimulates

the expression of core endocytic genes and promotes formation of endosomes carrying Akt.

Aim 2. To determine whether endocytosis is necessary for mTORC1 signaling. Deregulation in the endolysosomal system and mTORC1 signaling have been observed in neurodegenerative disorders including Alzheimer's disease (Nixon, 2005; Rosner et al., 2008). To better understand the molecular interplay between these two pathway and in turn offer insights into ways of re-regulating endocytic trafficking and mTORC1 in disease, I investigated the impact of nutrient uptake and receptor-mediated endocytosis on mTORC1 signaling. I found that perturbation of cellular endocytosis and associated molecular trafficking leads to changes in mTORC1 activity. These findings suggest that mTORC1 signaling is highly dependent on cellular endocytosis which also controls its reactivation on lysosomal membranes during nutrient deprivation.

Aim 3. To assess whether endocytosis is required for TFEB-mediated reactivation of mTORC1 and autophagic function during starvation. Starvation inhibits mTORC1 signaling and subsequently promotes TFEB-dependent induction of autophagy and lysosomal biogenesis (Napolitano and Ballabio, 2016; Settembre et al., 2011). Previous studies showed that under prolonged periods of starvation (up to 6 hours), mTORC1 signaling is re-established in an autophagy and TFEB-dependent manner (Chen and Yu, 2013; Di Malta et al., 2017). Under similar starvation conditions, TFEB upregulates expression of RagD, an mTORC1 tethering factor, to promote reactivation of mTORC1 (Di Malta et al., 2017). However It is still unclear how TFEB directs

mTORC1 re-tethering and its subsequent activation on lysosomal membranes under starvation conditions. Recently, the endolysosomal sugar transporter Spinter, and Clathrin proteins were shown to be required for mTORC1 activation under starvation, thus suggesting a role for endocytosis in the recovery of mTORC1 signaling. Since my preliminary data suggested that starvation stimulates endocytosis, I sought to see whether Dynamin-mediated endocytosis is required for mTORC1 reactivation. I found that cells require Dynamin GTPase activity for normal autophagic flux and reactivation of mTORC1 signaling under amino acid starvation conditions.

8. Chapter One

8.1. Introduction to Transcription Factor EB signaling pathway

The transcription factor EB (TFEB) signaling pathway regulates the induction of autophagy, a programmed cell degradation process necessary for maintenance of cellular proteostasis (Kromer et al., 2010; Napolitano and Ballabio, 2016; Yang and Klionsky, 2010). As a transcription factor, TFEB transcriptionally controls the biogenesis of autophagosomes and lysosomes, two intracellular compartments essential for autophagy (Napolitano and Ballabio, 2016). Subcellular localization of TFEB, which dictates its nuclear transcriptional activity, is largely controlled by two evolutionarily conserved serine/threonine protein kinases: the mechanistic target of rapamycin (mTOR) and the extracellular signal-regulated Kinase 2 (ERK2).

For many years, the expression of lysosomal genes was thought to be a constitutive process. Recent studies have now revealed that cells constantly regulate lysosomal function and number in response to their energetic or degradative needs (Puertollano, 2014). As mTORC1 is a well-established sensor and regulator of cellular energy status (Budanov and Karin, 2008; Laplante and Sabatini, 2012), it is unsurprising that the complex negatively regulates lysosomal biogenesis through inhibition of TFEB. Specifically, in fed cells, active mTORC1 phosphorylates TFEB sequester it in the cytoplasm and thereby preventing its nuclear entry (Martina et al., 2012). Conversely, in nutrient-deprived cells, the endolysosomal calcium efflux channel, Mucolipin 1 (MCOLN1) opens to promote local release of calcium ions and activation of the phosphatase Calcineurin that

dephosphorylates TFEB and allows for its nuclear translocation. Nuclear TFEB drives expression of autolysosomal genes required for biogenesis, transport and fusion autophagic vesicles (Medina et al., 2012; Martina et al., 2012; Napolitano and Ballabio, 2016).

An additional regulatory layer of autolysosomal biogenesis is maintained by ZKSCAN3, a member of the zinc finger transcription factors harboring Kruppel-associated box (KRAB) and SCAN domains (Chauhan et al., 2013). Members of this protein family bind to DNA in a zinc-dependent manner to repress gene transcription. ZKSCAN transcription factors play a role in several cellular functions including maintenance of the nucleolus, cell proliferation, and apoptosis (Urrutia, 2003). Recently, ZKSCAN3 was described to be a key transcriptional repressor of autophagy (Chauhan et al., 2013; Fullgrabe et al., 2014). This factor transcriptionally attenuates the expression of more than sixty genes encoding proteins involved in various steps of autophagy and lysosomal biogenesis and function (Chauhan et al., 2013). Interestingly, mTORC1 phosphorylates ZKSCAN3 to regulate its subcellular localization. In fed conditions, when mTORC1 is active, phosphorylated ZKSCAN3 shuttles into the nucleus to repress autophagy genes; under nutrient-deprived conditions, ZKSCAN3 accumulates in the cytoplasm enabling persistence of autophagy (Chauhan et al., 2013). Thus, TFEB and ZKSCAN3 are differentially regulated by mTORC1 to fine-tune the autolysosomal system. However, several key aspects of TFEB and ZKSCAN3 regulation remain unclear and the extent to which ZKSCAN3 interacts with the promoter of lysosomal genes to repress TFEB-responsive genes remains unknown. It should be

mentioned that the role of ZKSCAN3 in the endolysosomal pathway is currently questioned and debated in the field (Chaun et al., 2013; Chun-Yan and Zoncu, 2016).

8.1.1. Overview of the Microphthalmia family of transcription factors

TFEB is a member of the Microphthalmia family (MIT family) of basic-helix-loop-helix-leucine zipper (bHLH-Zip) transcription factors that bind a palindromic GTCACGTGAC 10-base-pair E-box motif identified in the promoter region of over 600 lysosomal genes (Napolitano and Ballabio, 2016; Raben and Peurtollano, 2016). This motif termed Coordinated Lysosomal Expression and Regulation (CLEAR) element contains a specific type of E-box sequence, CANNTG, that is recognized by other family members including the Microphthalmia-associated transcription factor (MITF), transcription factor E3 (TFE3) and transcription factor EC (TFEC) (Raben and Peurtollano, 2016). These MIT proteins share a conserved identical basic region required for DNA binding, a helix-loop-helix (HLH) and Zip regions necessary for their dimerization, and activation domain essential for transcriptional activation with the exception of TFEC, which has no activating domain but instead plays an inhibitory role during transcription (Napolitano and Ballabio, 2016; Zhao et al., 1993). All four MIT proteins (MITF, TFEB, TFEC, and TFE3) are evolutionary conserved in vertebrates and one MIT ortholog has been identified in lower organisms including *Drosophila melanogaster* (Hallsson et al., 2004; Napolitano and Ballabio, 2016) and *Caenorhabditis elegans* (Rheli et al., 1999).

MITF, along with TFE3, promote expression of several genes associated with biogenesis of lysosome-related organelles, melanosomes (Raben and Peurtollano, 2016), and osteoclast function (Hershey and Fisher, 2004; Motyckova et al., 2001). TFEB induces transcriptional activation of many autophagosome and lysosomal genes, including lysosomal transmembrane proteins, hydrolases and several subunits of the v-ATPase machinery resulting in the cellular increase of lysosome quantity. Therefore, TFEB is considered a master regulator of lysosomal function and autophagy.

8.1.2. Mechanism of TFEB activation

The regulation of TFEB activity begins with the recruitment, tethering and activation of mechanistic target of Rapamycin complex 1 (mTORC1) on the lysosomal surface, which is driven by two signaling axes: the amino acid-Rag-GTPase axis controlled by amino acids and the tuberous sclerosis 1 and 2 (TSC1/2)-Rheb-GTPase axis controlled by growth factors (Nnah et al., 2015). Under nutrient-rich conditions, TFEB is recruited and phosphorylated by mTORC1 at Ser142 and Ser211 on lysosomal membranes. This inhibitory phosphorylation in turn serves as a docking site for the chaperone 14-3-3, which then sequesters TFEB in the cytosol and prevents its translocation into the nucleus (figure 1) (Napolitano and Ballabio, 2016). Reversely, starvation by amino acid and serum deprivation inhibits RagGTPase-mediated recruitment of mTORC1 and Rheb GTPase-mediated activation of mTORC1 on lysosomal membranes respectively (Laplante and Sabatini, 2012). This in turn alleviates TFEB inhibition by mTORC1 and allows TFEB to translocate to the nucleus. Starvation also induces the efflux

of lysosomal calcium through a calcium channel named mucolipin 1 (MCOLN1) to activate the phosphatase Calcineurin, which dephosphorylates TFEB to promote its translocation into the nucleus (figure 2) (Medina et al., 2015; Napolitano and Ballabio, 2016). Depletion of MCOLN1 severely impairs lysosomal calcium release and activation of Calcineurin, and subsequently hinders activation of TFEB and induction of autophagy (Medina et al., 2015).

Other TFEB-activating stimuli such as exercise and lysosomal stress also induce activation of Calcineurin (Sancak et al., 2010). Endoplasmic reticulum stress (ER-stress) also activates Calcineurin and TFEB in an mTORC1-independent manner, and is controlled by protein kinase RNA-like endoplasmic reticulum kinase (PERK) (Martina et al., 2016). However, the molecular mechanisms that underlie PERK-mediated activation of TFEB is incompletely understood. Specific inhibition of Akt/protein kinase B-mediated phosphorylation of TFEB at Ser467 promotes nuclear translocation of TFEB and induction of cellular clearance (Palmieri et al., 2017).

In the nucleus, TFEB binds and activates expression of CLEAR-network genes associated with lysosome and autophagosome biogenesis including several vATPase subunits, MCOLN1, and the microtubule-associated protein 1A/1B-light chain (LC3) (Sardiello et al., 2009). Subsequent study has shown that by directly regulating the expression of the mTORC1 tethering factor RagD, TFEB controls a feedback mechanism that re-tethers mTORC1 to lysosomal membranes (Di Malta et al., 2017). The subsequent cellular processes that lead to the stimulation of mTORC1 kinase activity is still unclear.

8.1.3. Mechanistic Target of Rapamycin Complex1 and Other Cellular Kinases Regulating TFEB Activity

The activity of TFEB is strictly controlled by its phosphorylation status (Napolitano and Ballabio, 2016). Protein kinases such as the mechanistic target of rapamycin (mTOR) and extracellular signal-regulated kinase-2 (ERK2) are the two best-studied kinases that control TFEB activation. Protein kinase C-beta (PKCβ), which mediates the canonical NF-Kappa-B signaling pathway, has been reported to also phosphorylate and activate TFEB in osteoclasts (Ferron et al., 2013; Kang et al., 2001; Yamasaki et al, 2009). The complete mechanism of TFEB activation by PKCβ is still remains unclear.

mTOR is an evolutionarily conserved serine/threonine kinase that controls organismal growth, and is found deregulated in several multifaceted diseases including cancer, diabetes and neurodegeneration (Laplante and Sabatini, 2012; Nnah et al., 2015; Saxton and Sabatini, 2017). mTOR is a member of the phosphoinositide-3-kinase (PI3K)-related kinases that interact with several proteins to form two structurally and functionally distinct protein complexes termed mTOR Complex-1 (mTORC1) and Complex-2 (mTORC2) (Laplante and Sabatini, 2012; Sarbassov et al., 2006; Saxton and Sabatini, 2017; Wullschleger et al., 2006).

The composition of both mTOR complexes is well characterized. In addition to the mTOR catalytic subunit, both complexes contain Deptor, an inhibitor of mTOR (Peterson et al., 2009; Zhao et al., 2011), mLST8 (also known as GbL) (Jacinto et al., 2004; Kim et al., 2003), and the two structural proteins, Tti1/Tel2

(Kaizuka et al., 2010). Pras40, also an mTOR inhibitor, and Raptor are exclusive to mTORC1 (Haar et al., 2007; Hara et al., 2002; Sancak et al., 2007; Wang et al., 2007; Yonezawa et al., 2004). Whereas Rictor, mSin1 and Protor1/2 are mTORC2-specific components (Pearce et al., 2007; Sarbassov et al., 2006).

Raptor is a core regulatory component of mTORC1 necessary for proper subcellular localization of mTORC1 and recruitment of mTORC1 substrates through its interaction with the TOR signaling (TOS) motif identified in several canonical mTORC1 substrates (Nojima et al., 2003; Saxton and Sabatini, 2017; Schalm et al., 2003). PRAS40 regulates mTORC1 kinase activity by functioning as a direct inhibitor of substrate binding (Sancak et al., 2007; Wang et al., 2007). This negative regulation of mTORC1 by PRAS40 is achieved through its putative TOR signaling motif, FVMDE (Haar et al., 2007; Sancak et al., 2007; Wang et al., 2007).

mTORC1 integrates major intracellular and extracellular signaling pathways including growth factor signaling, amino acid sensing, energy status, and cellular stress (Betz and Hall, 2013; Laplante and Sabatini, 2012). Such mTORC1-mediated signal integration allows a well-controlled regulation and balancing of anabolic and catabolic processes such as protein and lipid synthesis, autophagy, lysosomal biogenesis, and energy metabolism that are essential for maintaining both homeostasis and promoting cell growth (Dibble and Cantley, 2015; Dibble and Manning, 2013; Menon et al., 2014; Nnah et al., 2015). This protein complex transits between cytoplasmic and endolysosomal membrane localization through an amino acid-dependent mechanism reliant upon the heterodimeric RagA/B-

RagC/D GTPases (Saxton and Sabatini, 2017; Wolfson et al., 2017). When localized to endolysosomal membranes, mTORC1 kinase activity is stimulated by complex association with Rheb (membrane-tethered Ras homolog enriched in brain) GTPase (Nnah et al., 2015; Saxton and Sabatini, 2017). Therefore, two sequential events are required for mTORC1 activation: translocation of the complex to endolysosomal membranes and subsequent stimulation of its kinase activity by the Rheb-GTP (Figure 2).

In addition to regulation of protein synthesis, mTORC1 also controls lysosomal biogenesis and degradation through phosphorylation and inhibition of members of the MIT family of transcription factors, including TFEB (Laplante and Sabatini, 2012; Luzio et al., 2014; Palmieri et al., 2011; Peña-Llopis et al., 2011; Sardiello, 2016; Vega-Rubin-de-Celis et al., 2017). As a master transcriptional regulator of cell catabolism, TFEB globally controls the expression of genes that regulate lysosomal and autophagosomal biogenesis (Napolitano and Ballabio, 2016; Palmieri et al., 2011; Sardiello et al., 2009). Under nutrient-rich conditions, TFEB is phosphorylated at serine residues Ser142 and Ser211 by mTORC1 to inhibit its nuclear translocation (Martina et al., 2012; Settembre et al., 2011, 2012) (Figure 2).

8.1.4. Regulation of TFEB by Extracellular Signal-regulated Kinase (ERK2)

Extracellular signal-regulated kinase 2 (ERK2), also known as mitogen-activated protein kinase 1 (MAPK1), is among a family of protein kinases that constitute the MAPK/ERK signaling pathway. When activated by dual phosphorylation at threonine-183 and tyrosine-185, ERK2/1 mediates intracellular signaling induced by hormones, growth factors, and cytokines to control many cellular processes including proliferation, differentiation, and transcription (Bertram et al., 1997; Vomastek et al., 2008). Like mTORC1, ERK2 also localizes to several subcellular compartments including endosomes and lysosomes (Nada et al., 2009; Napolitano and Ballabio, 2016; Pena-Llopis et al., 2011) and was identified as a regulator of TFEB subcellular localization through phosphorylation of TFEB at Ser142 (Sardiello, 2016). It is still unclear whether ERK2 phosphorylation of TFEB controls a separate signaling circuit that subsequently leads to autophagy induction.

8.1.5. Regulation of Autophagy and molecular clearance by TFEB

Autophagy is an evolutionarily conserved catabolic process induced in many cell types to degrade and recycle proteins and defective organelles (Kroemer et al., 2010; Mizushima et al, 2012; Yang and Klionsky, 2010). This degradative pathway is classified into three major categories: macroautophagy, microautophagy and chaperone-mediated autophagy (figure 1B). All of these autophagic processes converge in the lysosomal compartment to ensure proper intracellular degradation of targeted cargo, thus implicating TFEB as a master coordinator of autophagy.

The biogenesis of autophagosomes in mammalian cells begins with the formation of a phagophore assembly site that is mediated by the UNC-51-like kinase (ULK) complex, which contains ULK-1, Autophagy-related protein 13 (ATG13), and the scaffold protein FAK family kinase interacting protein of 200 kDa (FIP200) (Alers et al., 2012; Kaur and Debnath, 2015). Formation of the phagophore also requires interaction of ULK complex with class III phosphoinositide-3-kinase (PI3K) complex that consists of the vacuolar protein sorting-34 (VPS34), Beclin-1, vacuolar protein sorting-15 (VPS15) and ultraviolet irradiation resistance-associated gene (UVRAG) (Alers et al., 2012; Kaur and Debnath, 2015). Subsequent elongation and completion of the double-membrane vesicle is mediated by two ubiquitin-like conjugation pathways that involves production of the autophagy-related genes 5-12-16L (ATG5-ATG12-ATG16L) conjugate and phosphatidylethanolamine (PE) conjugation to the microtubule-associated protein light chain 3 (LC3-I/ATG8) to produced PE-conjugated LC3

(LC3-II) (Alers et al., 2012; Codogno et al, 2012; Feng et al., 2013; Kaur and Debnath, 2015). LC3-II subsequently recognizes and targets cargo to the expanding autophagosomal membrane that fuses with endosome or lysosomes to form amphisomes or autolysosomes respectively (Yang and Klionsky, 2010). Along with other auto-lysosomal genes, LC3 is a downstream target of TFEB (Sardiello et al., 2009).

Macroautophagy (or non-selective autophagy) is induced by starvation or cellular stress and involves the random engulfment and sequestration of cytoplasmic materials inside double-membrane vesicles known as autophagosomes. These autophagosomes carrying sequestered cargo are subsequently trafficked to lysosomes where their contents are degraded and recycled by lysosomal digestive enzymes (Kaur and Debnath, 2015; Mizushima et al., 2012).

Selective autophagic processes such as mitophagy in which defective organelles are selectively targeted for degradation is highly controlled and requires the interaction of specific cargo receptors with autophagic adapter proteins. In the case of mitophagy, accumulation of the kinase PINK1, which is continually degraded in healthy state, on mitochondrial membranes triggers recruitment of the E3 ubiquitin ligase, Parkin to initiate mitophagy (Catherine et al., 2015; Yang and Klionsky, 2010). Polyubiquitination of mitochondrial membrane proteins lead to recruitment of autophagy adapter proteins P62 (or SQSTM1), NBR1 and Ambra 1 that interacts with LC3-II to promote sequestration of targeted mitochondria inside autophagosomes (Kaur and Debnath, 2015; Yang and Klionsky, 2010). During

mitophagy, TFEB translocates to the nucleus to trigger transcription of autophagic genes in a PINK1- and Parkin-dependent manner (Catherine et al., 2015).

Chaperone-mediated autophagy involves selected degradation of substrates that harbor a pentapeptide motif KFERQ recognized by the heat shock cognate 70 kDa protein (Hsc70) chaperone (Bejarano and Cuervo, 2010; Cuervo, 2010; Dice, 2007; Kon and Cuervo, 2010). Hsc70 binds and translocates these substrates to the lysosome in a LAMP2A-dependent. The lysosomal protein LAMP2, like LC3, is also a downstream target of TFEB (Sardiello et al., 2009).

In addition to promoting intracellular-degradation of cytoplasmic contents, TFEB transcriptionally regulates lysosomal exocytosis (Medina et al., 2011) which plays major roles in several physiological processes including plasma membrane repair, immune response, and bone resorption (Andrews, 2000, 2005; Bossi and Griffiths, 2005; Jaiswal et al., 2002; Tucker et al., 2004). This TFEB-mediated exocytosis of lysosomes is achieved by elevation of intracellular calcium levels through lysosomal calcium channel, Mucolipin1 (MCOLN1) (Medina et al., 2011).

8.1.6. Role of TFEB in pathogenesis of human disease

Over the years, the role of autophagy in the maintenance of cellular homeostasis has been a subject of intense study. These studies have described autophagy as a regulator of biosynthetic and catabolic processes essential for cell survival, differentiation and tissue remodeling in various organisms (Napolitano and Ballabio, 2016; Levine and Klionsky, 2004; Shintani and Klionsky, 2004). As such, dysregulation of autophagic processes is central to the progression of certain human diseases including cancer, diabetes and neurodegeneration.

In cancer progression, autophagy can act as a tumor suppressor by removing damaged organelles that can generate free radicals and increase mutations (Luzio et al., 2014; Shitani and Klionsky, 2004) or it may positively influence tumorigenesis by promoting survival of cancer cells within the poor-nutrient environments of a tumor (Kaur and Debnath, 2015; Shitani and Klionsky, 2004). In neurodegeneration, impaired autophagic clearance of accumulated protein aggregates and defective organelles, especially “leaky” mitochondria, induce cytotoxic stress and eventually neuronal death (Menzies et al., 2015; Napolitano and Ballabio, 2016; Sardiello et al., 2009). Defective autophagic clearance of accumulated autophagosomes underlies progression of muscular dystrophy (Gatto et al., 2017).

Given its crucial role in autophagy and intracellular clearance, aberrant TFEB activity results in defective lysosomal biogenesis and function, and consequently causes the systematic breakdown of autophagic machineries observed in human diseases (Kaur and Debnath, 2015; Napolitano and Ballabio,

2016). For instance, increased expression and/or activity of TFEB is associated with non-small cell lung cancer motility (Giantromanolaki et al., 2015) and pancreatic cancer cell proliferation (Marchand et al., 2015). Chromosomal translocations that result in the fusion of TFEB coding region with the regulatory region of the non-coding MALAT1 gene leads to enhanced expression of full-length TFEB protein in patients with clear cell renal cell carcinoma (Kauffman et al., 2014). Defective TFEB signaling drives the progression of lysosomal storage diseases (LSDs) in which synthesis of defective lysosomal digestive enzymes lead to accumulation of substrates in lysosomal lumen (Parenti et al., 2015). Deregulated TFEB activity precedes the lysosomal and autophagic dysfunction observed in neurological disorders such as Alzheimer's and Parkinson's diseases (Menzies et al., 2015; Reddy et al., 2016; Sidransky et al., 2009).

Interestingly, induction of autophagy and intracellular clearance through overexpression of TFEB now serves as a therapeutic tool to counteract the progression of these diseases. Specifically, overexpression of TFEB in mouse models of several LSDs, including Batten disease, Pompe disease and Gaucher disease, have been shown to improve autophagy and reverses the disease phenotypes (Medina et al., 2011; Napolitanao and Ballabio, 2016; Song et al., 2013). Pharmacological or genetic activation of TFEB in cellular and mouse models of Alzheimer's or Parkinson's diseases improves lysosomal function and reduces amyloid-beta or alpha-synuclein aggregation, respectively (Decressac et al., 2013; Dehay et al., 2010).

While the role of TFEB in the regulation of autophagy in health and disease is well described, its function in regulating the endocytic pathway is currently not known.

8.2. Introduction to Cellular Endocytosis

8.2.1. Overview of Endocytosis

Endocytosis is the process by which cells engulf fluids, macromolecules and membrane components through invagination of the plasma membrane. This cellular process serves important cellular functions including uptake of extracellular nutrients, maintenance of cell polarity, regulation of intracellular signal transduction, and immune response (Doherty and McMahon, 2009; Mukherjee et al., 1997; Platta and Stenmark, 2011). While endocytosis can be subdivided into three main classes (pinocytosis, phagocytosis, and receptor-mediated endocytosis), the mechanisms of endocytosis are largely grouped into two main categories namely Dynamin-dependent and –independent pathways. Dynamin is a GTPase that controls fission and pinching-off of newly formed vesicles from intracellular membranes including the plasma membrane, Golgi apparatus and endoplasmic reticulum (Neefjes and Van der Kant, 2014; Wu and Yao, 2009). Dynamin-mediated endocytosis is regulated by Clathrin and Caveolin proteins, two coat proteins that regulate formation of Clathrin- and Caveolin-coated vesicles respectively. These two Dynamin-dependent pathways are the best studied of the endocytic mechanisms and have been implicated in various human diseases including cancer and neurodegeneration (Neefjes and Van der Kant, 2014; Wu and Yao, 2009).

Material taken into a cell by endocytosis are trafficked through a well-defined endocytic pathway. This pathway comprises of early endosomes, recycling endosomes, late endosomes and lysosomes, all of which contribute to proper trafficking and distribution of intracellular materials (Doherty and McMahon, 2009; Sorkin and Zastrow, 2009). Disruptions or mutations of proteins involved in endosomal transport of intracellular materials underlie the progression of several human disorders including cancer and neurodegenerative diseases (Nixon, 2005).

8.2.2. Mechanisms of Dynamin-dependent Endocytosis

Dynamin is a 100-kDa GTPase that regulates the formation of coated endocytic vesicles. It contains a phosphatidylinositol-4, 5-bisphosphate binding domain that tethers it to the membrane and a GTPase domain, which controls the rate at which vesicles pinch off from membranes (Fang et al., 2016; Hinshaw, 2000; Schmid and Frolov, 2011). Two well-characterized coated vesicles distinguished by their major coat proteins, Caveolae and Clathrin-coated vesicles (CCVs) are involved in Dynamin-dependent endocytosis (Doherty and McMahon, 2009).

Caveolae are small invaginations of the plasma membrane found on the surface of many mammalian cell types (Rothberg et al., 1992). They are most abundant in adipocytes and endothelial cells where they constitute up to one-third of the plasma membrane (Thorn et al., 2003). Integral membrane proteins named Caveolins form these Caveolae pits. Together with Dynamin, cholesterol and sphingolipids, Caveolins oligomerize to form caveolar vesicles (Rothberg et al., 1992). Three isoforms of the Caveolin protein, ranging from 18 to 22 kDa in size,

are expressed in mammalian cells: Caveolin-1 (Cav-1), Caveolin-2 (Cav-2) and Caveolin-3 (Cav-3). While Cav-3 is restricted to smooth and striated muscle cells, many other cells like neurons, endothelial cells, adipocytes and fibroblasts express Cav-1 and Cav-2 (Mora et al., 1999; Way and Parton, 1996). In general, Caveolins and Caveolae together are involved in diverse functions including endocytosis and vesicular transport (Yamamoto et al., 2006), cholesterol homeostasis (Frank et al., 2006; Bosch et al., 2011), and signal transduction (Yamamoto et al., 2006; Dobrowolski and De Robertis, 2012). Precisely, Caveolins/Caveolae mediate the canonical/β-Catenin-dependent Wnt signaling through their promotion of Glycogen Synthase Kinase-3 (GSK3) sequestration, a critical component of the Wnt signaling pathway (Dobrowolski and De Robertis, 2012). Subsequent studies suggested that sustained loss of Wnt signaling and failure to monitor the activity of GSK leads to hyperactivation of GSK3, hyperphosphorylation of Tau and presumably onset of Alzheimer's disease (Chichung-Lie et al., 2005; Gunnarsson et al., 2014).

Clathrin-coated vesicles were the first coated vesicles identified in mammalian cells. The major component of these vesicles is Clathrin, which forms the outer layer of the coat. Each subunit of Clathrin consists of three 190 kDa large and small 25 kDa polypeptide chains that form a three-legged structure known as a triskelion (Doherty and McMahon, 2009; Wu and Yao, 2009). Together, these Clathrin triskelion structures assemble into a framework of hexagons and pentagons to form coated pits on the cytosolic surface of intracellular membranes. Adaptor proteins such as Adaptor protein 2 (AP2) and Eps15 play essential roles

in the formation and targeting of membrane-bound cargo to Clathrin-coated pits. These cargos include transmembrane proteins and soluble proteins that interact with them (Boucrot et al., 2015; Doherty and McMahon, 2009).

Like Caveolin, Clathrin is involved in many cellular functions including endocytosis, vesicular transport, and mediation of intracellular signal transduction through internalization of various transmembrane receptors such as receptor tyrosine kinases (RTKs) and G-protein coupled receptors (Wu and Yao, 2009). As such, defects in the Clathrin-mediated endocytosis is associated with pathogenesis of many human diseases, such as neurodegeneration and cancer, in which signal transduction and vesicular trafficking are compromised (Chen et al., 2009, Doherty and McMahon, 2009; Wu and Yao, 2009).

8.2.3. Role of Dynamin-dependent Endocytosis in mTORC1-Signaling

mTORC1 signaling have been linked to endosome trafficking. In a genetic screen carried out by Li et al. (2010), members of the Rab and Arf family of small GTPases that control vesicular trafficking were associated to mTORC1 signaling (Li et al., 2010). In yeast, TOR localizes to endocytic compartments (Kunz et al., 2000; Chen and Kaiser, 2003; Wedaman et al., 2003) and in mammalian cell culture, mTORC1 localizes to late endosomes where it becomes receptive to activation by Rheb GTPase (Sancak et al., 2008, 2010; Flinn et al., 2010). Although the mechanism is poorly understood, studies in which mTORC1 activity was inhibited through disruption of early endosome maturation with constitutively active Rab5 or through depletion of hVps39, established a significant role for the endolysosomal system in mTORC1 signaling (Flinn et al., 2010). The role

endocytosis or accompanying vesicular trafficking in the assembly of mTOR complexes on endolysosomal compartments is still under investigation.

Emerging studies have now linked Dynamin activity in the regulation of autophagy in lower organisms such as Drosophila and Saccharomyces cerevisiae. Along with controlling fission of endocytic vesicles, Dynamin contributes to vacuolar fusion, autolysosomal and lysosomal biogenesis in fruit flies and yeast (Durieux et al., 2012; Peters et al., 2014; Schulze et al., 2013). Loss of function mutation in Dynamin protein results in defective endolysosomal acidification and defective autophagy in flies (Fang et al., 2015).

Three isoforms of Dynamin proteins exist in mammalian cells, all of which are expressed in a tissue-dependent manner. Dynamin 1 (Dyn1) is expressed in neurons and neuroendocrine cells, Dynamin 2 (Dyn2) is expressed in most cell types while the expression of Dynamin 3 (Dyn3) is restricted to testis, although minimal expression have been identified in brain, heart and lung tissues (Hanley et al., 1999). Although Dyn2 have been associated with the selective breakdown of lipid droplets in hepatocytes (Schulze et al., 2013), its specific role in mTOR-TFEB-mediated autophagy is incompletely understood.

8.3. Hypotheses of the Thesis

Defects in the endocytic pathway have been observed in several multifaceted diseases, such as neurodegeneration and cancer, in which mTORC1 signaling is deregulated (Khayati et al., 2016; Komatsu et al., 2016; Lipinski et al., 2010; Nixon, 2013; Reddy et al., 2016). Previously published work from our lab

demonstrated that mTORC1 constitutively tethers to endolysosomal membranes in Alzheimers' disease (AD) and remained largely insensitive to nutrient starvation. This hyperactive mTORC1 activity consequently inhibits cellular clearance mechanisms including autophagy.

Interestingly, cellular endocytosis and signal transduction are tightly intertwined processes. Endocytosis drives internalization of ligand-activated receptors, formation of specialized signaling platforms on early endosomes, or sequestration of inhibitory signaling molecules thereby leading to attenuation or generation of the signaling program, respectively (Dobrowolski and De Robertis, 2012; Sorkin and von Zastrow, 2009). While the role of endocytosis has been shown for some signaling pathways including Wnt, TGFβ, GPCR and others, studies assessing the role of endocytosis for mTORC1 signaling in the context of molecular clearance remain scarce.

Preliminary data from our lab and the previous work done by Di Malta et al., (2017) suggest that, in a regulatory feedback loop, TFEB controls mTORC1 activity during starvation. Also our preliminary data show that inhibition and subsequent dissociation of tuberous sclerosis complex 2 (TSC2) by active Akt is required to tether mTORC1 to endolysosomal membranes and is dependent on endosomal trafficking. These data show that the endocytic pathway plays a crucial role in the activation of the mTORC1 signaling during prolonged starvation, an important step to sustain autophagy and drive lysosomal biogenesis. Therefore, I **hypothesized that cellular endocytosis and accompanying molecular trafficking, controls mTORC1 signaling and that during starvation *TFEB-driven endocytosis***

***directs the mTORC1 reactivation*.** To test this hypothesis, I determined whether endocytosis is necessary for mTORC1 signaling and assessed whether TFEB controls cellular endocytosis. Furthermore, I sought to test whether endocytosis is required for TFEB-mediated reactivation of mTORC1 and autophagic function during starvation.

8.4. Chapter One Figures

8.4.1. Figure1

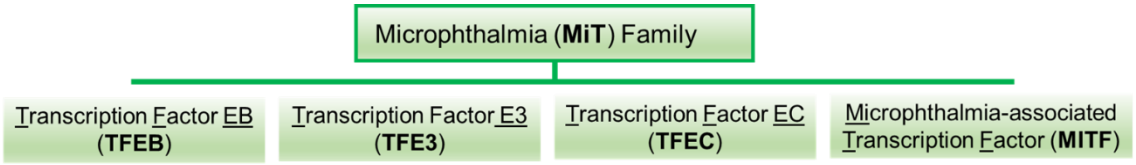

Figure 1A: TFEB is a Member of the Microphthalmia Family (MIT Family) of basic-helix-loop-helix-leucine zipper (bHLH-Zip) transcription factors that bind a palindromic GTCACGTGAC 10-base-pair E-box motif identified in the promoter region of over 600 lysosomal genes (Napolitano and Ballabio, 2016; Raben and Peurtollano, 2016)

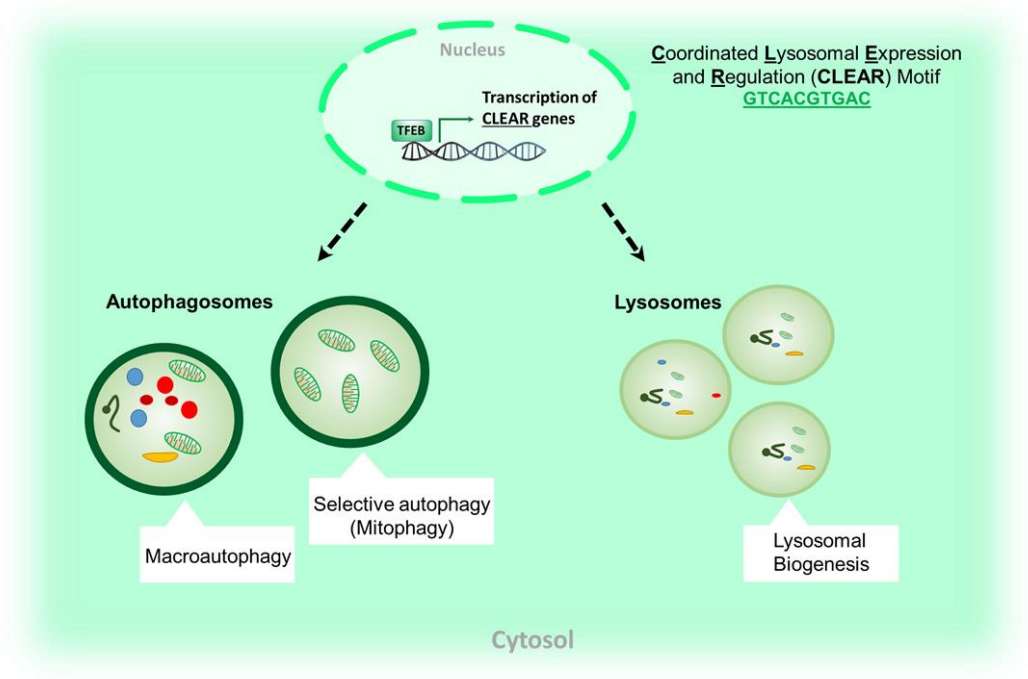

Figure 1B: TFEB Controls Autolysosomal Biogenesis and Autophagy.

Nuclear TFEB activates the expression of CLEAR genes that direct the biogenesis of Autophagosomes and Lysosomes, two intracellular compartments that are crucial for all three categories of autophagy namely, non-selective/macroautophagy, selective/microautophagy and Chaperone-mediated autophagy.

8.4.2. Figure 2

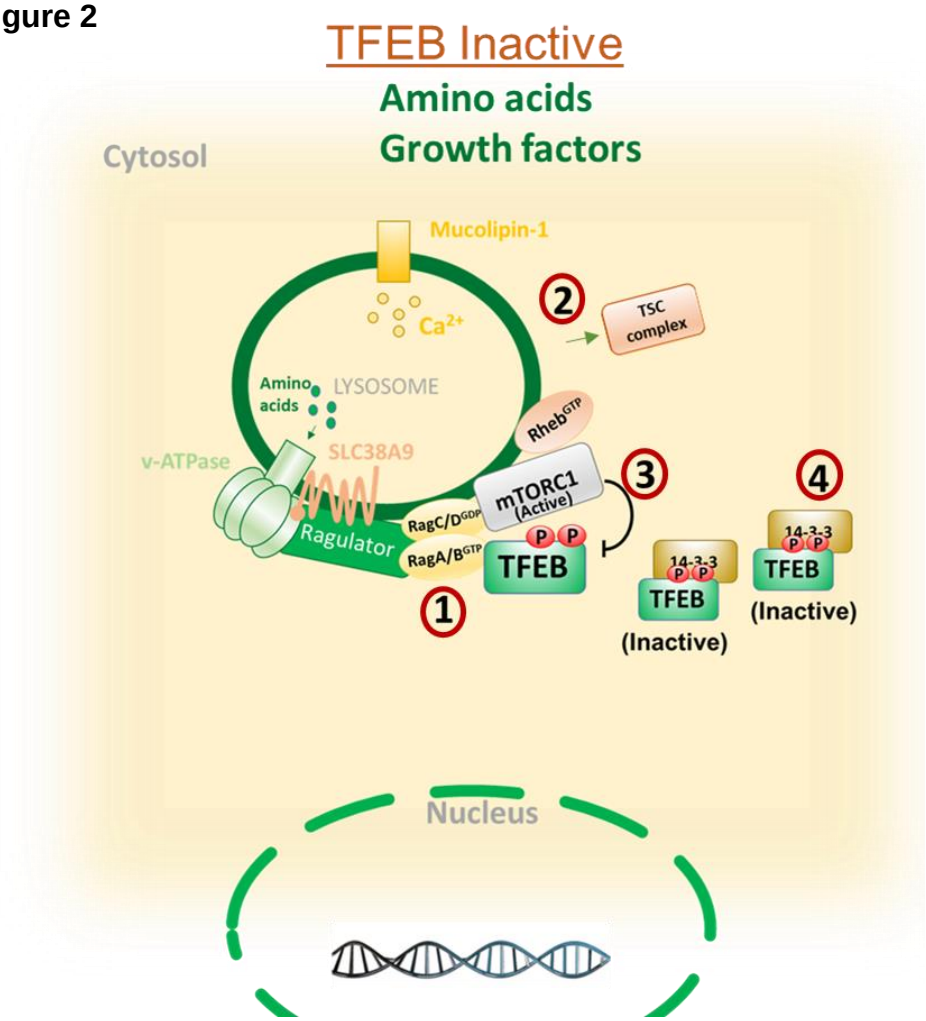

Figure 2A: Amino Acids and Growth Factors Activate mTORC1 Signaling to Inhibit Nuclear Translocation of TFEB. 1) Amino acids mediate the Rag-GTPase-dependent recruitment of mTORC1 to lysosomal membranes; 2) the PI3K/Akt signaling pathway, initiated by the presence of insulin/growth factors, subsequently directs the phosphorylation and inhibition of Tuberous sclerosis (TSC) complex that inhibits Rheb-GTPase. TSC complex inhibition releases Rheb, allowing it to activate mTORC1. 3) Active mTORC1 phosphorylates TFEB, which is recruited to lysosomal membranes through Rag GTPase, at Serine

residues142 and 211. 4) This, in turn, leads to the sequestration of TFEB in the cytoplasm by the cytoplasmic 14-3-3 chaperone protein.

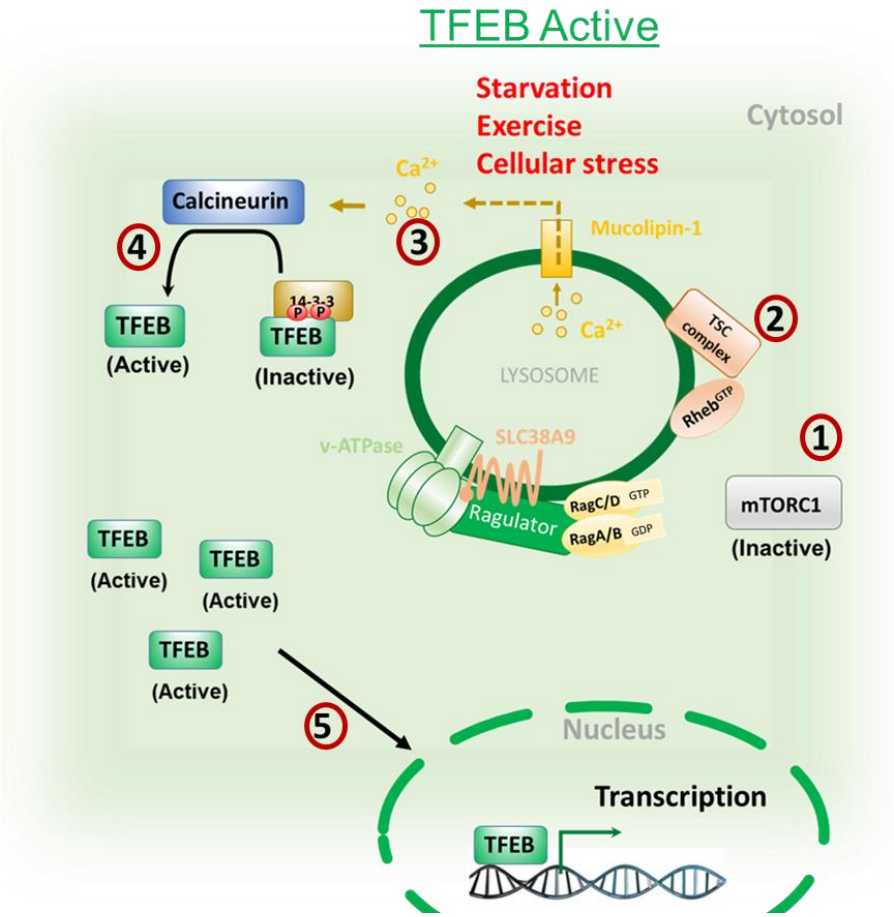

Figure 2B: Starvation, Exercise or Cellular Stress Activates TFEB Signaling. 1-2) Starvation by amino acid/growth factor deprivation, physical exercise or cellular stress promotes inhibition and relocalization of mTORC1 from the lysosomal membrane to the cytosol while re-tethering TSC2 to lysosomal membranes to inhibit Rheb. 3) These stimuli cause the efflux of lysosomal calcium from the calcium channel, Mucolipin-1 that 4) activates Calcineurin, a phosphatase

that subsequently 4) dephosphorylates TFEB to 5) promote activation and nuclear translocation TFEB

9. Chapter Two

9.1. Materials & Methods

9.1.1. Materials

The following primary antibodies were used for immunoblotting and immunostaining: Rab5 (#C8B1, Cell Signaling Technology, Danvers, MA), EEA1 (#N19, Sigma-Aldrich), Clathrin light chain (#3F133, ThermoFischer), Caveolin (cat. #610059; BD Transduction), SLC38A9 (cat. #HPA043785; Sigma-Aldrich), mTOR (cat. #7C10, cat. #2983; Cell Signaling Technology), TSC2 (cat. #4308; Cell Signaling Technology), Phospho-p70S6K (Thr389, cat. #9205; Cell Signaling Technology), P70S6K (cat. #2708; Cell Signaling Technology), mouse lysosomal-associated membrane protein 2 (LAMP2) (cat. #ABL-93; DSHB), human LAMP2 (cat. #H4B4; DSHB), microtubule-associated protein light chain 3 (LC3) a/b (cat. #4108; Cell Signaling Technology), p62/SQSTM1 (cat. #GP62-C; Progen, Heidelberg, Germany), mCherry (cat. #5993-100; BioVision, Milpitas, CA, USA), HA (cat. #H9658; Sigma-Aldrich), Flag (cat. #F3165; Sigma-Aldrich), Phospho-Akt (Thr308, cat. #2965P; Cell Signaling Technology), pan-Akt (total, cat. #4691, Cell Signaling Technology), Phospho-PDK1 (Ser241, cat. #3438; Cell Signaling Technology), β-Actin (cat. #JLA20; DSHB, Iowa City, IA, USA). Secondary antibodies coupled to either Infrared Dyes (IRDye 680 and IRDye 800, LICOR), or to HRP (Jackson IR) were used for immunoblotting analysis, those coupled to fluorochromes (Jackson IR) were used for immunostaining. Amino acids were reconstituted in water or 1 M hydrochloric acid followed by a neutralization with sodium hydroxide. Stock solutions were diluted in respective culture media to

obtain the stated amino acid concentrations. All amino acid starvation experiments were carried out as previously described (Khayati et al., 2016). RPMI medium without leucine/L-glutamine (#R899912) was supplied by United States Biological (Salem, MA, USA). The amino acids L-leucine (L800) was supplied by Sigma-Aldrich. HBSS 10X (#14065-056, Life Technologies), hydroxyl-Dynasore (cat. #SML0340; Sigma-Aldrich), Ciliobrevin-A (cat. #4529), Dulbecco's Modified Eagle's Medium (Sigma-Aldrich), Fetal Bovine serum (FBS) (cat. #10438, Life Technologies), dialyzed Fetal Bovine Serum (Life Technologies), Chloroquine (Sigma), BioT transfection reagent (cat. #B01-00; Bioland Sci).

Cell culture

Mouse neuroblastoma cell line, CAD cells stably expressing TFEB-Flag were generated in our laboratory as described previously by Khayati et al., (2017). Mouse Embryonic Fibroblasts (MEFs), NIH-3T3 fibroblasts and HEK-293T cells were cultured in Dulbecco's modified Eagle's medium (DMEM) supplemented with 10% fetal bovine serum (FBS) and glutamine.

9.1.2. Methods

Amino acid deprivation assay:

Cells were first plated and allowed to stabilize in RPMI 1640 containing 10% dialyzed FBS (dFBS) along with both Leucine and Glutamine. For Leucine and glutamine deprivation, the media was replaced with 10% dFBS in RPMI1640 without Leucine and glutamine for the indicated time points. For Dynasore and Ciliobrevin drug treatments, cells were first plated and allowed to stabilize in complete RPMI media containing 10% dFBS and Leucine/glutamine. These cells were pre-incubated with the indicated concentrations of Dynasore and Ciliobrevin-A for 2 hours in complete RPMI media before starting the leucine/glutamine deprivation experiments for the indicated time points. For Dynasore/Ciliobrevin-A treatments under leucine/glutamine deprivation, stabilized cells were incubated with the indicated concentrations of DMSO and Ciliobrevin-A in leucine/glutamine-free RPMI medium containing 10% dFBS for the indicated time points. For Dynamin-2 plasmid transfections and leucine/glutamine deprivation, cells were first transfected with the indicated plasmids before incubating them in leucine/glutamine-free RPMI medium containing 10% dFBS for the indicated time points.

Plasmid DNA and transfections:

WT-Dynamin 2-mCherry was a gift from Christien Merrifield (Addgene plasmid #27689), Dominant negative Dynamin 2-GFP was a gift from Pietro De Camilli (Addgene, plasmid # 22197). pcDNA3-Akt-PH-GFP was a gift from Craig Montel (Addgene plasmid #18836). WT-TFEB-Flag was cloned in our laboratory

by amplifying human Tcfeb cDNA with the following PCR primers: Tfeb_for: GAA TTC GCC ACC ATG GCG TCA CGC ATA GGG T and Tfeb-Flag_rev: TCT AGA TCA CTT GTC ATC GTC CTT GTA GTC CAG CAC ATC GCC CTC. The TFEB-Flag amplicon was cloned into the pCS2+ vector backbone using EcoRI and XbaI restriction sites. TFEBS211A-Flag, and TFEBS142A-Flag point mutations were generated using the QuikChange Lightning Site-Directed Mutagenesis Kit, following manufacturer's instructions. All constructs were transfected using BioT plasmid transfection protocol (Bioland Scientific). For knock-down experiments, the following siRNA reagents were used: ONTARGET plus SMARTpool siRNA for Clathrin light chain B (#M-004003-00), siRNA for Tfeb (#D-009798-03), and control (scrambled) siRNA were purchased from GE Dharmacon. siRNAs were transfected as described using the BioT reagent protocol (Bioland Sci.), knock-down efficiency of gene expression was validated by immunoblot.

Immunostaining:

Cells grown on fibronectin-coated coverslips were rinsed in PBS once and fixed in 4% paraformaldehyde in 37ºC for 10 minutes and for 5 minutes at RT. Cultures were rinsed in PBS and blocked in 5% normal goat serum, 0.5% BSA, and 0.5% TritonX100 in PBS for 45 minutes at room temperature. Primary antibody working solutions were made in blocking buffer and incubated overnight at 4ºC. Cultures were rinsed in PBS and placed in secondary antibodies for 45 min. The specimens were rinsed and mounted. Confocal images were obtained using a Zeiss Cell Observer spinning-disc microscope (Zeiss, Thornwood, NY).

SDS PAGE and Western blot analysis:

Cell lysates were prepared with lysis buffer (10% glycerol, 1% NP40, 20mM Tris (pH7.4), 2.5 mM EDTA (pH8), 2.5mM EGTA (pH8), including Roche Protease inhibitor cocktail (#04693116001). Lysates were spun down at 17,000rpm for 15 minutes at 4°C. The cleared supernatant was collected and protein concentration assayed using the BCA method and run on a 10-12% SDS-PAGE gels. The protein was transferred onto PVDF (Immobilon) membranes. The membranes were blocked in 5% Milk, 0.1% Triton-X 100 in TBS for 1 hour. After incubation with primary antibodies (overnight) and secondary antibodies (45 minutes), the membranes were washed and analyzed by either the LI-COR Odyssey system or developed by ECL (Pierce).

Dextran-TMR uptake assay for cellular endocytosis:

Cells were first plated in 24-well plates and allowed to stabilize in a complete DMEM medium containing 10% FBS, pen-strep and supplemented with glutamine. These cells were pre-incubated with the indicated drugs for 2 hours before addition of Dextran-tetramethylrhodamine (Dextran-TMR, #D1863; Life technologies) or endothelial growth factor (EGF)-Rhodamine (#E3481, ThermoFisher) for 2-4 hours at 37C, 5% CO_2. Cells were fixed and prepared for confocal microscopic analyses, or trypsinized with 0.5% Trypsin EDTA, spun down, and re-suspended in 1X phosphate buffer saline (PBS) pH 7.4. Re-suspended cells were counted, transferred into a 96-well plate and analyzed using a Promega GloMax plate reader to measure signal intensity of internalized Dextran-TMR.

Quantitative Assessment of TFEB localization in cultured cells:

Nuclear or cytoplasmic localization of TFEB-GFP in stably expressing HeLa cells were assessed using the OPERA system (Perkin Elmer). TFEB-GFP expressing cells were grown on plates that were treated in indicated compounds overnight and monitored using 20 × water immersion objective. The OPERA system acquires >6 fields/well using two exposures (laser 405 nm for Hoechst and laser 488 nm for TFEB-GFP) and blindly assesses for nuclear vs cytoplasmic localization expressed as a ratio of an average nuclear GFP intensity/average cytosol GFP intensity in cells.

Cell fractionation:

Endosomal cell fractionation was carried out as described (de Araújo et al., 2015; Bilic et al., 2007). Cells were seeded in 6-well plates with a doxycycline-containing nutrient-rich media for 24 hours. Cells were harvested in 1x TNE buffer (50 mM Tris-HCl, pH 7.4; 100mM NaCl and 0.1 mM EDTA without protease inhibitors) and spun down at 400g for 5 minutes. The cell pellet was collected and spun in 300 µl of 1X TNE Buffer containing protease and phosphatase inhibitors, and sheared by pipetting through a 25G needle (40 strokes). 200 µl of the cell suspension was transferred into a fresh microcentrifuge tube containing 200 µl of 1X TNE Buffer (containing protease/phosphatase inhibitors and 2% Triton-X 100) followed by a 30-minute incubation in 4^{o} C with gentle agitation. 30 µl of the sheared cell suspension was transferred to a fresh tube and used as 10% input. After incubation, the 400 µl of sheared cell suspension was mixed with 700 µL of 60% OptiPrep solution and gently pipetted to the bottom of a 3.5 ml centrifuge tube and layered with 600 µl of 40%, 30%, 20%, and 15% OptiPrep solutions prepared

with 1X TNE buffer containing protease/phosphatase inhibitors to produce OptiPrep gradients. The prepared samples were spun at 55,000 g for 4 hours at 4°C using a Sorvall ultracentrifuge. A total of 17 fractions (200 µl each) were collected and used in immunoblot analyses.

Quantitative PCR analyses:

For RNA isolation, CAD cells were plated at 75% confluency and grown overnight with or without doxycycline to induce expression of TFEB-Flag. DMSO, Dynasore, or Ciliobrevin were added to the cells the following morning for up to 6 h prior to lysis and preparation of total RNA using TRIZOL (LifeTech), chloroform and ethanol absolute for precipitation. Two µg of total RNA were used for cDNA synthesis (Single Strand cDNA Synthesis kit, Fermentas), cDNA was diluted 10-fold and used for qPCR analyses using SYBRgreen (Biosystems) and the Roche Lightcycler 480. Following primer sequences (PGA-PrimerBank) were used for the presented analyses: LC3_for: CGC TTG CAG CTC AAT GCT AAC, LC3_rev: CTC GTA CAC TTC GGA GAT GGG; p62/SQSTM1_for GAA CTC GCT ATA AGT GCA GTG T, p62/SQSTM1_rev: AGA GAA GCT ATC AGA GAG GTG G; TFEB_for: GCA GCC ACC TGA ACG TGT A; TFEB_rev: TGT TAG CTC TCG CTT CTG AGT; MCOLN1_for: GCG CCT ATG ACA CCA TCA A; MCOLN1_rev: TAT CCT GGA CTG CTC GAT; CTSF_for: ACG CCT ATG CAG CCA TAA AG; CTSF_rev: CTT TTG CCA TCT GTG CTG AG; CTSB_for TTA GCG CTC TCA CTT CCA CTA cc; CTSB_rev: TGC TTG CTA CCT TCC TCT GGT TA; Actin_for: TTG CTG ACA GGA TGC ACG AAG, Actin_rev: CCA CCG ATC CAC ACA GAG TA

Statistics:

Experiments involving cultured cells were repeated independently for at least 3 times (n = 3) with triplicates and results represented as the average of the three experiments with error bars indicating calculated standard error of the mean (SEM). Statistical analyses were performed using Microsoft Excel and further confirmed with Prism 6 software. Means between two groups were compared using 2-tailed, unpaired Student's t-test while means between more than two independent groups were compared using ANOVA followed by indicated post hoc tests for intergroup comparisons. Significant differences of means were indicated as * ≤ 0.05, ** ≤ 0.01, and *** ≤ 0.001, while 'ns' denotes no significant difference.

10. Chapter Three

10.1. TFEB-driven endocytosis coordinates mTORC1 signaling and autophagy

Highlights of this study

- TFEB induces expression of a multitude of endocytic genes, including Clathrin, Caveolin, Rab5, and Rab7
- TFEB up-regulates cellular endocytosis and trafficking of p-Akt (Thr308), SLC38A9, and RagD to lysosomes
- mTOR tethering to lysosomal membranes as well as mTORC1 activity strictly depend on endocytic trafficking
- TFEB re-localized into the nucleus upon starvation to drive mTORC1 reactivation, autophagy, and lysosomal biogenesis in an endocytosis-dependent manner

10.1.1 Abstract

The mechanistic target of rapamycin complex 1 (mTORC1) is a central cellular kinase that integrates major signaling pathways, allowing a well-controlled regulation of anabolic and catabolic processes including autophagy and lysosomal biogenesis. Essential to the aforementioned process is the regulatory activity of transcription factor EB (TFEB). In a regulatory feedback loop modulating transcriptional levels of RagD GTPase, TFEB controls mTORC1 re-activation and induction of anabolic processes upon nutrient replenishment. I now show that TFEB promotes assembly of an mTORC1-containing nutrient sensing complex through formation of endosomes which carry the associated proteins, RagD, the amino acid transporter SLC38A9, and activated protein kinase B (Thr308-Akt). TFEB-induced signaling endosomes en route to lysosomes are required to dissociate TSC2, re-tether and activate mTORC1 on endolysosomal membranes during prolonged starvation. TFEB-triggered endocytosis is required for delivery of mTORC1 activators, lysosomal biogenesis, and autophagy flux. Studies presented in this thesis

identify TFEB-mediated endocytosis as a critical process driving lysosomal biogenesis and emphasizes the role of endolysosomal system in molecular clearance.

10.1.2 Introduction

The mechanistic target of Rapamycin complex 1(mTORC1) is an evolutionarily conserved serine/threonine kinase that controls organismal growth, and has been found deregulated in several multifaceted diseases including cancer and neurodegeneration (Laplante and Sabatini, 2012; Nnah et al., 2015). mTORC1 integrates major intracellular and extracellular signaling pathways including growth factor signaling, amino acid sensing, energy status, and cellular stress (Betz and Hall, 2013; Laplante and Sabatini, 2012). Such mTORC1-mediated signal integration allows a well-controlled regulation and balancing of anabolic and catabolic processes such as protein and lipid synthesis, autophagy, lysosomal biogenesis, and energy metabolism that are essential for maintaining both homeostasis and promoting cell growth (Dibble and Manning, 2013; Nnah et al., 2015). mTORC1 transits between cytoplasmic and endolysosomal membrane localization through an amino acid-dependent mechanism reliant upon the heterodimeric RagA/B-RagC/D GTPases (Saxton and Sabatini, 2017; Wolfson et al., 2017). When localized to endolysosomal membranes, mTORC1 kinase activity is stimulated by complex association with Rheb (membrane-tethered Ras homolog enriched in brain) GTPase (Nnah et al., 2015; Saxton and Sabatini, 2017). Therefore, two sequential events are required for mTORC1 activation: translocation of the complex to endolysosomal membranes and subsequent stimulation of its kinase activity by the GTP-bound Rheb (Laplante and Sabatini, 2012; Nnah et al., 2015).

mTORC1 is known to control lysosomal biogenesis and degradation through phosphorylation and inhibition of different members of the basic helix-loop-helix leucine zipper family of transcription factors, including TFEB (Laplante and Sabatini, 2012; Luzio

et al., 2014; Palmieri et al., 2011; Peña-Llopis et al., 2011; Sardiello, 2016). As a master transcriptional regulator of cell catabolism, TFEB globally controls the expression of genes that regulate lysosomal and autophagosomal biogenesis (Napolitano and Ballabio, 2016; Sardiello et al., 2009). However, although both lysosomal biogenesis and autophagy both depend on active endocytosis, an association between TFEB activity and modulation of the endocytic pathway has yet to be discovered.

Besides a deregulation of mTORC1 signaling, defects in endolysosomal trafficking are associated with cancer and severe neurodegenerative diseases, including Alzheimer's, Parkinson's, amyotrophic lateral sclerosis and myelination disorders (Khayati et al., 2016; Komatsu et al., 2006; Lipinski et al., 2010; Nixon, 2013; Reddy et al., 2016). Generally speaking, endocytosis and signal transduction are tightly intertwined processes. Endocytosis drives internalization of ligand-activated receptors, formation of specialized signaling platforms on early endosomes, or sequestration of inhibitory signaling molecules, this way contributing to attenuation or generation of the signal, respectively (Dobrowolski and De Robertis, 2012; Sorkin and von Zastrow, 2009). While the role of endocytosis has been shown for other pathways including Wnt, TGFβ, GPCR and others, studies assessing the role of endocytosis for mTORC1 signaling in the context of molecular clearance are yet to be conducted.

Here I show that overexpression of TFEB induces cellular endocytosis and formation of endosomes carrying activated protein kinase B (Thr308-Akt), the amino acid transporter SLC38A9 and the tethering molecule RagD, which are crucial components of the lysosomal nutrient sensing complex (Settembre et al., 2013) tightly linked to mTORC1 activity. Pharmacological and genetic inhibition of either endocytosis or retrograde trafficking abolished mTORC1 activity without affecting total levels of pT308-Akt and active TFEB in the nucleus. We further observed that these TFEB-induced endosomes en route to lysosomes were required to dissociate TSC2 and tether mTORC1 to lysosomal

membranes, this way restoring its activity during prolonged periods of starvation. Importantly, we demonstrate that TFEB-triggered endocytosis is a critical step required for mTORC1 activation, lysosomal biogenesis, and sustained autophagy.

10.1.3 Results

10.1.3.1. TFEB increases cellular endocytosis and assembly of mTORC1-containing lysosomal nutrient sensing complex

TFEB drives lysosomal biogenesis and molecular clearance through endolysosomal exocytosis and autophagy. All of these TFEB-driven processes depend on cellular endocytosis. Therefore, I asked whether cellular endocytosis is regulated by TFEB activity. In collaboration with Dr. Ballabio's group (TIGEM, Italy), we carried out ChIP-seq analyses (Palmieri et al., 2011) that identified 46 known endocytic genes including Rab5, Rab7, Clathrin, and Caveolin to be transcriptionally regulated by TFEB (Figure 10.1.5.**1A** and Table 1, Appendix Table 2). Expression of wildtype or the constitutively active mutant form of TFEB (TFEB-FLAG or TFEB-S211A-FLAG, respectively) in HeLa cells strongly induced an increase in the number of Early Endosomal Antigen-1 (EEA1)-positive endosomes as determined by immunofluorescence and immunoblot analyses (Figure 10.1.5.**1B**). TFEB-overexpressing cells showed a robust increase of Caveolin 2 and Clathrin light chain protein levels (Figure 10.1.5.**1C** and Figure 10.1.5.**1D**), two major endocytic coat proteins. I assessed the effect of TFEB overexpression as well as starvation on the localization of Caveolin proteins and uptake of epidermal growth factor (EGF)-Rhodamine. In amino acid-starved cells, membrane-bound EGF-Rhodamine and Caveolin were efficiently internalized (Figure 10.1.5.**1G**-**1H**), similar to cells expressing WT or TFEB-S211A (Figure 10.1.5.**1I**). Amino acid starvation increased total intracellular Caveolin levels in a TFEB-dependent manner (Figure 10.1.5.**1J**). I further found that TFEB-GFP expressing cells increased uptake of extracellular Dextran-Tetramethylrhodamine (TMR) in microscopic and densitometric analyses, similar increase of Dextran-TMR uptake was observed in cells treated with the lysosomal inhibitor Chloroquine, the mTOR inhibitor Torin1, or during prolonged starvation, all being conditions known to translocate TFEB into the nucleus (Figure 10.1.5.**1E**). Importantly, the

increased endocytic uptake of Dextran-TMR in amino acid-starved cells was dependent on TFEB expression, as TFEB knockdown cells showed low levels of intracellular Dextran-TMR signal when compared to control cells (Figure 10.1.5.**1F**). Collectively, these analyses establish that TFEB regulates the expression of a number of endocytic genes needed to drive the activity of the endocytic pathway under starvation conditions.

Recent studies show that TFEB-mediated transcription of RagD promotes mTORC1 activity and tumor growth (Di Malta et al., 2017). As endocytosis plays a crucial role in the activation of many signaling pathways (Dobrowolski and De Robertis, 2012; Sorkin and von Zastrow, 2009), I wondered whether TFEB-driven endocytic trafficking could be important for the formation of signaling endosomes and for lysosomal delivery of crucial components of the nutrient sensing complex to activate mTORC1. To investigate this hypothesis, I used stable neuroblastoma cell line (CAD cells) expressing a doxycycline (DOX)-inducible TFEB-FLAG to conduct endosomal fractionation assays to quantitatively assess the levels of Rab5-positive early endosomes, the TSC complex, phospho-Akt (Thr308), and the arginine transporter SLC38A9 when TFEB is overexpressed. These cells were cultured in nutrient-rich medium, with or without doxycycline, for 24 hours prior to endosomal fractionation (Figure 10.1.5.**2A**-**2C**). OptiPrep-fractions of TFEB-expressing cells showed an enrichment of Rab5-positive early endosomes and increased levels of endosomal pPDK1 (pSer241) and p-Akt (Thr308) when compared to controls. While levels of the arginine transporter SLC38A9 were only slightly changed, the mTORC1-tethering molecule RagD was strongly upregulated in endosomal fractions of TFEB overexpressing cells (compare Figure 10.1.5.**2B** vs Figure 10.1.5.**2A** and quantifications in Figure 10.1.5.**2C**). The mTORC1 inhibitor TSC2 was detected in the endosomal fractions of untreated controls but was largely absent in TFEB-expressing cells (Figure 10.1.5.**2A** vs Figure 10.1.5.**2B**). Importantly, no significant difference in p-Akt (Thr308) and SLC38A9 could be detected in the whole-cell, pre-fractionation lysates of TFEB-expressing and

control cells (Figure 10.1.5.**2D**, 10% input), whereas Rab5 levels were increased and TSC2 protein levels decreased in TFEB-expressing cells.

I next assessed whether TFEB overexpression induces formation of endosomes carrying the active form of Akt (Figure 10.1.5.**2E**). I expressed the Akt-Pleckstrin-homology-domain (PH)-GFP bioprobe that under unstimulated, baseline conditions remains cytoplasmic and/or plasma membrane-associated. Overexpression of TFEB-FLAG strongly relocalized Akt-PH-GFP to the partially Rab5-positive endocytic compartment indicating an increase in endosomal phosphatidylinositol-3-phosphate (PI3P) levels and increased binding of Akt to these lipids through its PH-domain, which is considered the necessary step in the activation of Akt (Ebner et al., 2017). To verify endosomal localization of RagD and mTORC1, we examined cells expressing Rab5QL-DsRed by confocal microscopy. These cells form enlarged endosomes making it possible to assess the presence of proteins on endosomal membranes. We confirmed the localization of RagD and mTOR on endosomal membranes that was further increased upon TFEB-FLAG overexpression (see Figure 10.1.5.**2F**). Together, these data show that TFEB activity potently increased endocytic activity and formation of pPDK1/pAkt/RagD/mTOR-positive endosomes.

10.1.3.2. Dynamin-mediated cellular endocytosis and retrograde trafficking are necessary for mTORC1 re-activation during prolonged starvation

During periods of long starvation, re-activation of mTORC1 precedes induction of autophagic lysosome reformation (ALR) that is necessary for replenishing lysosome quantity and maintaining lysosome homeostasis (Chen and Yu, 2013; Rong et al., 2012; Yu et al., 2010; Zhang et al., 2016). Previous studies suggested that degradation of autolysosomal content was sufficient to reactivate mTORC1 while recent findings have shown that other factors contribute to mTORC1 reactivation (Rong et al., 2011, 2012; Yu et al., 2010).

Here, I assessed the role of TFEB-mediated endocytosis in the reactivation of mTORC1 signaling during long-term starvation. I utilized CAD cells stably expressing a doxycycline-inducible, FLAG-tagged WT-TFEB (WT-TFEB-FLAG). WT-TFEB-FLAG cells were cultured in nutrient-rich media with or without doxycycline for 24 hours after which mTORC1 activity was assessed by determining phosphorylation levels of mTORC1 substrates, including P70S6K. Doxycycline-treated CAD cells showed a two-fold increase in phospho-P70S6K protein levels compared to the untreated controls (Figure 10.1.5.**2G**), likewise HEK-293T cells overexpressing WT or constitutively active TFEB showed increased phospho-P70S6K protein level (Figure 10.1.5.**2H**), suggesting that increased levels of TFEB promotes upregulation of mTORC1 activity.

Previous studies demonstrated that lysosome-bound mTORC1 is localized close to the periphery where plasma membrane-bound activators, such as phospho-Akt, interact to activate the complex (Korolchuk et al., 2011). Current models of mTORC1 re-activation during prolonged starvation have not linked endocytic trafficking as an essential step in activating mTORC1 (Chen and Yu, 2013; Rong et al., 2012; Yu et al., 2010; Zhang et al., 2016). To elucidate the role of endocytosis and retrograde trafficking during mTORC1 re-

activation, I assessed mTORC1 reactivation in TFEB overexpressing and knockdown cells after exposure to Dynasore (a specific inhibitor of the Dynamin GTPase), treatment with Ciliobrevin A (an inhibitor of the Dynein motor protein inhibitor) or in cells expressing WT or dominant negative forms of Dynein (Figure 10.1.5.**4**). Compared to DMSO-treated cells, mTORC1 signaling remained inhibited in cells treated with Dynasore or Ciliobrevin containing medium and subsequently deprived of amino acids for six hours (compare relative p-P70 levels in Figure 10.1.5.**4A**).

To specifically target Dynamin-mediated endocytosis and observe the effect of its inhibition on mTORC1 reactivation, HEK 293T cells were transiently transfected with WT or dominant negative forms of Dynamin2 (Dynamin2-K44A) followed by prolonged amino acid deprivation. In control cells, mTORC1 activity was inhibited within 1 hour of starvation and recovery of activity was observed after 4 hours of amino acid deprivation, while cells expressing WT-Dynamin2 did not fully inhibit mTORC1 activity at any of the investigated time points (Figure 10.1.5.**4B**). In contrast, cells expressing Dynamin2-K44A showed an overall low mTORC1 activity and mTORC1 activity was not restored even following prolonged starvation (Figure 10.1.5.**4B**), further underlining the importance of endocytic trafficking in mTORC1 signaling.

Since TFEB increased cellular endocytosis and mTORC1 activity in fed condition, I set out to see whether modulation of TFEB expression would impact recovery of mTORC1 activity during long-term starvation. Depletion of endogenous TFEB in HEK293 cells inhibited reactivation of mTORC1 while overexpression of TFEB promoted basal levels and faster recovery of mTORC1 activity (Figure 10.1.5.**4C**) in an endocytosis-dependent manner (Figure 10.1.5.**4D**) (compare relative pP70 levels in TFEB-overexpressing cells vs TFEB-overexpressing cells treated with Dynasore). These data identifies TFEB-mediated endocytosis in mTORC1 reactivation during prolonged starvation.

10.1.3.3. Endocytic trafficking controls mTORC1 activity and promotes lysosomal biogenesis

Since the inhibition of endocytic trafficking affected mTORC1 activity during starvation, I asked if endocytosis and retrograde trafficking generally controls mTORC1 signaling in fed conditions. When cells were cultured in hypertonic sucrose media to inhibit all forms of cellular endocytosis, mTORC1 dissociated from lysosomes, while TSC2 localized to lysosomal membranes (Figure 10.1.5.**3G** and 10.1.5.**3H**). Treating cell with Dynasore (Figure 10.1.5.**3A-B**) or Ciliobrevin (Figure 10.1.5.**3E**) for 4 or 2 hours, respectively, similarly resulted in mTORC1 re-localization to the cytosol while TSC2 was associated with lysosomes (LAMP2 staining). In addition, phosphorylation of P70S6K, a standard read-out for mTOR1 activity, was inhibited in a series of experiments attenuating cellular endocytosis and vesicular trafficking, including culturing in sucrose (Figure 10.1.5.**3I**), treatment with Dynasore (Figure 10.1.5.**3C**), overexpression of DN-Dynamin2 (Figure 10.1.5.**3D**), treatment with Ciliobrevin (Figure 10.1.5.**3K**), or overexpression of DN-Rab5 (Figure 10.1.5.**3F**) under nutrient-rich conditions. Note that overexpression of wildtype Dynamin or Rab5 increased relative pP70/S6K1 levels indicating increased mTORC1 activity (Figure 10.1.5.**3D** and 10.1.5.**3F**). Localization of components of the LYNUS other than mTOR confirmed effective treatment with the used compounds (see Figure 10.1.5.**3J** showing decreased lysosomal localization of the arginine transporter SLC38A9 in Dynasore-treated cells, indicating transport of this protein via the endocytic pathway).

Since attenuation of TFEB-mediated signaling inhibits mTORC1 activity, I assessed cellular localization of TFEB as well as transcription of a number of TFEB target genes. Interestingly, inhibition of Dynamin or Dynein-mediated endocytic trafficking re-localized TFEB-FLAG to the nucleus in P8B11-HeLa cells (Figure 10.1.5.**5A-C**) and increased

transcription of TFEB-target genes, including LC3, p62/SQSTM1, MCOLN1, CTSB, CTSF, and TFEB (Figure 10.1.5.**5D**). In addition, long-term inhibition of endocytic trafficking for 16-24 hours efficiently reduced total LAMP2 signal intensity as well as the total number of lysosomes per cell (Figure 10.1.5.**5E**). Thus, interestingly, while inhibition of the endocytic pathway promoted nuclear TFEB activity, this activity appeared ineffective in its ability to increase the number of lysosomes in individual cells. I concluded that inhibition of the endocytic pathway does not inhibit mTORC1 activity solely through TFEB.

10.1.3.4. Inhibition of retrograde trafficking consequently disrupts endolysosomal acidification and autophagy flux.

Previous studies demonstrated mTORC1 to be re-activated in an autophagy-dependent manner during long periods of starvation (Yu et al., 2010). Di Malta et al. (2017) showed that TFEB-driven mTORC1 activity is independent of autophagy while the data presented here shows TFEB-mediated endocytic trafficking drives assembly of the nutrient sensing complex and reactivates mTORC1. Since reactivation of mTORC1 is a critical step preceding lysosomal restoration and autophagy flux, I assessed whether TFEB-mediated endocytosis regulates lysosomal homeostasis, acidification, and autophagy flux. In cells exposed to Ciliobrevin, I observed fewer acidic vesicles (Figure 10.1.5.**6A**) and an inhibition of autophagy flux (Figure 10.1.5.**6B** and 10.1.5.**6C**). Autophagy flux encompasses the biogenesis of autophagosomes, their fusion with lysosomes to form autolysosomes, and their subsequent degradation (Hamasaki et al., 2013; Jiang and Mizushima, 2014; Sardiello, 2016). Post-translational modification of LC3-I to LC3-II through phosphatidylethanolamine conjugation to LC3-I and degradation of P62/SQSTM1 are a widely accepted markers for detecting autophagy flux in experiments conducted in the presence of lysosomal inhibitors such as Chloroquine to assess total levels of LC3-II and P62/SQSTM1 (Hamasaki et al., 2013; Kroemer et al., 2010; Yang and Klionsky, 2010). I assessed the levels of these markers in cells cultured in an amino acid-free media containing either DMSO (Figure 10.1.5.**6B**) or Ciliobrevin (Figure 10.1.5.**6C**). During starvation, in DMSO treated cells, LC3-II and P62/SQSTM1 levels decreased over time (Figure 6B), whereas in cells treated with Ciliobrevin, LC3-II and P62/SQSTM1 proteins accumulated over time (compare Figure 10.1.5.**6B** to 10.1.5.**6C**), cells exposed to Dynasore showed a similar phenotype. To assess the impact of TFEB-mediated endocytosis on autophagy flux, I first assessed the levels of LC3-II and

P62/SQSTM1 in cells overexpressing TFEB-FLAG before and after pharmacological inhibition of endocytic trafficking. TFEB expressing cells showed an accelerated decline of LC3-II and P62/SQSTM1 levels during starvation, indicating enhanced autophagy flux (Figure 10.1.5.**6D**). However, inhibition of endocytic trafficking with Ciliobrevin, abolished TFEB-mediated increase of autophagic flux (Figure 10.1.5.**6E** vs 10.1.5.**6D**), further underlining the importance of endocytic function in TFEB-mediated lysosomal signaling.

10.1.4. Discussion

I identified a novel role of TFEB in coordinating endocytic trafficking of essential components of the lysosomal nutrient sensing complex to mediate mTORC1 signaling, autophagy flux, and lysosomal biogenesis. TFEB induces expression of a number of core endocytic genes including Caveolin, Clathrin EEA1, Rab5, and others, which results in increased endocytic rates in baseline and amino acid starvation conditions (Figure 10.1.5.**1**, Table 1 and Appendix Table 2). TFEB-induced endocytic trafficking is required for proper assembly of the mTORC1-tethering complex on endosomes containing the amino acid transporter SLC38A9, RagD, and pAkt (Figure 10.1.5.**2**). Our collaborators recently showed that TFEB transcriptional activity is required for mTORC1 signaling (Di Malta et al., 2017); in particular, TFEB induces transcription of RagD to drive mTORC1 lysosomal tethering.

In this study, I expanded this model and showed that TFEB-induced endocytosis promotes trafficking of proteins required for tethering as well as activation of mTORC1, such as active pAkt that is required to phosphorylate and inactivate TSC2 (Figures 10.1.5.**2A-D**). TFEB-mediated endocytosis is critical for assembly and activation of mTORC1 during long-term starvation (Figure 10.1.5.**3**) and in the presence of nutrients (Figure 10.1.5.**4**), a necessary step in lysosomal reformation that drives lysosomal biogenesis. Previous studies showed that mTORC1 activation is driven by anterograde

shuttling of lysosomes to the periphery where plasma membrane-bound activators, including activated growth factor receptors, interact and activate mTORC1 (Korolchuk et al., 2011). Other studies suggested that autophagic flux is sufficient to reactivate mTORC1, while recent findings have shown that other factors contribute to mTORC1 reactivation (Rong et al., 2011, 2012; Yu et al., 2010). This project extended the current models by the requirement of TFEB-mediated endocytic trafficking of mTORC1 activators to the lysosome (Figure 10.1.5.**7**) in an autophagy-independent manner (Di Malta et al., 2017). Re-activation of mTORC1 during long periods of starvation is required for the induction of autophagic lysosome reformation and therefore lysosomal homeostasis (Chen and Yu, 2013; Rong et al., 2012; Yu et al., 2010; Zhang et al., 2016). I found that TFEB-triggered endocytosis is required for re-activation of mTORC1 and autophagy. Furthermore, my data propose a sequence of events driving lysosomal reformation: starvation-induced inhibition of mTORC1 promotes nuclear TFEB signaling that mediates formation of signaling endosomes to tether and activate mTORC1 and promote autophagy (Figure 10.1.5.**7**). Thus, TFEB functions as a coordinator of cellular endocytosis driving assembly of lysosomal nutrient sensing machinery that tethers and reactivates mTORC1 during starvation to autophagy.

10.1.5. Figures, Tables and Descriptions

10.1.5.1. Table 1, Figure 1

Gene Symbol	Gene Description	Chromosome	Endosomal related function
ACAP2	arf-GAP with coiled-coil, ANK repeat and PH	chr3	protein localization to endosome
AP1S2	AP-1 complex subunit sigma-2	chrX	post-Golgi vesicle-mediated transport
AP4M1	AP-4 complex subunit mu-1	chr7	Golgi to endosome transport
ARAP1	arf-GAP with Rho-GAP domain, ANK repeat and PH	chr11	small GTPase mediated signal transduction
ARFGEF2	brefeldin A-inhibited guanine	chr20	intracellular vesicular trafficking
ATP6V0B	V-type proton ATPase 21 kDa proteolipid subunit	chr1	transmembrane transport
ATP6V0D1	V-type proton ATPase subunit d 1	chr16	transmembrane transport
ATP6V0E1	V-type proton ATPase subunit e 1	chr5	transmembrane transport
ATP6V1A	V-type proton ATPase catalytic subunit A	chr3	transmembrane transport
ATP6V1C1	V-type proton ATPase subunit C 1	chr8	transmembrane transport
ATP6V1E1	V-type proton ATPase subunit E 1 isoform c	chr22	transmembrane transport
ATP6V1G1	V-type proton ATPase subunit G 1	chr9	transmembrane transport
ATP6V1H	V-type proton ATPase subunit H isoform 1	chr8	transmembrane transport
BLOC1S3	biogenesis of lysosome-related organelles	chr19	secretion of lysosomal enzymes
CHMP4A	charged multivesicular body protein 4A	chr14	endosomal transport
CLCN7	h(+)/Cl(-) exchange transporter 7 isoform b	chr16	chloride transmembrane transport
CLTA	clathrin light chain A isoform a	chr9	endocytosis
CLTC	clathrin heavy chain 1	chr17	receptor-mediated endocytosis
GIT2	G protein-coupled receptor kinase interacting	chr12	regulation of ARF GTPase activity
IGF2R	cation-independent mannose-6-phosphate receptor	chr6	receptor-mediated endocytosis
M6PR	cation-dependent mannose-6-phosphate receptor	chr12	endosome to lysosome transport
MCOLN1	mucolipin-1	chr19	transmembrane transport
MFSD1	major facilitator superfamily domain-containing	chr3	transmembrane transport
MTM1	myotubularin	chrX	endosome to lysosome transport
PDCD6IP	programmed cell death 6 interacting protein	chr3	binds to endophilins, proteins that regulate membrane shape during endocytosis
PICALM	phosphatidylinositol-binding clathrin assembly	chr11	receptor-mediated endocytosis
PIP4K2C	phosphatidylinositol-5-phosphate 4-kinase type-2	chr12	phosphatidylinositol metabolic process
PIP5K1A	phosphatidylinositol-4-phosphate 5-kinase type-1	chr1	phagocytosis
PLA2G6	85 kDa calcium-independent phospholipase A2	chr22	positive regulation of exocytosis
PPT1	palmitoyl-protein thioesterase 1 isoform 1	chr1	receptor-mediated endocytosis
RAB21	RAB21, member RAS oncogene family	chr12	protein transport
RAB5A	ras-related protein Rab-5A	chr3	endocytosis
RAB7A	ras-related protein Rab-7a	chr3	endosome to lysosome transport
RAB7L1	ras-related protein Rab-7L1 isoform 3	chr1	small GTPase mediated signal transduction
SLC36A1	proton-coupled amino acid transporter 1	chr5	transmembrane transport
SLC37A3	sugar phosphate exchanger 3 isoform 1	chr7	transmembrane transport
SNX13	sorting nexin-13	chr7	intracellular trafficking
SNX16	sorting nexin-16 isoform b	chr8	endosome to lysosome transport
SNX2	sorting nexin-2	chr5	endocytosis
SPG20	spartin	chr13	regulating endosomal trafficking
STX4	syntaxin 4	chr16	post-Golgi vesicle-mediated transport
STX6	syntaxin-6	chr1	retrograde transport, endosome to Golgi
SYNRG	synergin gamma isoform 4	chr17	intracellular protein transport
TOM1	target of myb1 membrane trafficking protein	chr22	endocytosis
TPP1	tripeptidyl-peptidase 1 preproprotein	chr11	proteolysis
VPS35	vacuolar protein sorting-associated protein 35	chr16	retrograde transport, endosome to Golgi

Table 1: Set of 46 endocytic genes directly regulated by TFEB

ChIP-seq (1Kb) analyses of stable HeLa cells overexpressing TFEB, as previously described by our collaborators in Palmieri et al (2011), showed that TFEB interacted with the promoter region of 46 genes involved in regulation and maintenance of cellular endocytosis.

1A.

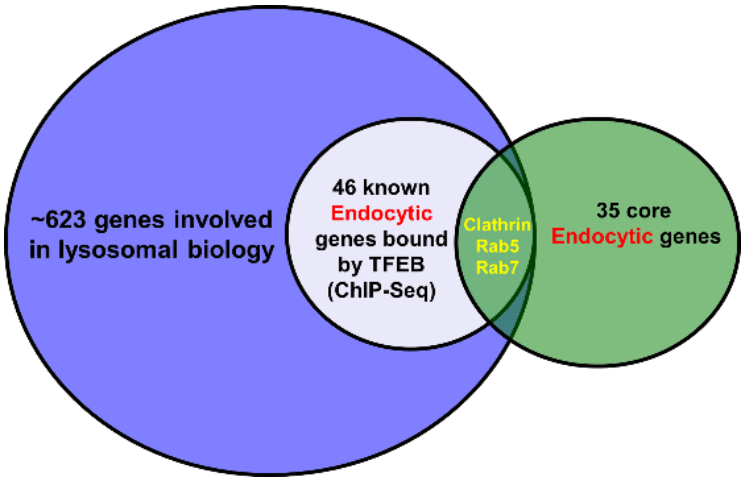

Putative endocytic genes induced by TFEB-GFP expression	ChIP-seq (-/+ 1Kb_TSS)
EEA-1	YES
CAV1-3	YES
CLTA	YES
EGFR	YES (position +968)
DBNL	YES (position -443)
OPA1	YES (position +147)
ELMO2	YES (position +213)
LRP12	YES (position +317)
see supplementary table 2	

Figure 1: TFEB regulates cellular endocytosis

TFEB interacted with the promoter regions of endocytic genes

1A. HeLa cells overexpressing TFEB were subjected to chromatin immunoprecipitation and DNA sequence analyses. The Venn diagram illustrates the relationship between the 46 endocytic genes identified in ChIP-seq. analyses, and subsequently confirmed by qPCR to be regulated by TFEB, and core putative endocytic genes that regulate endocytic processes. The Table below lists putative endocytic genes identified in the TFEB ChIP-Seq analyses. The full list of the 46-endocytic genes bound by TFEB is represented in the Table 1, while all 623 endocytic genes regulated by TFEB and identified in Lysoplex analyses (Di Fruscio et al., 2015) are listed in Table 2 (please see Appendices).

1B.

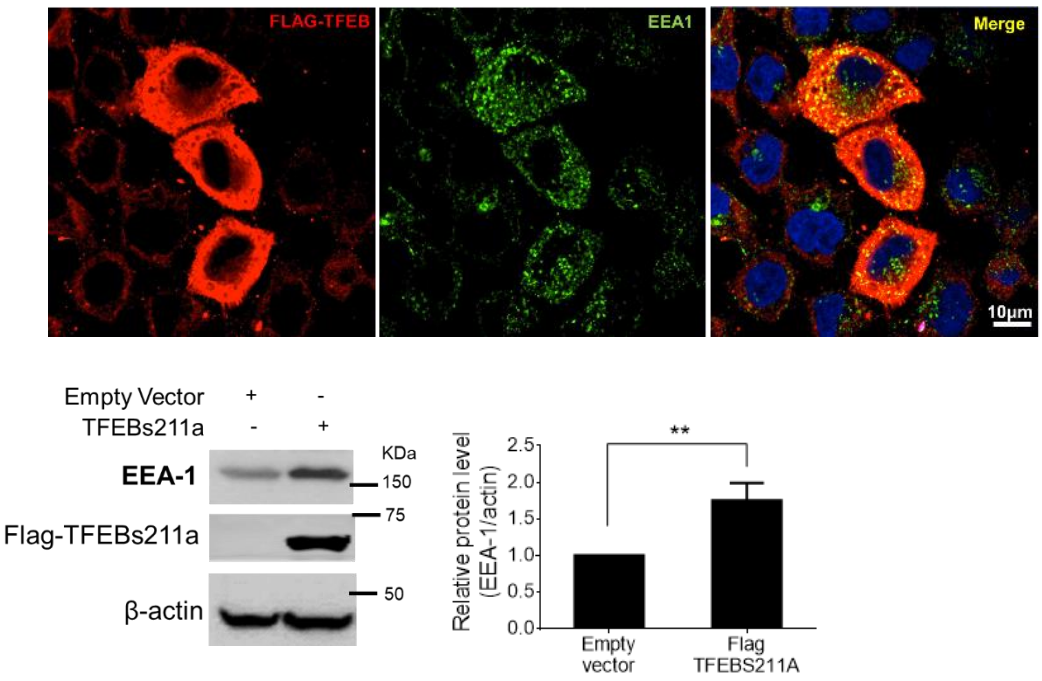

Figure 1: TFEB regulates cellular endocytosis

Protein level of early endosomal antigen-1 (EEA-1) increased dramatically in cells overexpressing TFEB

1B. Immunofluorescence images represent HeLa cells transiently transfected with FLAG-TFEB construct for 48 hours, and co-stained with anti-EEA-1(488) and anti-FLAG (596) antibodies. EEA-1 is a Rab5 GTPase effector protein whose role in the formation of early endosomes is indispensable. Cells overexpressing FLAG-TFEB showed a significant increase in the number of EEA-1 positive endosomes. EEA-1 puncta in FLAG-TFEB transfected versus un-transfected cells were counted using ImageJ plugin, and quantified using student'-t-test.

Immunoblots, quantified with ImageJ, represent experiments in which the constitutively active form of TFEB (s211a) was transiently overexpressed in HeLa cells for 48 hours followed by EEA-1 western blot analyses. EEA-1 protein level increased significantly in lysates of TFEBs211a overexpressing cells compared to those expressing an empty vector control. The inserted bar graph represents quantitative evaluation of relative EEA-1 protein levels from three independent experiments with replicates. The relative EEA-1 protein level was determined by normalizing EEA-1 levels to beta-actin levels. Data are represented as mean ± SEM, n = 3 independent experiments, $^{**}p \leq 0.01$; Student's t-test

1C.

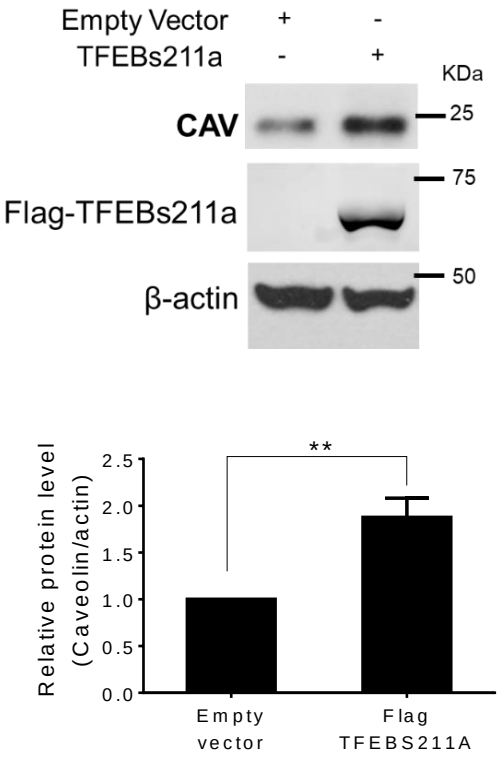
Empty Vector + -
TFEBs211a - +
KDa
CAV
25
75
Flag-TFEBs211a
β-actin
50
Relative protein level (Caveolin/actin)
2.5
2.0
1.5
1.0
0.5
0.0
**
Empty vector
Flag TFEBS211A

Figure 1: TFEB regulates cellular endocytosis

Caveolin protein levels increased in cells lysates of TFEBs211a-overexpressing cells

1C. HEK-293T cells were transiently transfected with TFEBs211a for 48 hours. The level of Caveolin proteins, which was detected by immunoblots, increased in TFEBs211a-overexpressing cells compared to those transfected with an empty vector.

Immunoblots were quantified in ImageJ and the relative protein levels were determined by normalizing Caveolin levels to beta-actin. Bar graph represents quantitative analyses of relative Caveolin protein levels and data are represented as mean ± SEM, n = 3 independent experiments with replicates, **p ≤ 0.01; Student's t-test

1D.

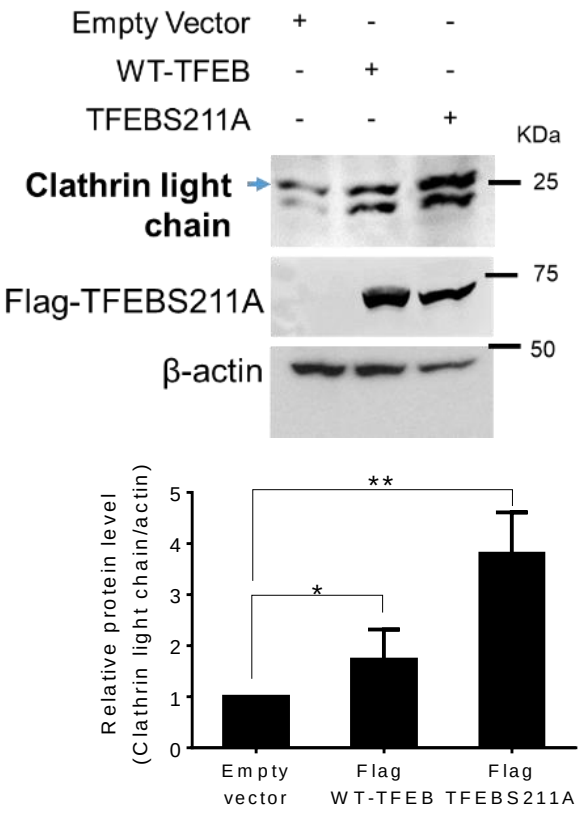
Empty Vector + - -
WT-TFEB - + -
TFEBS211A - - +
KDa
Clathrin light chain
25
Flag-TFEBS211A
75
β-actin
50
Relative protein level (Clathrin light chain/actin)
0
1
2
3
4
5
**
*
Empty vector
Flag WT-TFEB
Flag TFEBS211A

Figure 1: TFEB regulates cellular endocytosis

Clathrin Light Chain protein levels increased in cells lysates of TFEB-overexpressing cells

1D. HEK-293T cells were transiently transfected with TFEBs211a for 48 hours. The level of Clathrin Light Chain (CLC) proteins (upper bands), detected by immunoblots, increased in both WT-TFEB and TFEBs211a-overexpressing cells compared to those transfected with an empty vector.

Immunoblots were quantified in ImageJ and the relative CLC levels were determined by normalizing CLC levels to beta-actin. Bar graph represents quantitative analyses of relative protein levels. Data are represented as mean ± SEM, n = 3 independent experiments with replicates, **p ≤ 0.01; Student's t-test

1E.

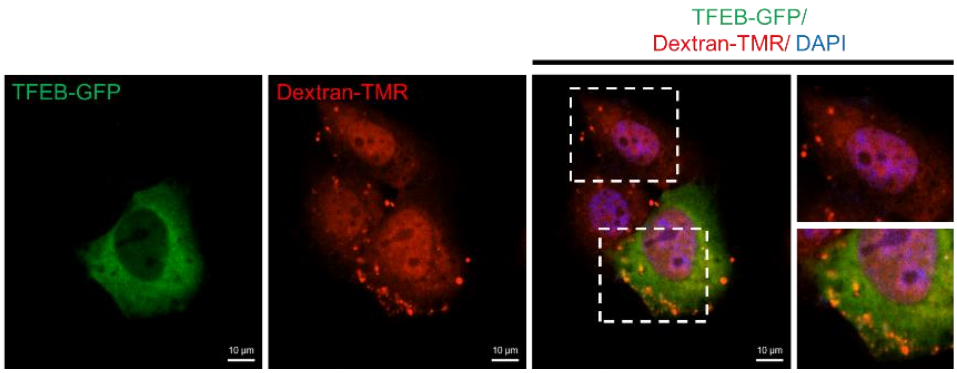
TFEB-GFP/
Dextran-TMR/ DAPI
TFEB-GFP
Dextran-TMR
10 µm
10 µm
10 µm

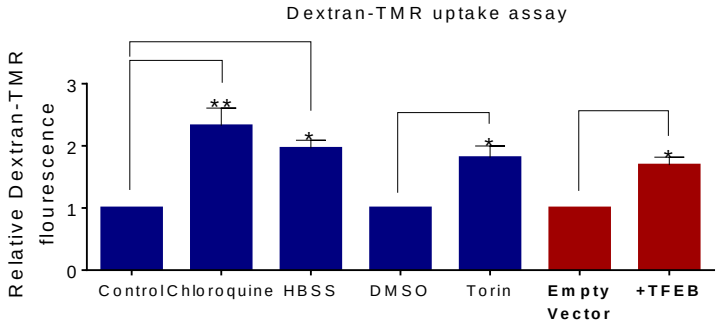
Dextran-TMR uptake assay
Relative Dextran-TMR flourescence
3
2
1
0
**
*
*
*
Control
Chloroquine
HBSS
DMSO
Torin
Empty Vector
+TFEB

Figure 1: TFEB regulates cellular endocytosis

Endocytosis-mediated uptake of Dextran-TMRhodamine increased in cells overexpressing TFEB

1E. HEK-293T cells transiently overexpressing TFEB-GFP for 48 hours were incubated in nutrient-rich medium containing Dextran-TMRhodamine for one hour in 37C after a 10-minute incubation on ice, followed by a 10-minute fixation with 4% paraformaldehyde and subjected to confocal microscopy analyses. Cells expressing TFEB-GFP showed increased number of Dextran-TMR-positive puncta compared to untransfected cells. Panels on the right show magnifications of the outlined areas in merged images. Bar graph represents quantitative Dextran-TMR uptake assays assessing Rhodamine fluorescence intensities in cells. Note that TFEB-overexpression, Chloroquine, Torin and Amino acid starvation potently increased Dextran-TMR uptake. Data are represented as mean ± SEM, n = 3 independent experiments with replicates, *$p \leq 0.05$; **$p \leq 0.01$; ANOVA (Tukey HSD post hoc test), Scale bar: 10μm.

1F.

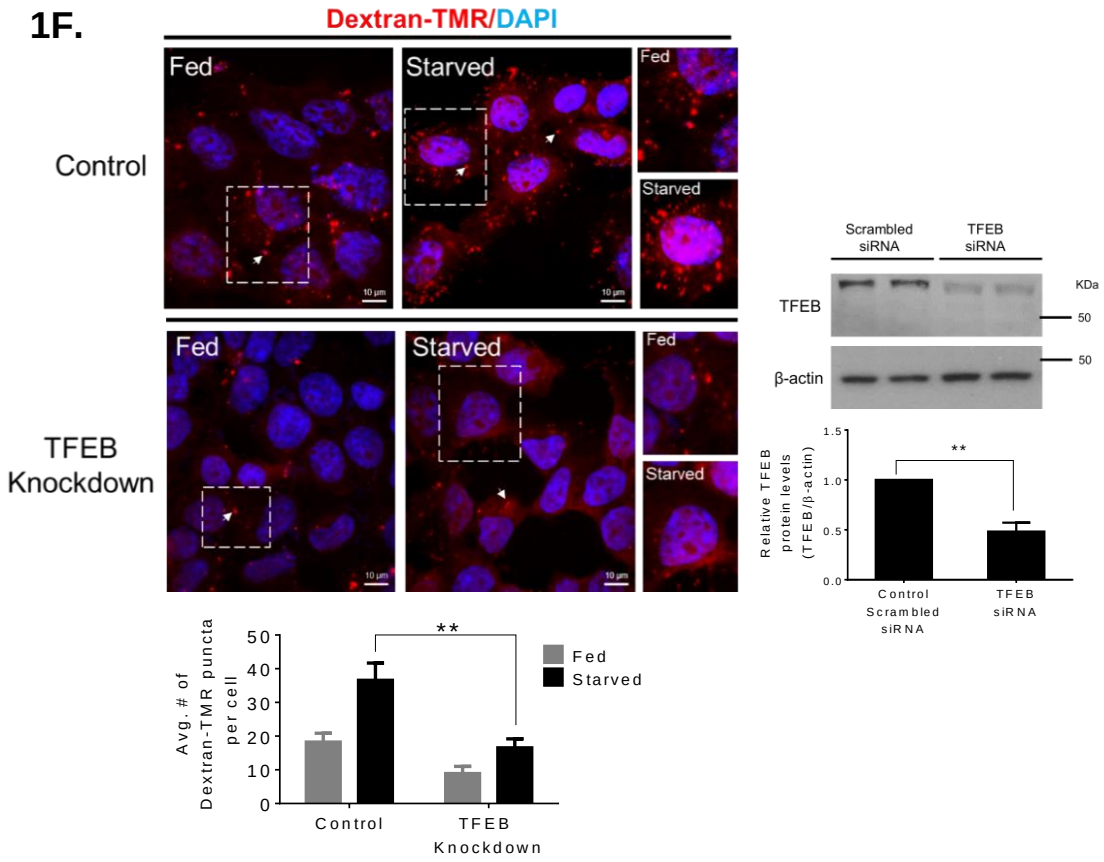
Dextran-TMR/DAPI
Control
TFEB Knockdown
Fed
Starved
Fed
Starved
Fed
Starved
Fed
Starved
10 μm
Scrambled siRNA
TFEB siRNA
KDa
TFEB
β-actin
50
50
Relative TFEB protein levels (TFEB/β-actin)
1.5
1.0
0.5
0.0
**
Control Scrambled siRNA
TFEB siRNA
Avg. # of Dextran-TMR puncta per cell
50
40
30
20
10
0
**
Fed
Starved
Control
TFEB Knockdown

Figure 1: TFEB regulates cellular endocytosis

Amino acid starvation-induced endocytosis of Dextran TMRhodamine in a TFEB-dependent manner

1F. Wild-type HEK-293T cells were incubated with either control non-targeting/scrambled siRNA or TFEB specific siRNA for 72 hours. TFEB deficient HEK-293T cells show lower rate of uptake compared to control cells, in both fed and amino acid-starved conditions. Panels on the right are magnifications of the outlined areas in images of fed or starved cells. Bar diagram represents quantitative assessment of Dextran-TMR uptake in control or TFEB-knockdown cells under fed or starved conditions (average number of Dextran-TMRhodamine puncta per cell in control vs. TFEB KD cells). Note that amino acid starvation increases endocytic Dextran-TMR uptake and is dependent on TFEB expression. Immunoblot analyses represent TFEB knockdown efficiency in HEK-293T cells. Bar graph represents quantitative evaluation of TFEB protein levels. Immunoblots were quantified in ImageJ. The relative protein levels were determined by normalizing TFEB protein levels to beta-actin.

Dextran-TMRhodamine puncta in control versus TFEB-KD cells were counted using ImageJ plugin, and quantified using student's t-test. Data are represented as mean ± SEM, n = 3 independent experiments with replicates, **p ≤ 0.01; Student's t-test, Scale bar: 10μm.

1G.

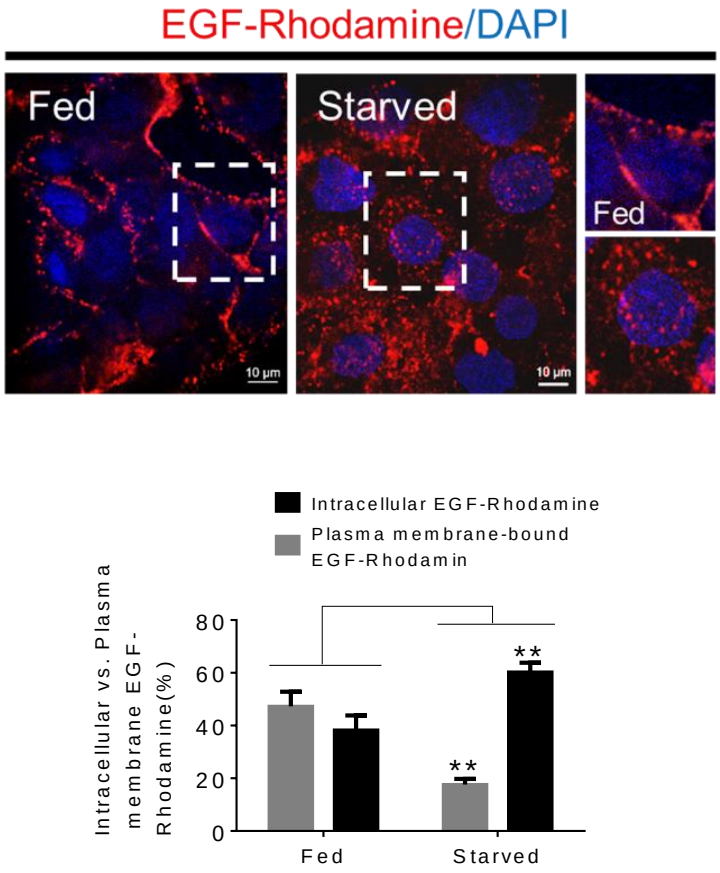
EGF-Rhodamine/DAPI
Fed
Starved
Fed
10 µm
10 µm
Intracellular EGF-Rhodamine
Plasma membrane-bound EGF-Rhodamin
Intracellular vs. Plasma membrane EGF-Rhodamine(%)
80
60
40
20
0
**
**
Fed
Starved

Figure 1: TFEB regulates cellular endocytosis

Plasma membrane-bound EGF-Rhodamine relocalized to the cytoplasm in cells incubated with amino acid deficient media

1G. WT-HEK-293T cells were incubated with either amino acid-deprived- or complete-media containing EGF-Rhodamine for 30 minutes in 37C after a 10-minute incubation on ice. Following a 10-minute fixation with 4% PFA, EGF-Rhodamine was visualized under a confocal microscope. Bar graph represents quantitative assessment of cells with intracellular vs. plasma membrane-bound EGF-Rhodamine. Data are represented as mean ± SEM, n = 3 independent experiments with replicates; **p ≤ 0.01; ANOVA, Scale bar: 10μm.

1H.

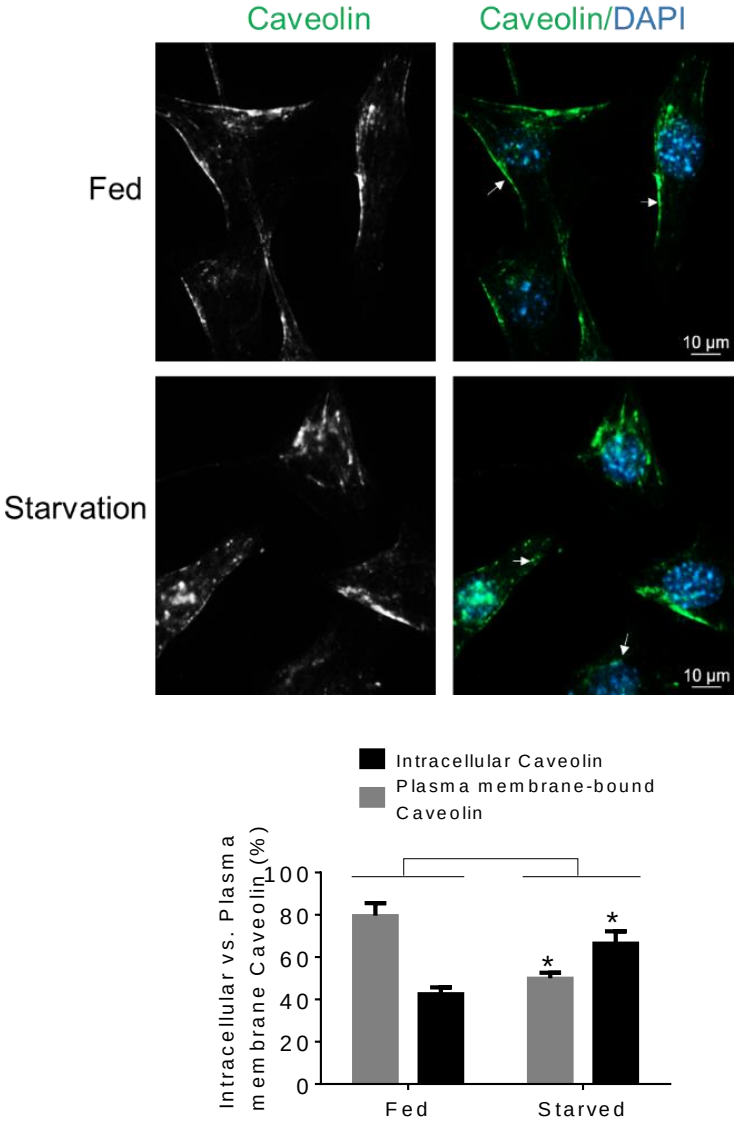
Caveolin
Caveolin/DAPI
Fed
Starvation
10 µm
10 µm
Intracellular Caveolin
Plasma membrane-bound Caveolin
Intracellular vs. Plasma membrane Caveolin (%)
100
80
60
40
20
0
*
*
Fed
Starved

Figure 1: TFEB regulates cellular endocytosis

Endogenous plasma membrane-bound Caveolin proteins relocalized to the cytoplasm of cells incubated with amino acid-deficient media

1H. WT-NIH-3T3 fibroblasts were cultured with either amino acid-deprived- or nutrient-rich media for 2 hours at 37C followed by immunofluorescence analyses of Caveolin protein. Plasma membrane-bound Caveolin relocalized to intracellular compartments upon starvation (compare magnified images of Fed vs. Starved cells. Bar graph represents quantitative assessment of cells with intracellular vs. plasma membrane-bound Caveolin proteins. Data are represented as mean ± SEM, n = 3 independent experiments with replicates; *p ≤ 0.05; student's t-test, Scale bar: 10μm.

1l.

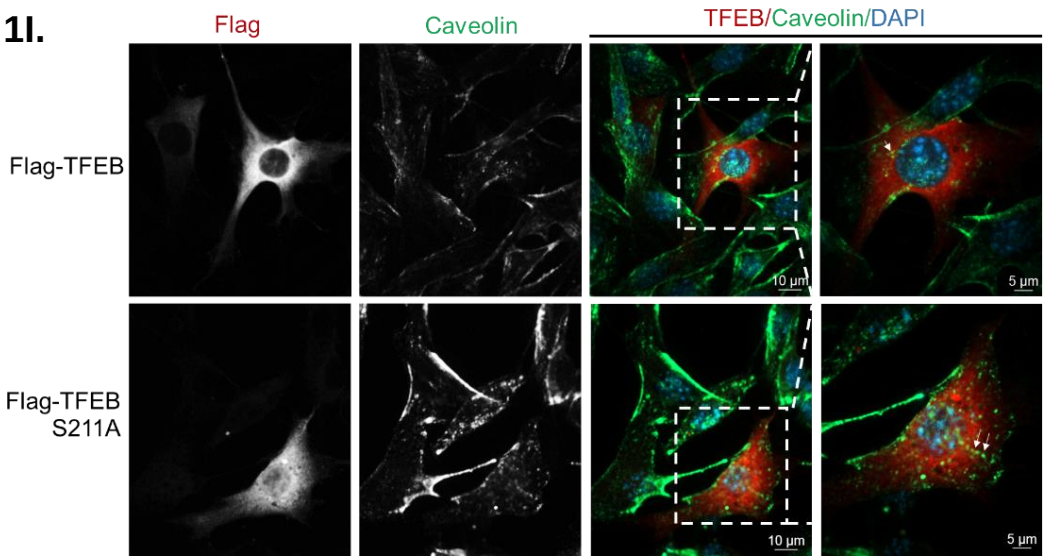
Flag
Caveolin
TFEB/Caveolin/DAPI
Flag-TFEB
Flag-TFEB S211A
10 µm
5 µm
10 µm
5 µm

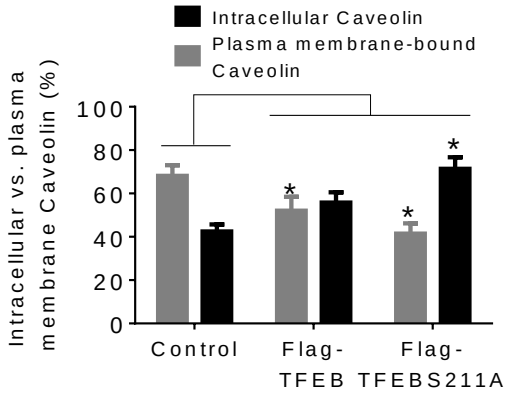
Intracellular Caveolin
Plasma membrane-bound Caveolin
Intracellular vs. plasma membrane Caveolin (%)
100
80
60
40
20
0
*
*
*
Control
Flag-TFEB
Flag-TFEBS211A

Figure 1: TFEB regulates cellular endocytosis

Endogenous plasma membrane-bound Caveolin proteins relocalized to the cytoplasm of cells overexpressing TFEB.

1I. Localization of endogenous Caveolin proteins in WT-NIH-3T3 fibroblasts transiently overexpressing TFEB-FLAG or TFEB-S211A-FLAG for 48 hours. Internalized Caveolin proteins were detected in TFEB overexpressing cells and compared to untransfected cells which had more plasma membrane-bound Caveolin. Panels on the right are magnifications of the outlined areas in merged images. Bar graph represents quantitative assessment of number of cells with intracellular vs. plasma membrane-bound Caveolin proteins. Data are represented as mean ± SEM, n = 3; *p ≤ 0.05; ANOVA followed by Tukey post hoc intergroup analyses, Scale bars: 10 μm and 5 μm.

1J.

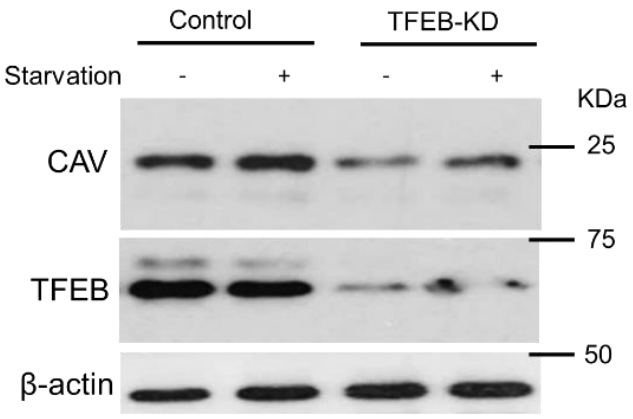
Control
TFEB-KD
Starvation
-
+
-
+
KDa
CAV
25
TFEB
75
β-actin
50

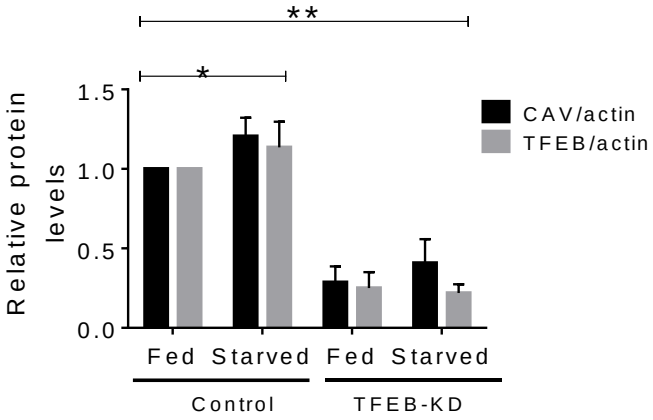
**
*
Relative protein levels
1.5
1.0
0.5
0.0
CAV/actin
TFEB/actin
Fed
Starved
Fed
Starved
Control
TFEB-KD

Figure 1: TFEB regulates cellular endocytosis

The level of endogenous Caveolin proteins increased in amino acid-starved cells in a TFEB-dependent manner

1J. HEK-293T cells were incubated with either control siRNA or TFEBsiRNA for 72 hours and subjected to amino acid starvation for 5 hours followed by immunoblot assessment of endogenous Caveolin protein levels. TFEB deficient and starved cells showed reduced level of endogenous Caveolin proteins compared to control cells. Bar graph represents quantitative analyses of relative protein levels. Data are represented as mean ± SEM, n = 3 independent experiments with replicates; *p ≤ 0.05; **p ≤ 0.01; ANOVA followed by Tukey post hoc analyses.

10.1.5.2. Figure 2

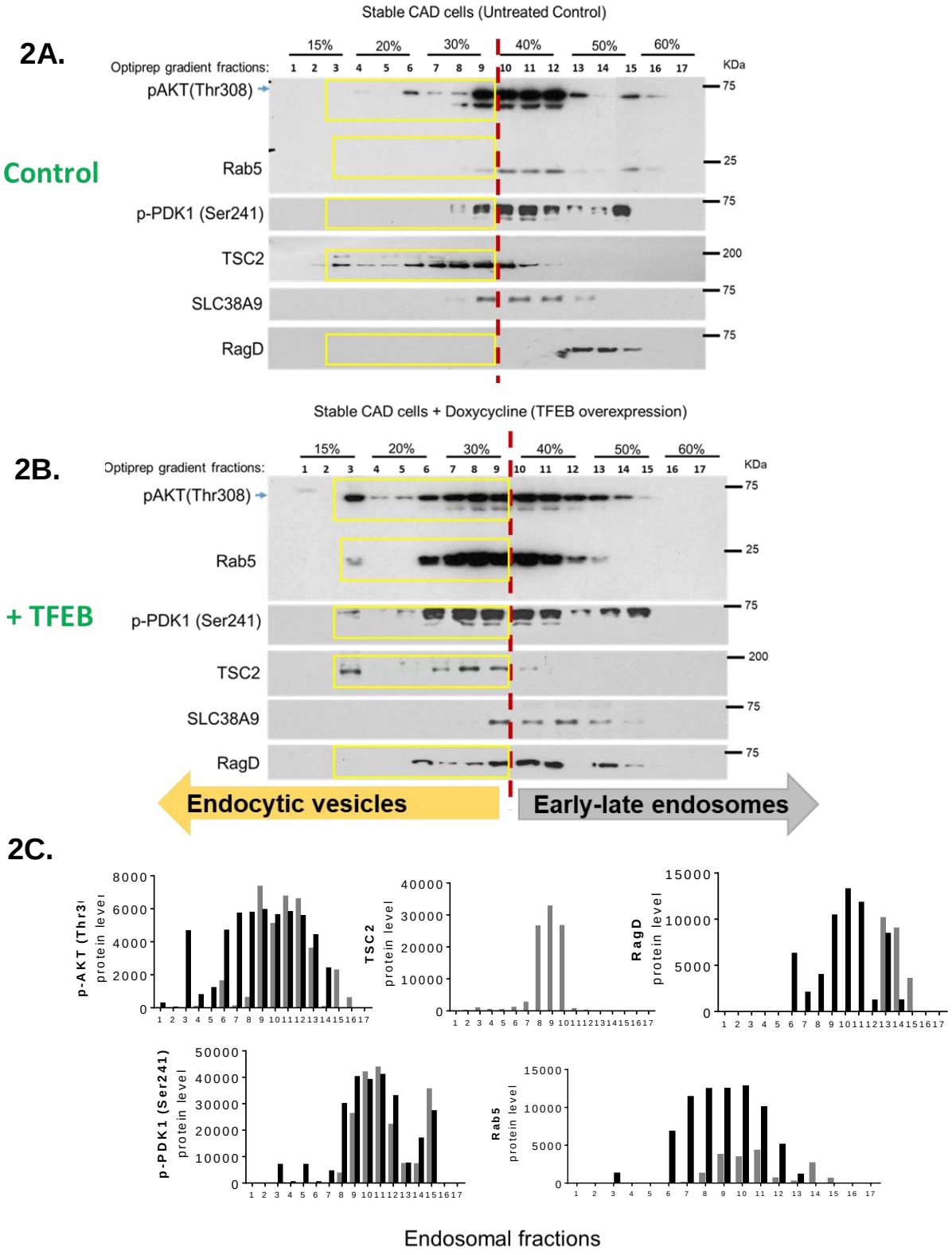

Figure 2: Overexpression of TFEB induces the formation of signaling endosomes to assemble the lysosomal nutrient-sensing complex.

The quantity of Rab5, pAkt (Thr308) and RagD in less-dense OptiPrep endosomal fractions increased with the overexpression of TFEB

(2A-2C) Stable CAD cells expressing a Doxycycline-inducible TFEB were treated with Doxycycline (Dox.) for 24 hours and subjected to endosomal fractionation. TFEB-overexpressing CAD cells showed increased quantity of Rab5-positive endosomes, endosomal phospho-Akt (Thr308), and the mTORC1 tethering molecule RagD in endosomal fractions (compare immunoblots of untreated control cells in 2A to Dox.-treated cells in 2B). Bar graphs in 2C represents protein levels in endosomal fractions of untreated versus Dox.-treated cells. Data are represented as mean ± SEM, n = 3 independent experiments without replicates; grey bars represent OptiPrep fractions of control CAD cells while black bars represent OptiPrep fractions of cells treated with doxycycline.

2D.

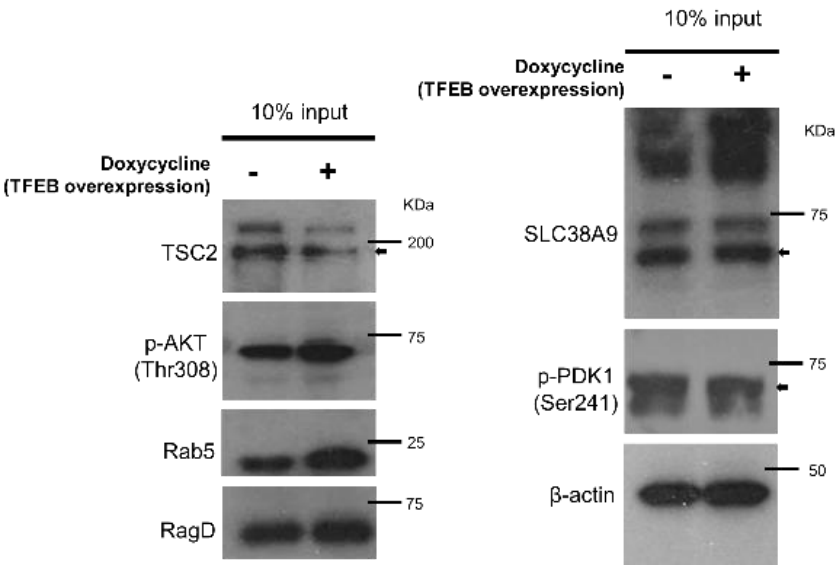
10% input
Doxycycline
(TFEB overexpression)
-
+
KDa
TSC2
200
p-AKT
(Thr308)
75
Rab5
25
RagD
75
10% input
Doxycycline
(TFEB overexpression)
-
+
KDa
SLC38A9
75
p-PDK1
(Ser241)
75
β-actin
50

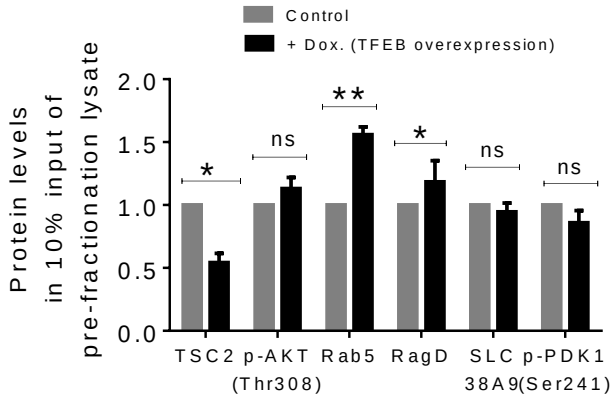
Control
+ Dox. (TFEB overexpression)
Protein levels
in 10% input of
pre-fractionation lysate
2.0
1.5
1.0
0.5
0.0
*
ns
**
*
ns
ns
TSC2
p-AKT
(Thr308)
Rab5
RagD
SLC
38A9
p-PDK1
(Ser241)

Figure 2: Overexpression of TFEB induces the formation of signaling endosomes to assemble the lysosomal nutrient-sensing complex.

Protein levels of Rab5 and RagD increased, while TSC2 protein levels decreased in 10% input of pre-fractionated lysates.

2D. 10% input of pre-fractionated lysates from control and Dox.-treated CAD cells were analyzed by immunoblot. Dox.-treated CAD cells showed increased levels of Rab5 and RagD proteins compared to the control. Protein levels of the Rheb-GTPase inhibitor TSC2 are significantly decreased in TFEB-expressing cells. Bar graph represents quantitative analyses of relative protein levels in 10% input of pre-fractionated lysates. Data are represented as mean ± SEM, n = 3 independent experiments, *$p \leq 0.05$; **$p \leq 0.01$; ANOVA followed by Tukey post hoc analyses.

2E.

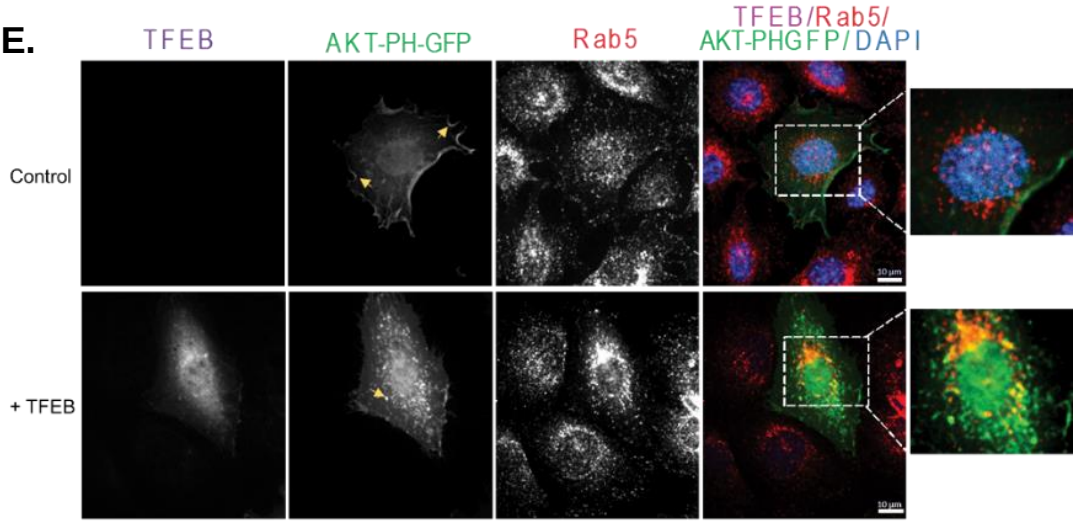
TFEB
AKT-PH-GFP
Rab5
TFEB/Rab5/
AKT-PHGFP/DAPI
Control
+ TFEB

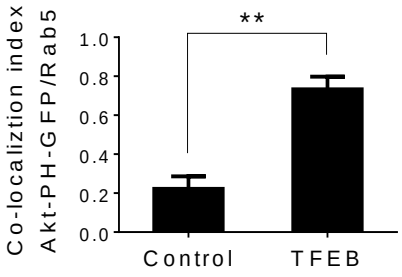
Co-localiztion index
Akt-PH-GFP/Rab5
**
1.0
0.8
0.6
0.4
0.2
0.0
Control
TFEB

Figure 2: Overexpression of TFEB induces the formation of signaling endosomes to assemble the lysosomal nutrient-sensing complex.

Active Akt relocalized to early endosomal compartments in TFEB overexpressing cells

2E. NIH-3T3 fibroblasts were transiently co-transfected with FLAG-TFEB and Akt-PH-GFP for 24 hours followed by immunostaining of early endosomes with anti-Rab5 antibody. The otherwise plasma membrane-bounded or cytoplasmic bioprobe Akt-PH-GFP relocalized to Rab5-positive endosomes in TFEB overexpressing fibroblasts, indicating an increase in phosphatidylinositol-3-phosphate (PI3P) levels and activation of Akt. Bar graph represent quantitative evaluation of Akt-PH-GFP co-localization with Rab5. Analyses of co-localization was done with ImageJ Coloc2 plugin and co-localization data analyzed in excel. Data are represented as mean ± SEM, n = 3 independent experiments, **p ≤ 0.01; student's t-test; Scale bar: 10μm

2F.

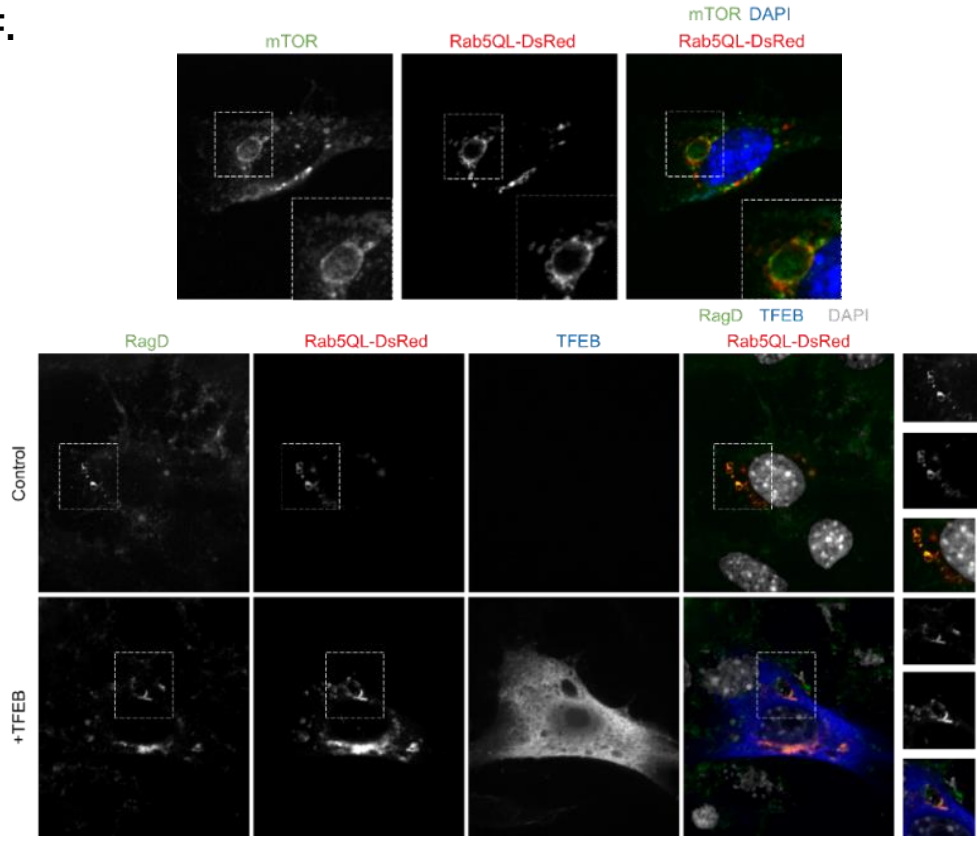
mTOR
Rab5QL-DsRed
mTOR DAPI
Rab5QL-DsRed
RagD
Rab5QL-DsRed
TFEB
RagD TFEB DAPI
Rab5QL-DsRed
Control
+TFEB

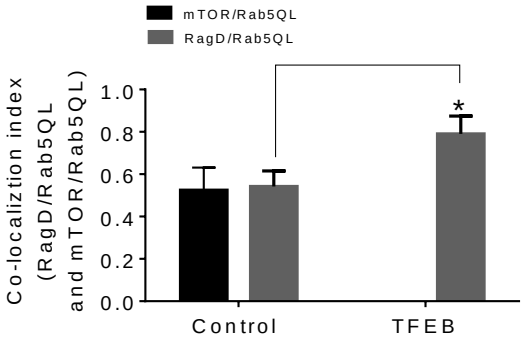
mTOR/Rab5QL
RagD/Rab5QL
Co-localiztion index
(RagD/Rab5QL
and mTOR/Rab5QL)
1.0
0.8
0.6
0.4
0.2
0.0
*
Control
TFEB

Figure 2: Overexpression of TFEB induces the formation of signaling endosomes to assemble the lysosomal nutrient-sensing complex.

mTOR and RagD colocalized with early endosomal membranes in TFEB-overexpressing cells

2F. NIH-3T3 fibroblasts were transiently co-transfected with FLAG-TFEB and Rab5QL-DsRed for 24 hours followed by anti-mTOR and anti-RagD immunostaining. Localization of the endogenous mTOR kinase and its tethering molecule RagD to Rab5QL-positive endosomes increased with expression of TFEB-FLAG. Bar graph represents quantitative evaluation of mTOR or RagD co-localization with Rab5QL-DsRed endosomes carried out with Coloc2 plugin in ImageJ. Scale bar: 10μm. Data are represented as mean ± SEM, n = 3 independent experiments without replicates, *p ≤ 0.05; student's t-test

2G.

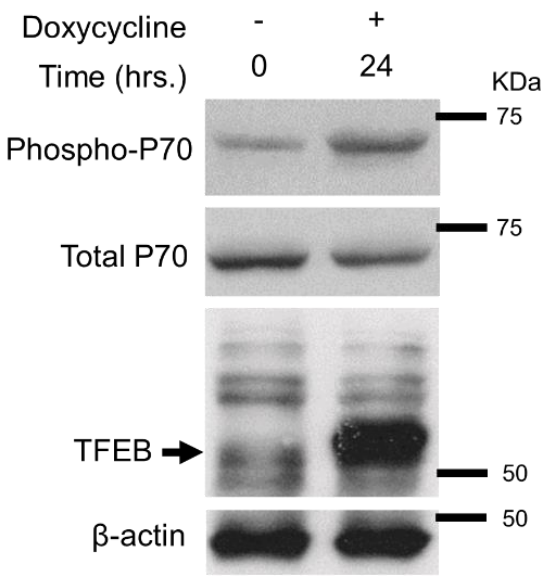
Doxycycline
-
+
Time (hrs.)
0
24
KDa
Phospho-P70
75
Total P70
75
TFEB
50
β-actin
50

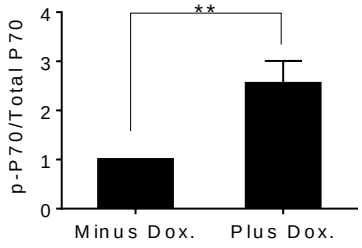
**
p-P70/Total P70
4
3
2
1
0
Minus Dox.
Plus Dox.

Figure 2: Overexpression of TFEB induces the formation of signaling endosomes to assemble the lysosomal nutrient-sensing complex.

Quantity of phospho-P70 proteins, indicative of active mTORC1 signaling, increased in stable CAD cells incubated with doxycycline for 24 hours.

2G. Stable CAD cells expressing doxycycline-inducible FLAG-TFEB were incubated with nutrient-rich media ± Doxycycline for 24 hours. mTORC1 activity was then assessed by phospho-P70/total P70 immunoblots. Bar graph represents relative protein levels of p-P70. Data are represented as mean ± SEM, n = 3 independent experiments with replicates, **p ≤ 0.01; student's t-test.

2H.

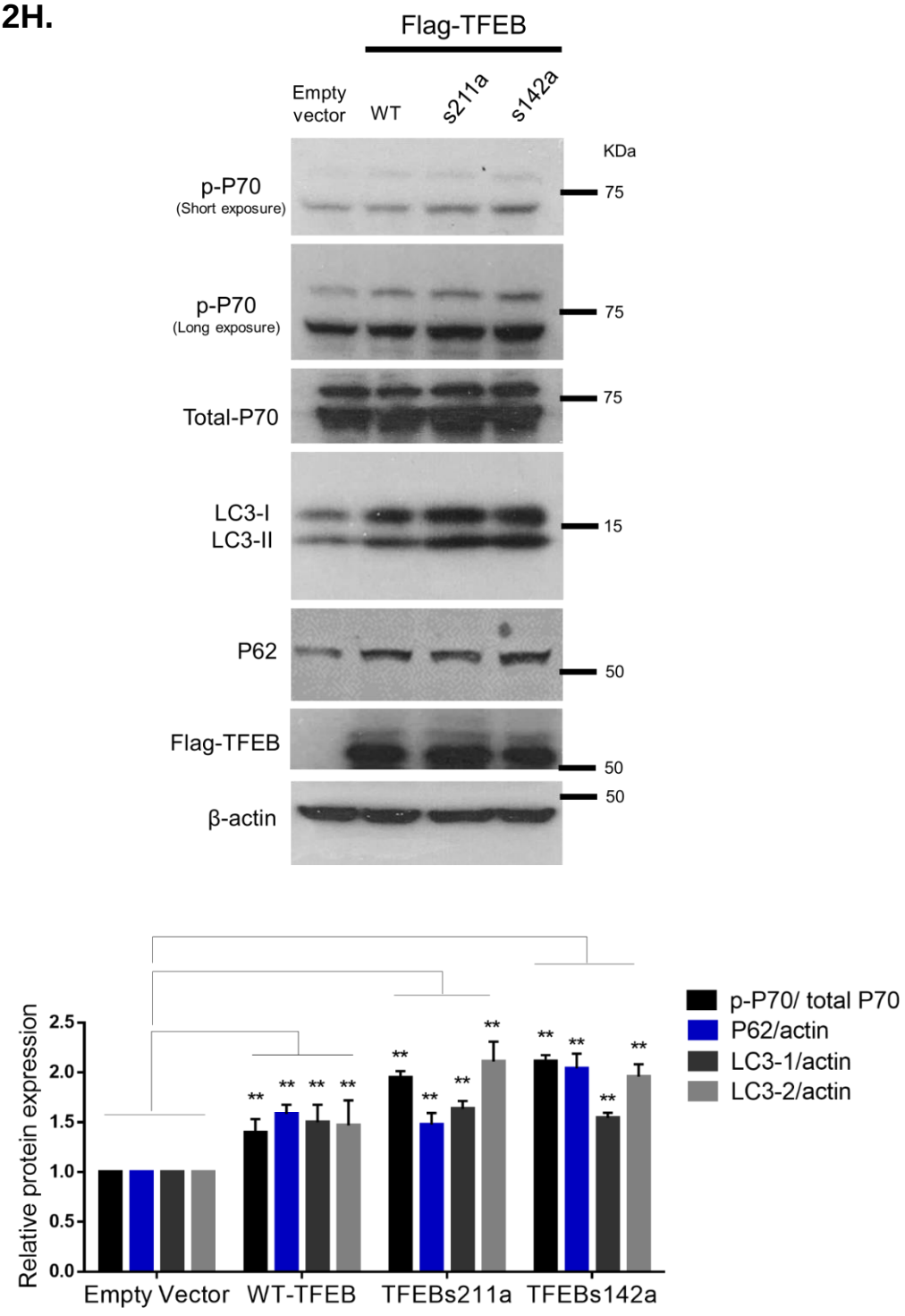
Flag-TFEB
Empty vector
WT
s211a
s142a
KDa
p-P70 (Short exposure)
p-P70 (Long exposure)
Total-P70
LC3-I
LC3-II
P62
Flag-TFEB
β-actin
75
75
75
15
50
50
50
Relative protein expression
2.5
2.0
1.5
1.0
0.5
0.0
Empty Vector
WT-TFEB
TFEBs211a
TFEBs142a
p-P70/ total P70
P62/actin
LC3-1/actin
LC3-2/actin

Figure 2: Overexpression of TFEB induces the formation of signaling endosomes to assemble the lysosomal nutrient-sensing complex.

TFEB overexpression induced autophagy and increased mTORC1 activity in fed HEK-293T cells

2H. 48 hour-transient overexpression of WT-TFEB-FLAG or its constitutively active mutants, TFEB-S211A-FLAG/TFEB-S142A-FLAG increased mTORC1 activity and increased the protein levels of autophagy markers in HEK-293T cells. Lysates of HEK-293T cells transiently overexpressing TFEB for 48 hours were collected and analyzed by immunoblot for mTORC1 activity represented by phospho-P70 immunoblots, induction of autophagy represented by LC3 and P62 immunoblots. Bar graph represents relative protein levels of p-P70, P62 and LC3-I and LC3-II. Data are represented as mean ± SEM, n = 3 independent experiments with replicates, **p ≤ 0.01; ANOVA followed by Tukey post hoc intergroup comparisons.

10.1.5.3. Figure 3

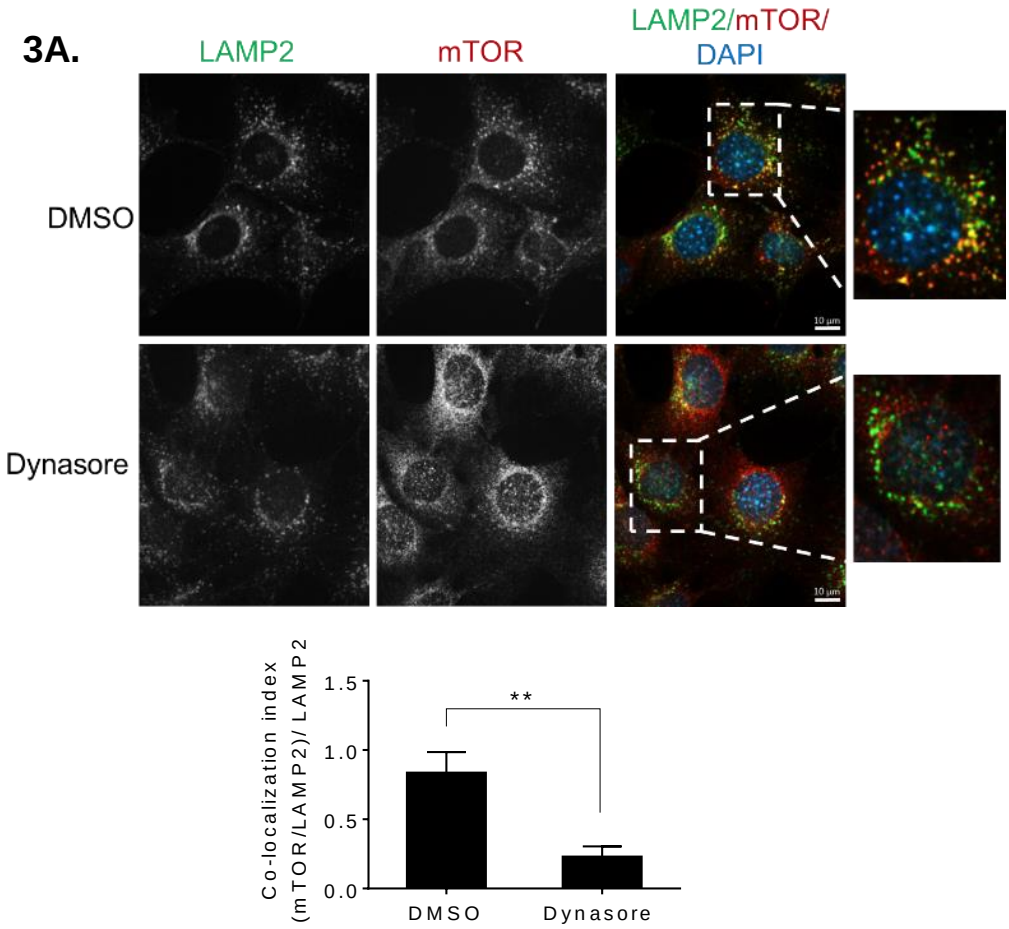

Figure 3: Endocytic trafficking controls mTOR tethering and signaling.

Lysosome-bound mTOR relocalized to the cytosol of cells incubated with Dynasore drug

3A. WT-NIH3T3 fibroblasts were incubated in complete media containing [80µM] Hydroxyl-Dynasore for 4 hours followed by co-localization analyses of mTOR with lysosomal LAMP2 protein. Dynasore-mediated inhibition of Dynamin GTPase dispersed mTOR into the cytosol. Panels on the right are magnifications of the outlined areas in merged images Bar graph represents quantitative evaluation of lysosomal mTORC1. Data are represented as mean ± SEM, n = 3 independent experiments with replicates, **p ≤ 0.01; student's t-test, Scale bar: 10µm.

3B.

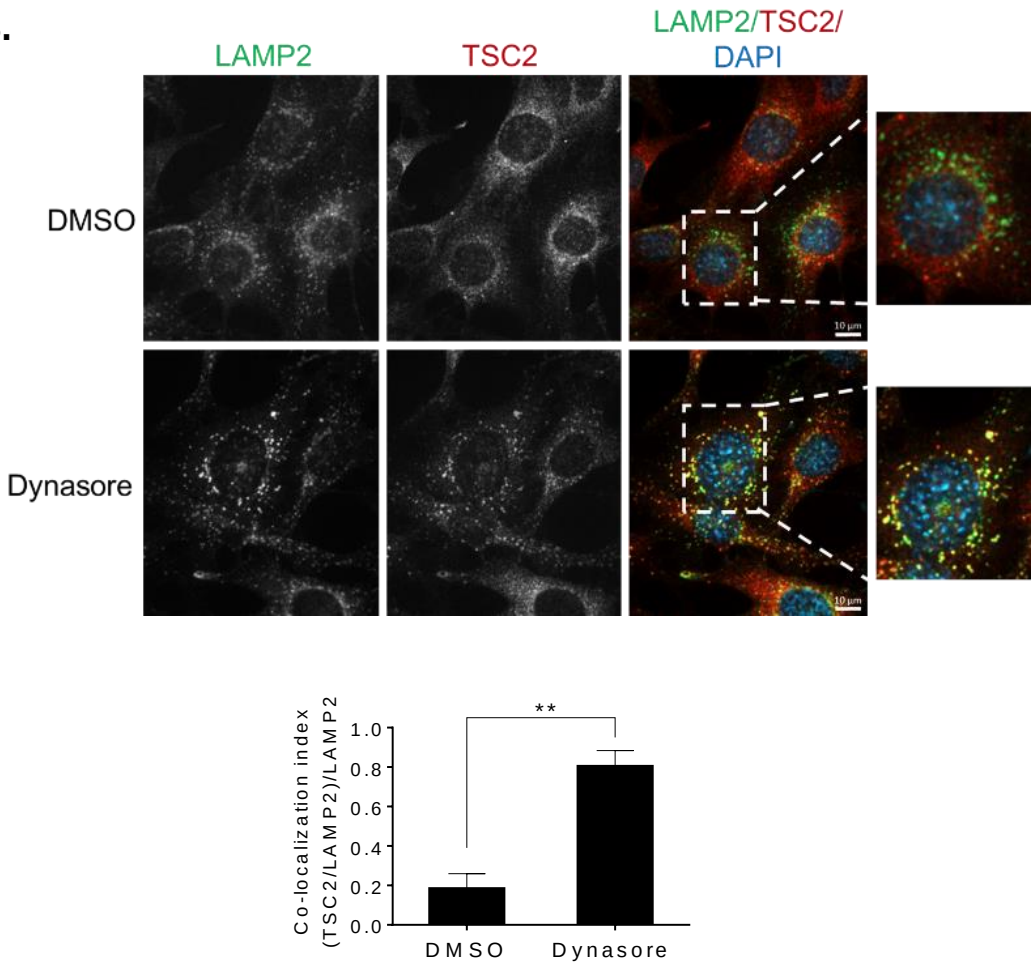
LAMP2
TSC2
LAMP2/TSC2/
DAPI
DMSO
Dynasore
10 μm
10 μm
Co-localization index
(TSC2/LAMP2)/LAMP2
1.0
0.8
0.6
0.4
0.2
0.0
**
DMSO
Dynasore

Figure 3: Endocytic trafficking controls TSC2 tethering and signaling.

Cytosolic TSC2 proteins relocalized to lysosomal membranes in cells incubated with Dynasore

3B. WT-NIH3T3 fibroblasts were incubated in complete media containing [80µM] Hydroxyl-Dynasore for 4 hours followed by co-localization analyses of TSC2 with lysosomal LAMP2 protein. Dynasore-mediated inhibition of Dynamin GTPase caused the re-tethering of TSC2 to lysosomal membranes. Panels on the right are magnifications of the outlined areas in merged images Bar graph represents quantitative evaluation of lysosomal TSC2. Data are represented as mean ± SEM, n = 3 independent experiments with replicates, **p ≤ 0.01; student's t-test, Scale bar: 10µm.

3C.

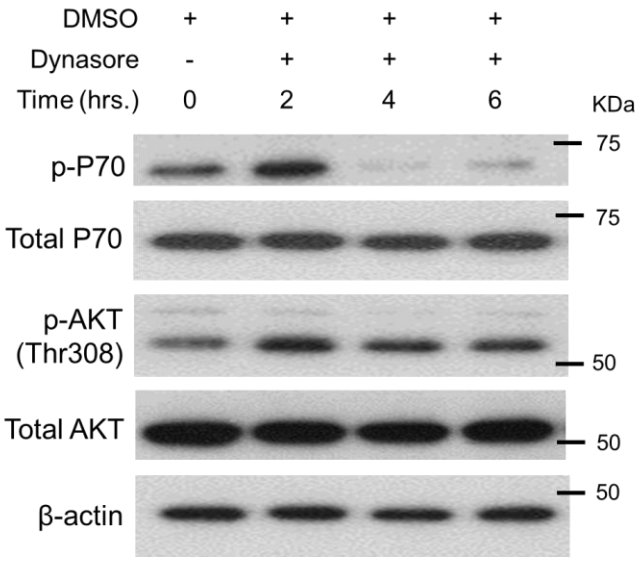
DMSO + + + +
Dynasore - + + +
Time (hrs.) 0 2 4 6
KDa
p-P70
75
Total P70
75
p-AKT (Thr308)
50
Total AKT
50
β-actin
50

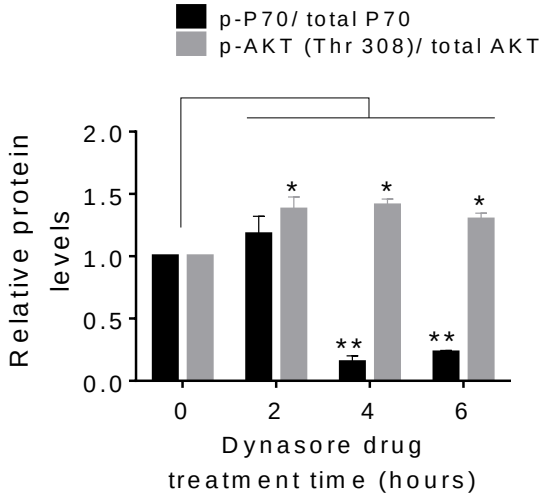
p-P70/ total P70
p-AKT (Thr 308)/ total AKT
Relative protein levels
2.0
1.5
1.0
0.5
0.0
*
*
*
**
**
0
2
4
6
Dynasore drug treatment time (hours)

Figure 3: Endocytic trafficking controls mTORC1 tethering and signaling.

Dynasore treatment attenuates mTORC1 signaling

3C. WT-NIH3T3 fibroblasts were incubated in complete media containing [80μM] Hydroxyl-Dynasore for the indicated time points. Dynasore treatment inhibits mTORC1 activity under fed conditions and has no significant effect on relative phospho-Akt (Thr308) protein levels. Bar graph represents quantitative analysis of relative protein levels of phospho-P70 and phospho-Akt (Thr308). Data are represented as mean ± SEM, n = 3 independent experiments with replicates, *p ≤ 0.05, **p ≤ 0.01; student's t-test.

3D.

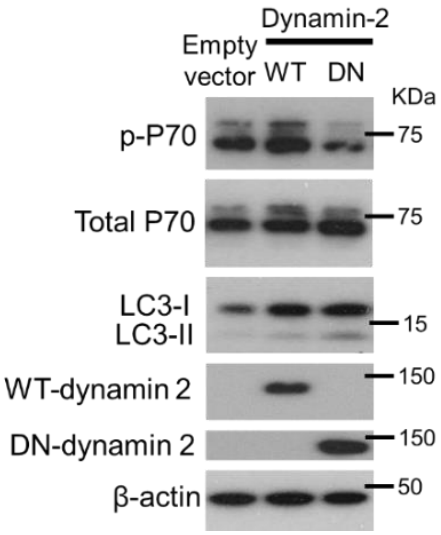
Dynamin-2
Empty vector
WT
DN
KDa
p-P70
75
Total P70
75
LC3-I
LC3-II
15
WT-dynamin 2
150
DN-dynamin 2
150
β-actin
50

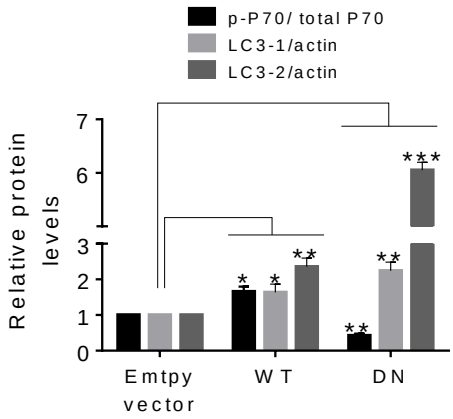
p-P70/ total P70
LC3-1/actin
LC3-2/actin
Relative protein levels
0
1
2
3
6
7
Emtpy vector
WT
DN

Figure 3: Endocytic trafficking controls mTORC1 tethering and signaling.

Genetic Inhibition of Dynamin-mediated endocytosis attenuates mTORC1 signaling

3D. Lysates of HEK-293T cells transiently expressing either WT-Dynamin2 or dominant negative Dynamin2 (DYN-2-K44A) for 48 hours were analyzed for mTORC1 activity and induction of autophagy via p-P70 and LC3 immunoblots respectively. Competitive inhibition of Dynamin-2 with DYN-2-K44A reduced mTORC1 activity while overexpression of the wild-type form increased mTORC1 signaling in HEK-293T cells. Increasing LC3 II level indicative of autophagy induction and buildup of autophagosomes were observed in DYN2-K44A overexpressing cells. Bar graph represents the quantitative analyses of relative protein levels of phospho-P70, LC3-1 and 2. Data are represented as mean ± SEM, n = 3 independent experiments with replicates, *p ≤ 0.05; **p ≤ 0.01; ***p ≤ 0.001; students t-test.

3E.

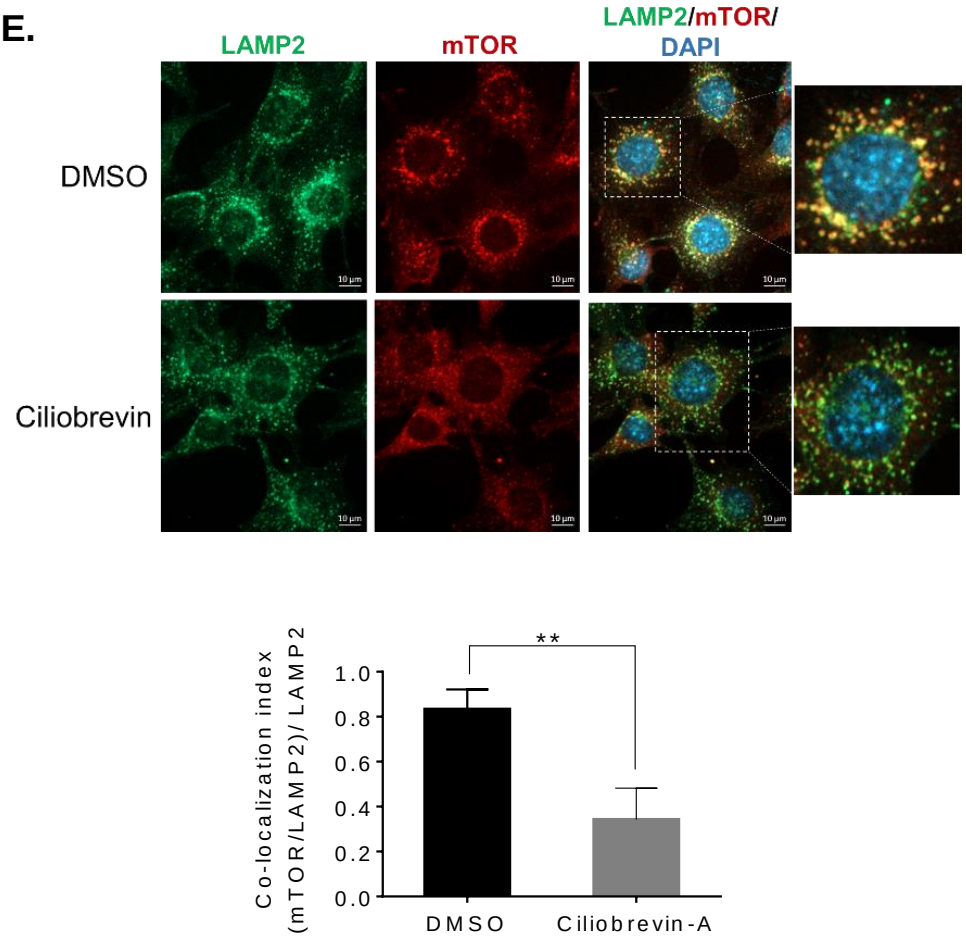
LAMP2
mTOR
LAMP2/mTOR/
DAPI
DMSO
Ciliobrevin
10 µm

Co-localization index
(mTOR/LAMP2)/ LAMP2
**
1.0
0.8
0.6
0.4
0.2
0.0
DMSO
Ciliobrevin-A

Figure 3: Endocytic trafficking controls mTORC1 tethering and signaling.

Inhibition of Dynein mediated retrograde trafficking leads to relocalization of mTORC1

3E. WT-NIH3T3 fibroblasts were incubated in complete media containing [100µM] Ciliobrevin-A for 2 hours followed by co-localization analyses of mTOR with lysosomal LAMP2 protein. Ciliobrevin-A-mediated inhibition of Dynein activity dispersed mTOR into the cytosol. Panels on the right are magnifications of the outlined areas in merged images Bar graph represents quantitative evaluation of lysosomal mTORC1. Data are represented as mean ± SEM, n = 3 independent experiments with replicates, **p ≤ 0.01; student's t-test, Scale bar: 10µm.

3F.

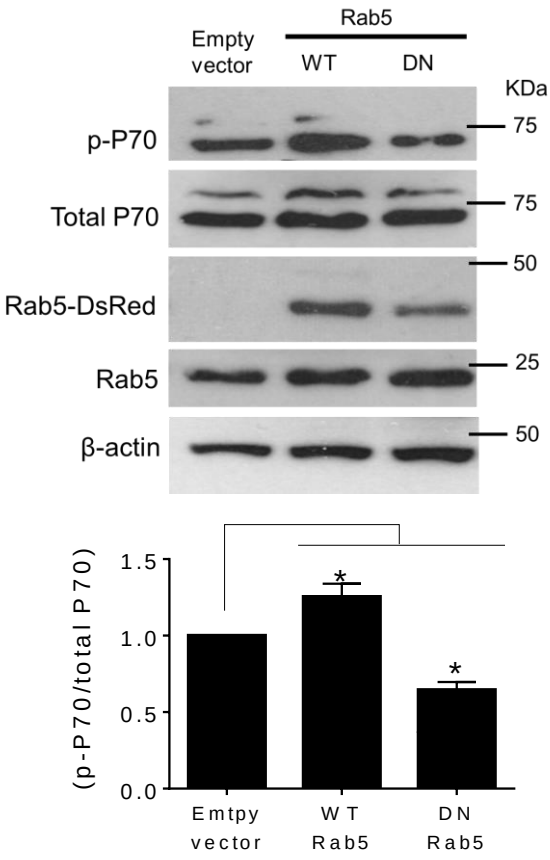
Rab5
Empty vector
WT
DN
KDa
p-P70
Total P70
Rab5-DsRed
Rab5
β-actin
75
75
50
25
50
(p-P70/total P70)
1.5
1.0
0.5
0.0
*
*
Emtpy vector
WT Rab5
DN Rab5

Figure 3: Endocytic trafficking controls mTORC1 tethering and signaling.

Competitive Inhibition of early endosomal biogenesis attenuates mTORC1 signaling

3F. Lysates of HEK-293T cells transiently expressing either WT-Rab5 or dominant negative Rab5 for 48 hours were collected and analyzed for mTORC1 activity and induction of autophagy via p-P70 immunoblots. mTORC1 activity was significantly lower in cells expressing DN-Rab5 while increased mTORC1 signaling was seen in cells transiently expressing WT-Rab5 cells. Bar graph represents the quantitative analyses of relative protein levels of phospho-P70 normalized to total P70. Data are represented as mean ± SEM, n = 3 independent experiments with replicates, *p ≤ 0.05; ANOVA followed by Scheffe post hoc test.

3G.

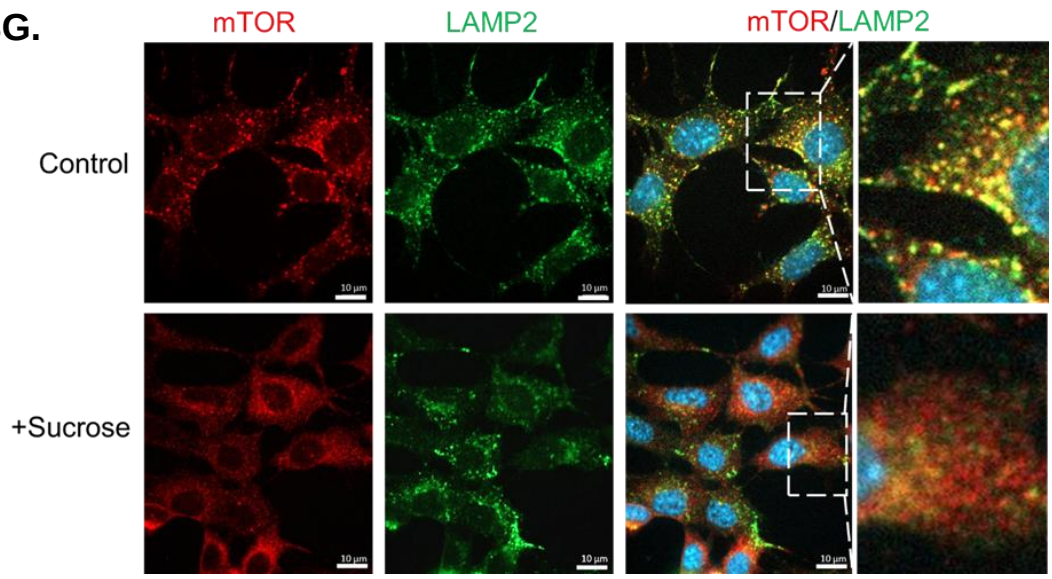
mTOR
LAMP2
mTOR/LAMP2
Control
+Sucrose
10 µm

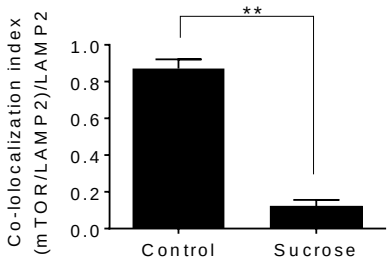
**
Co-lolocalization index
(mTOR/LAMP2)/LAMP2
1.0
0.8
0.6
0.4
0.2
0.0
Control
Sucrose

Figure 3: Endocytic trafficking controls mTORC1 tethering and signaling.

Inhibition of general endocytosis with hypertonic sucrose medium leads to relocalization of mTORC1

3G. WT-NIH3T3 fibroblasts were incubated in complete medium containing 0.45M sucrose for 1 hour followed by co-localization analyses of mTOR with lysosomal LAMP2 protein. Hypertonic sucrose media dispersed mTORC1 into the cytosol. Panels on the right are magnifications of the outlined areas in merged images. Bar graph represents quantitative evaluation of lysosomal mTOR. Data are represented as mean ± SEM, n = 3 independent experiments, **p ≤ 0.01; student's t-test, Scale bar: 10μm.

3H.

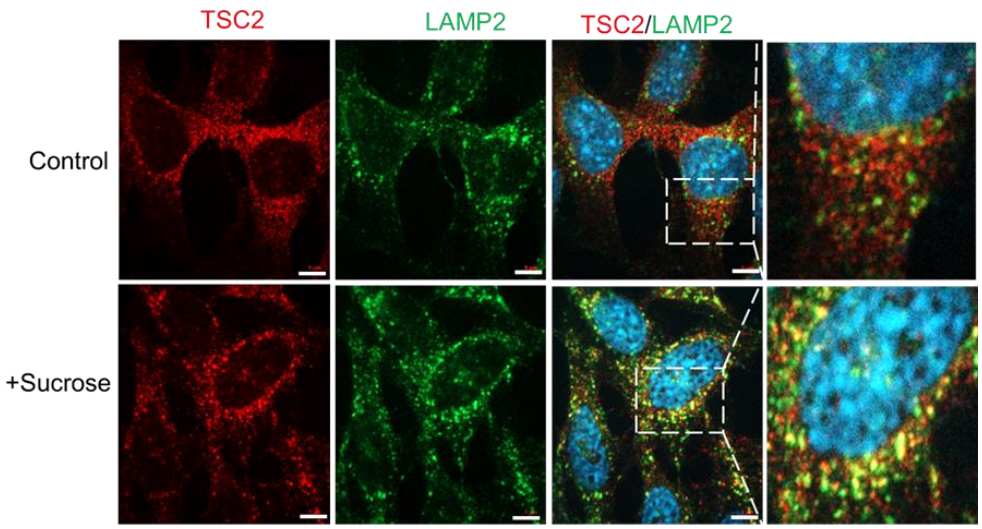
TSC2
LAMP2
TSC2/LAMP2
Control
+Sucrose

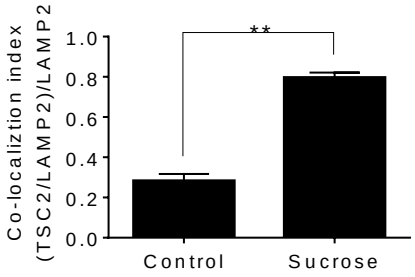
Co-localiztion index (TSC2/LAMP2)/LAMP2
1.0
0.8
0.6
0.4
0.2
0.0
**
Control
Sucrose

Figure 3: Endocytic trafficking controls mTORC1 tethering and signaling.

Inhibition of general endocytosis with hypertonic sucrose medium leads to relocalization of TSC2

3H. WT-NIH3T3 fibroblasts were incubated in complete medium containing 0.45M sucrose for 1 hour followed by co-localization analyses of TSC2 with lysosomal LAMP2 protein. Hypertonic sucrose media relocalized TSC2 to lysosomal membranes. Panels on the right are magnifications of the outlined areas in merged images. Bar graph represents quantitative evaluation of lysosomal TSC2. Data presented as mean ± SEM, n = 3 independent experiments, **p ≤ 0.01; student's t-test, Scale bar: 10μm.

3I.

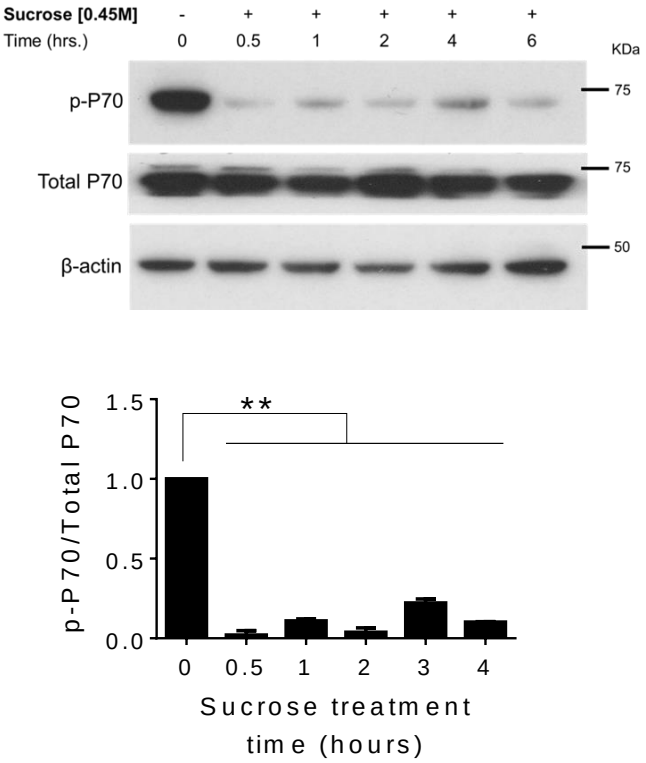
Sucrose [0.45M] - + + + + +
Time (hrs.) 0 0.5 1 2 4 6
KDa
p-P70
75
Total P70
75
β-actin
50
p-P70/Total P70
1.5
1.0
0.5
0.0
**
0 0.5 1 2 3 4
Sucrose treatment time (hours)

Figure 3: Endocytic trafficking controls mTORC1 tethering and signaling.

Hypertonic sucrose medium inhibited mTORC1 signaling in cells

3I. WT-NIH3T3 fibroblasts were incubated in complete media containing 0.45M sucrose for the indicated time points followed by p-P70 immunoblot analyses for mTORC1 activity. P70 phosphorylation was inhibited within 30 minutes of incubation with hypertonic sucrose media. Bar graph represents quantitative evaluation of relative protein levels of p-P70. Data are represented as mean ± SEM, n = 3 independent experiments with replicates, **p ≤ 0.01; student's t-test

3J.

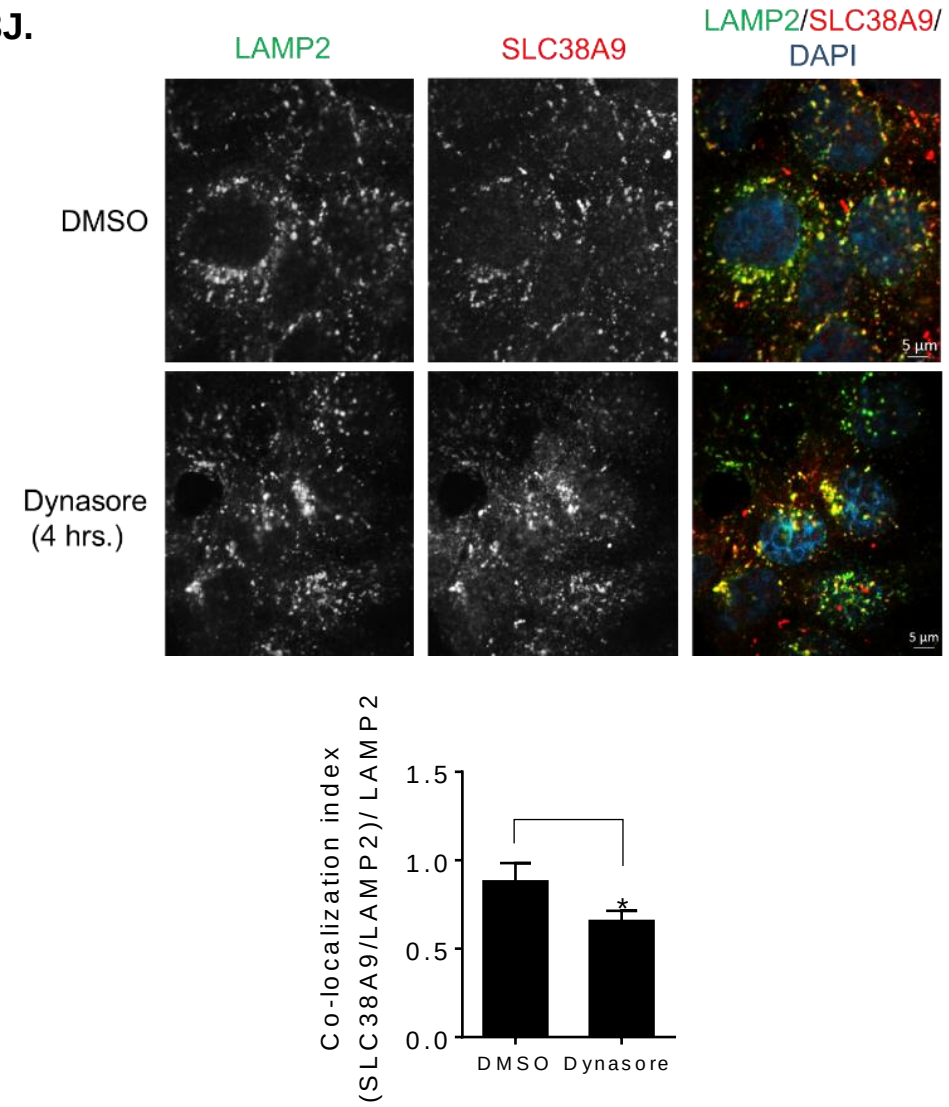
LAMP2
SLC38A9
LAMP2/SLC38A9/
DAPI
DMSO
Dynasore
(4 hrs.)
5 µm
5 µm
Co-localization index
(SLC38A9/LAMP2)/ LAMP2
1.5
1.0
0.5
0.0
*
DMSO
Dynasore

Figure 3: Endocytic trafficking controls mTORC1 tethering and signaling.

Dynasore drug treatment reduced the quantity of lysosomal arginine transporter

3J. WT-NIH3T3 fibroblasts were incubated in complete medium containing [80µM] concentration of Hydroxyl-Dynasore for 4 hours followed by co-localization analyses of SLC38A9 with lysosomal LAMP2 protein using ImageJ. Bar graph represents quantitative evaluation of lysosomal SLC38A9. Data are represented as mean ± SEM, n = 3 independent experiments, *p ≤ 0.05; student's t-test, Scale bar: 5µm.

3K.

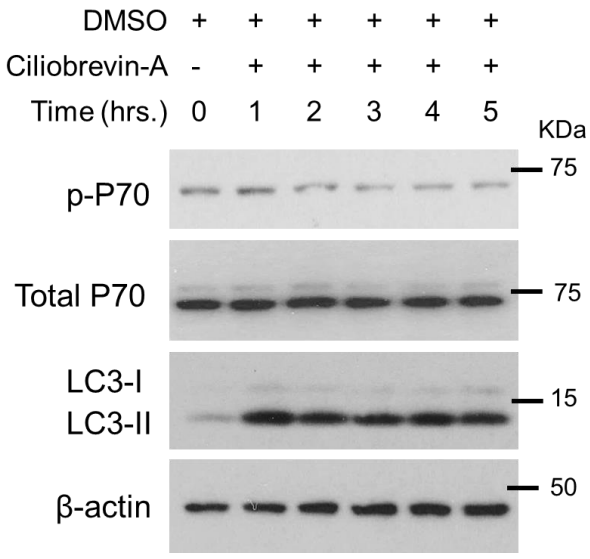
DMSO + + + + + +
Ciliobrevin-A - + + + + +
Time (hrs.) 0 1 2 3 4 5
KDa
p-P70
75
Total P70
75
LC3-I
LC3-II
15
β-actin
50

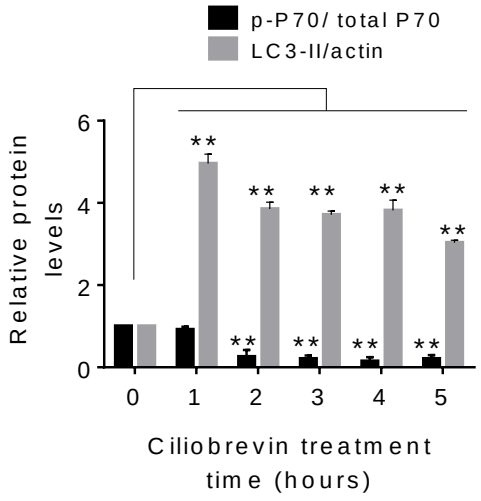
p-P70/ total P70
LC3-II/actin
Relative protein levels
6
4
2
0
**
0 1 2 3 4 5
Ciliobrevin treatment time (hours)

Figure 3: Endocytic trafficking controls mTORC1 tethering and signaling.

Ciliobrevin Drug treatment attenuated mTORC1 signaling

3K. Time course analyses of Ciliobrevin-mediated inhibition of Dynein showed a swift accumulation of LC3-II with gradual inhibition of mTORC1 activity. HEK-293T cells were treated with Ciliobrevin for the indicated time points followed by a phospho-P70 and LC3 immunoblot analyses for mTORC1 activity and autophagosome biogenesis, respectively. Bar graphs represent quantitative assessment of relative protein levels. Data are represented as mean ± SEM, n = 3 independent experiments with replicates, **p ≤ 0.01; ANOVA followed by Scheffe post hoc analyses.

10.1.5.4. Figure 4

4A.

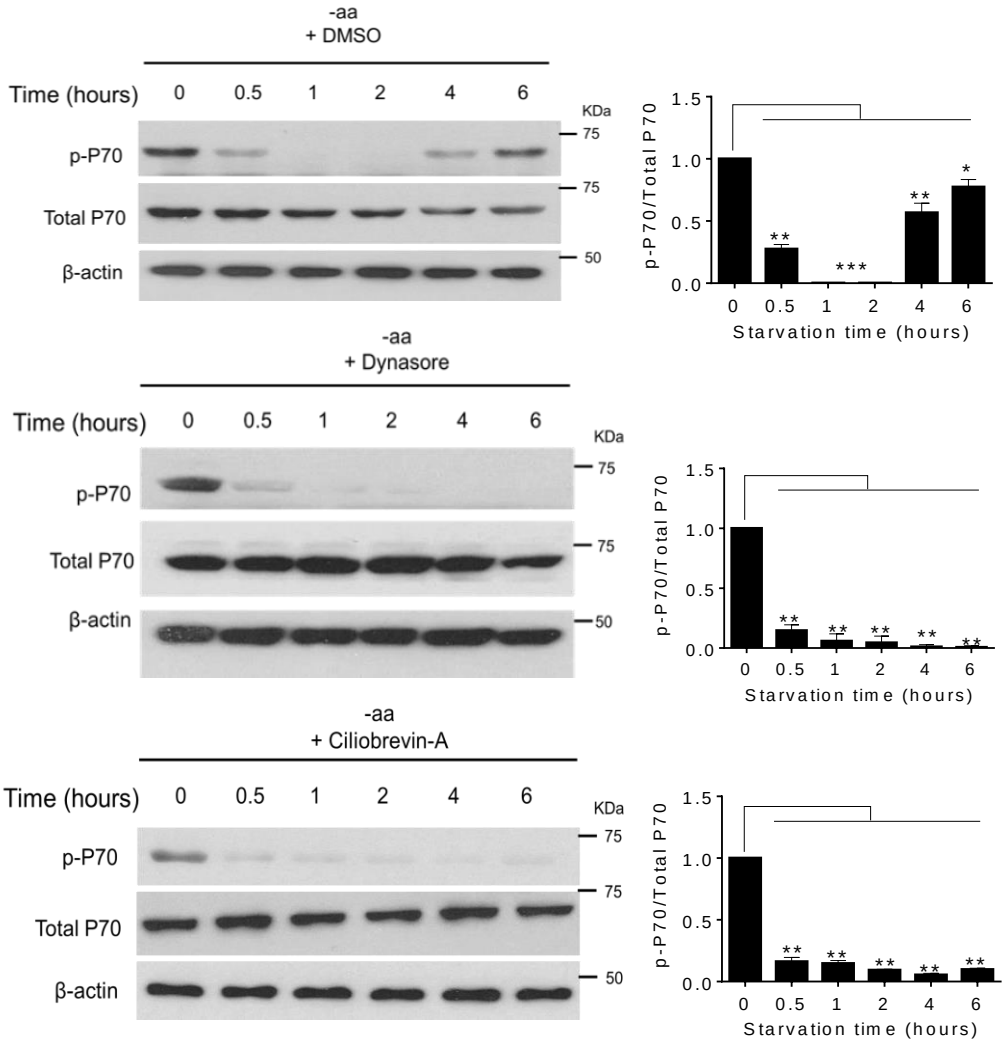

Figure 4: Recovery of mTORC1 activity during prolonged starvation occurs in a TFEB-driven endocytosis-dependent manner.

Pharmacological inhibition of Dynamin-mediated endocytosis and dynein-mediated retrograde trafficking inhibits amino acid starvation-induced reactivation of mTORC1

4A. mTORC1 activity was assessed in amino acid (Leucine/Glutamine) starved HEK-293T cells for the indicated time points. Relative phospho-P70/S6K1 levels indicative of mTORC1 activity were assessed by Western blots. Reactivation of mTORC1 was observed after 6 hours of starvation in DMSO-treated control cells, but remained suppressed in Hydroxyl-Dynasore or Ciliobrevin-A-treated and starved cells. Bar graphs represent quantitative evaluation of relative phospho-P70 protein levels. Data are represented as mean ± SEM, n = 3 independent experiments with replicates, *p ≤ 0.05; **p ≤ 0.01; ***p ≤ 0.001; ANOVA followed by Scheffe post hoc analyses.

4B.

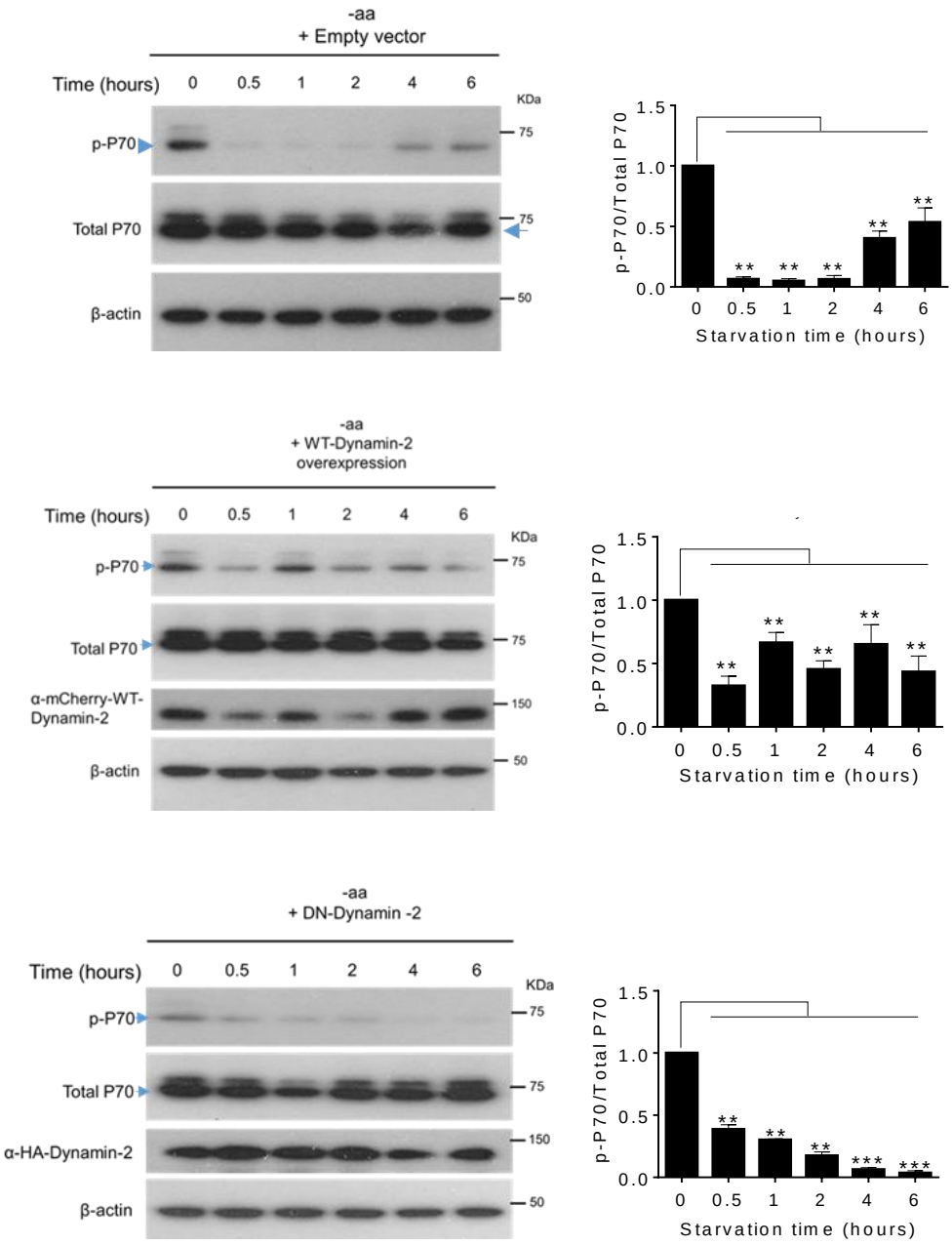
-aa
+ Empty vector
Time (hours) 0 0.5 1 2 4 6
KDa
p-P70
Total P70
β-actin
75
75
50
p-P70/Total P70
Starvation time (hours)
-aa
+ WT-Dynamin-2
overexpression
Time (hours) 0 0.5 1 2 4 6
KDa
p-P70
Total P70
α-mCherry-WT-Dynamin-2
β-actin
75
75
150
50
p-P70/Total P70
Starvation time (hours)
-aa
+ DN-Dynamin -2
Time (hours) 0 0.5 1 2 4 6
KDa
p-P70
Total P70
α-HA-Dynamin-2
β-actin
75
75
150
50
p-P70/Total P70
Starvation time (hours)

Figure 4: Recovery of mTORC1 activity during prolonged starvation occurs in a TFEB-driven endocytosis-dependent manner.

Genetic inhibition of Dynamin-mediated endocytosis and Dynein-mediated retrograde trafficking inhibits amino acid starvation-induced reactivation of mTORC1

4B. mTORC1 activity was assessed in amino acid (Leucine/Glutamine) starved HEK-293T cells transiently overexpressing either a WT-Dynamin2 or dominant negative (DN)-Dynamin2 for the indicated time points. Relative phospho-P70/S6K1 levels indicative of mTORC1 activity were assessed by Western blots. Faster recovery of mTORC1 signaling was observed in HEK-293Tcells overexpressing WT-Dynamin-2 while the overexpression of DN-Dynamin-2 efficiently inhibited mTORC1 reactivation during starvation (compare WT-Dynamin-2 and DN-Dynamin-2 expressing cells to those expressing an empty vector control). Arrows indicate specific p-P70 bands. Bar graphs represent quantitative evaluation of relative phospho-P70S6K protein levels. Data are represented as mean ± SEM, n = 3 independent experiments with replicates, **p ≤ 0.01; ***p ≤ 0.001; ANOVA followed by Scheffe post hoc analyses.

4C.

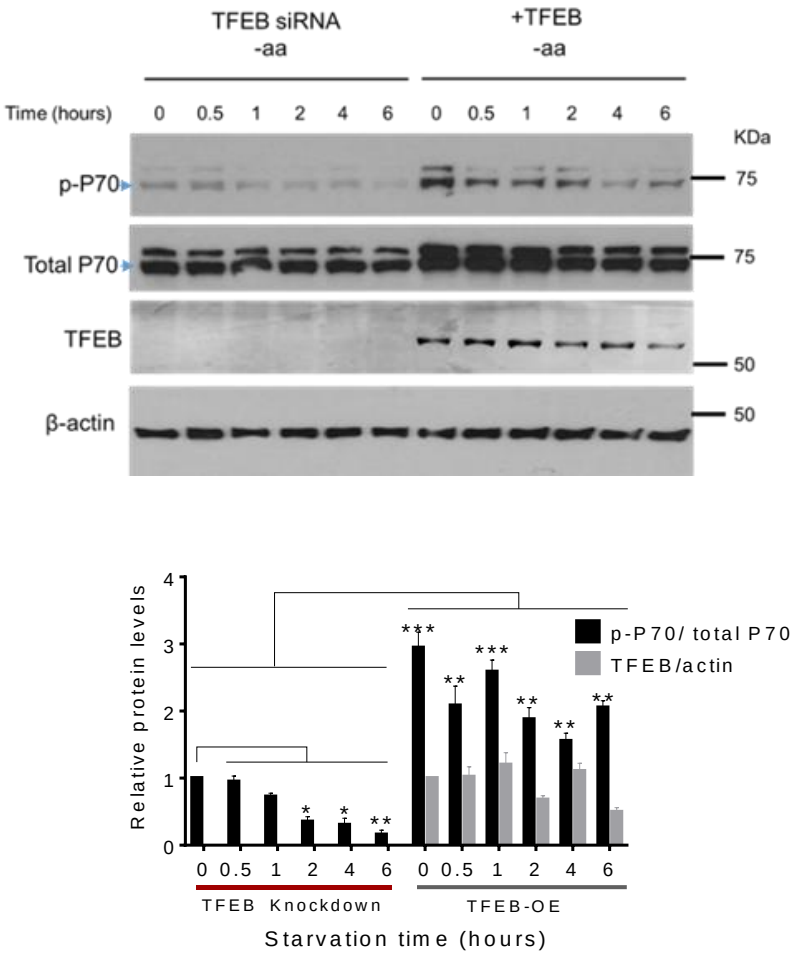
TFEB siRNA
-aa
+TFEB
-aa
Time (hours)
0 0.5 1 2 4 6 0 0.5 1 2 4 6
KDa
p-P70
Total P70
TFEB
β-actin
75
75
50
50
Relative protein levels
p-P70/ total P70
TFEB/actin
TFEB Knockdown
TFEB-OE
Starvation time (hours)

Figure 4: Recovery of mTORC1 activity during prolonged starvation occurs in a TFEB-driven endocytosis-dependent manner.

TFEB overexpressing cells, compared to cells deficient of TFEB, show a robust reactivation of mTORC1 during amino acid starvation

4C. mTORC1 activity was assessed in amino acid (Leucine/Glutamine) starved TFEB-KD or TFEB overexpressing HEK-293T cells for the indicated time points. Relative phospho-P70/S6K1 levels indicative of mTORC1 activity was assessed by western blots. Arrows indicate specific p-P70 bands. Depletion of endogenous TFEB inhibits mTORC1 reactivation while overexpression of FLAG-TFEB increased basal mTORC1 activity and promoted faster recovery of mTORC1 signaling during prolonged starvation. Bar graphs represent quantitative evaluation of relative phospho-P70 and TFEB protein levels. Data are represented as mean ± SEM, n = 3 independent experiments, *p ≤ 0.05; **p ≤ 0.01; ***p ≤ 0.001; ANOVA followed by Scheffe post hoc analyses.

4D.

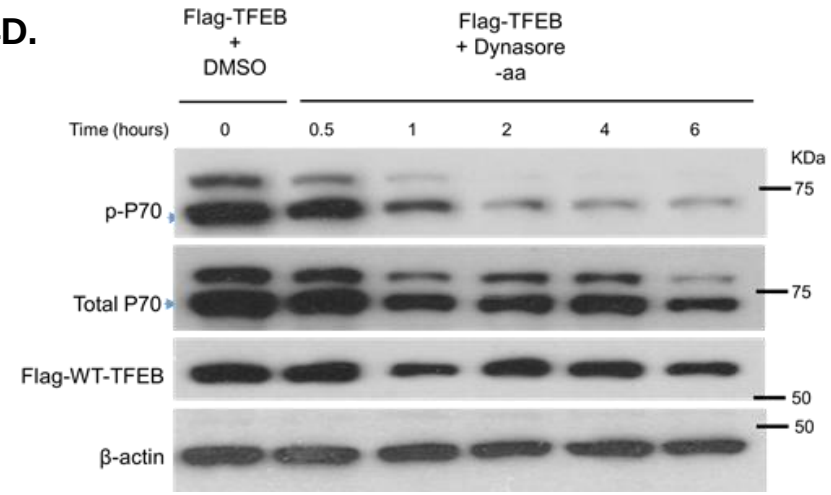
Flag-TFEB
+
DMSO
Flag-TFEB
+ Dynasore
-aa
Time (hours)
0
0.5
1
2
4
6
KDa
p-P70
Total P70
Flag-WT-TFEB
β-actin
75
75
50
50

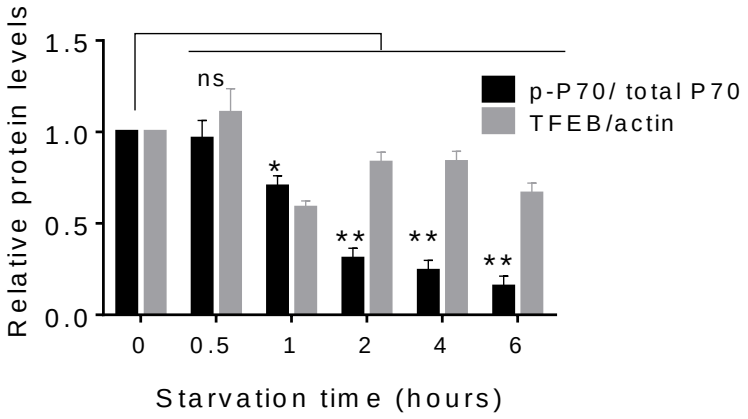
Relative protein levels
1.5
1.0
0.5
0.0
ns
*
**
**
**
p-P70/ total P70
TFEB/actin
0
0.5
1
2
4
6
Starvation time (hours)

Figure 4: Recovery of mTORC1 activity during prolonged starvation occurs in a TFEB-driven endocytosis-dependent manner.

TFEB overexpressing cells show a robust reactivation of mTORC1 during amino acid starvation in a Dynamin-dependent manner

4D. mTORC1 activity was assessed in amino acid (Leucine/Glutamine) starved HEK-293T cells transiently overexpressing TFEB and treated with Hydroxyl-Dynasore for the indicated time points. Relative phospho-P70 levels indicative of mTORC1 activity was quantified by Western blots. Arrows indicate specific p-P70 bands. Overexpression of FLAG-TFEB increased basal mTORC1 activity and promoted faster recovery of mTORC1 signaling during prolonged starvation in a Dynamin-dependent manner. Bar graphs represent quantitative evaluation of relative phospho-P70 and TFEB protein levels. Data are represented as mean ± SEM, n = 3 independent experiments, ns denotes no significant difference, *$p \leq 0.05$; **$p \leq 0.01$; ANOVA followed by Scheffe post hoc analyses.

10.1.5.5. Figure 5

5A.

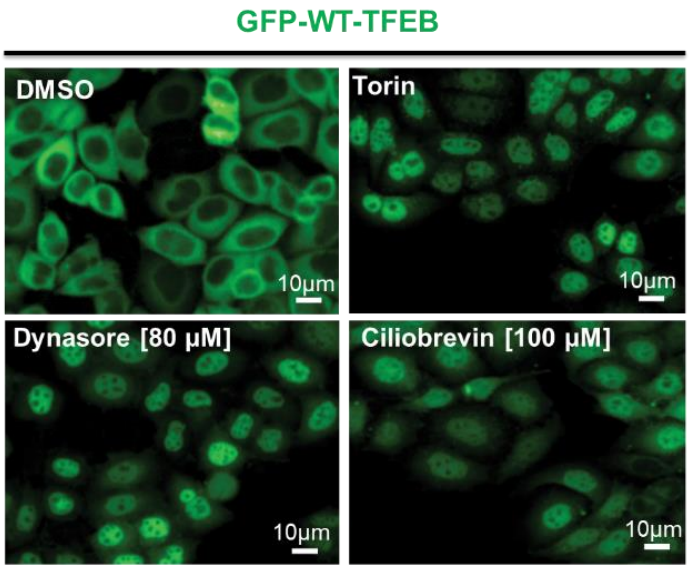

Figure 5: Inhibition of endosomal trafficking translocates TFEB into the nucleus and reduces the quantity of LAMP2 positive vesicles.

Pharmacological Inhibition of Dynamin or Dynein causes nuclear translocation of TFEB

5A. Inhibition of Dynamin or Dynein with Ciliobrevin or Dynasore re-localizes TFEB to the nucleus. GFP-WT-TFEB was transiently transfected into HeLa cells for 48 hours followed by Dynasore or Ciliobrevin-A treatments with the indicated concentrations. Nuclear TFEB was then assessed by confocal microscopy and quantitatively represented in the graphs in (5B and 5C).

5B.

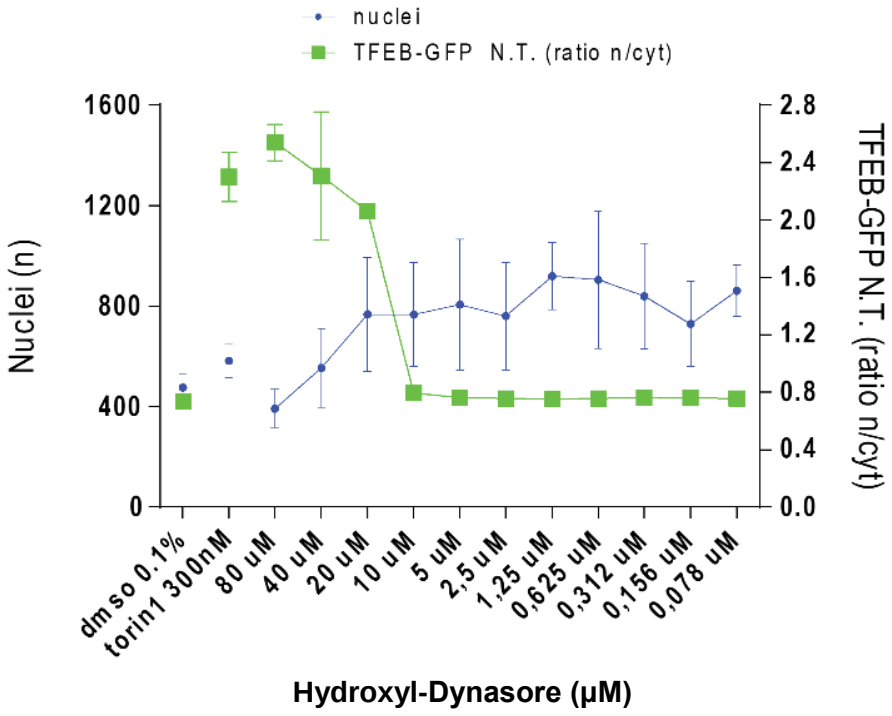
nuclei
TFEB-GFP N.T. (ratio n/cyt)
Nuclei (n)
TFEB-GFP N.T. (ratio n/cyt)
1600
1200
800
400
0
2.8
2.4
2.0
1.6
1.2
0.8
0.4
0.0
dmso 0.1%
torin1 300nM
80 uM
40 uM
20 uM
10 uM
5 uM
2,5 uM
1,25 uM
0,625 uM
0,312 uM
0,156 uM
0,078 uM
Hydroxyl-Dynasore (µM)

Figure 5: Inhibition of endosomal trafficking translocates TFEB into the nucleus and reduces the quantity of LAMP2 positive vesicles.

Pharmacological Inhibition of Dynamin or Dynein causes nuclear translocation of TFEB

5B. Inhibition of Dynamin with Dynasore re-localizes TFEB to the nucleus. GFP-WT-TFEB was transiently transfected into HeLa cells for 48 hours followed by 4 hour-Dynasore treatments with the indicated concentrations. Analyses of nuclear versus cytoplasmic TFEB was carried out by confocal microscopy and quantitatively represented in the graph. Data are represented as mean ± SEM, n = 3 independent experiments

5C.

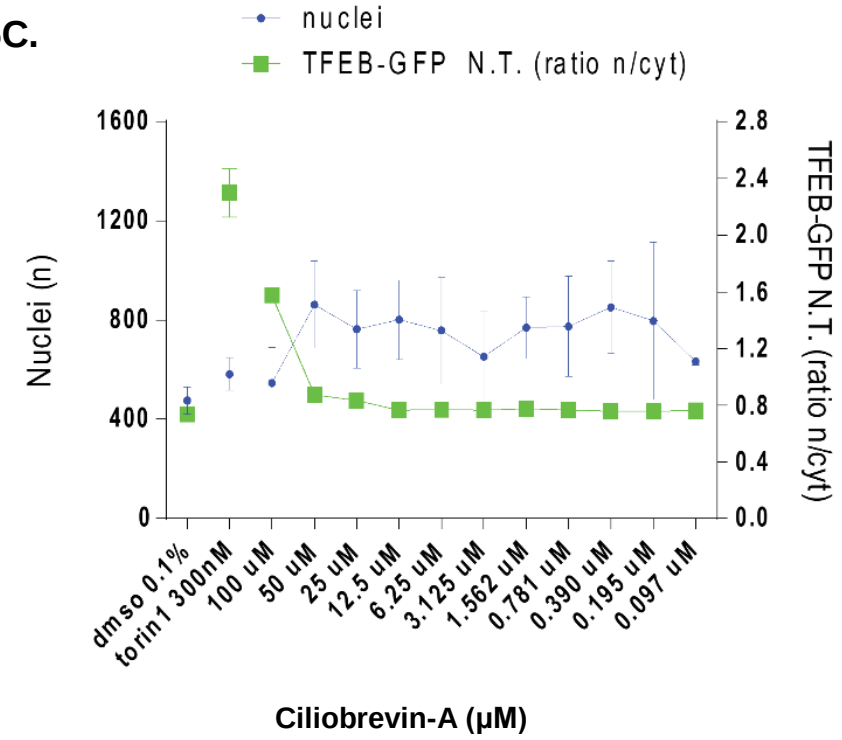
nuclei
TFEB-GFP N.T. (ratio n/cyt)
Nuclei (n)
TFEB-GFP N.T. (ratio n/cyt)
1600
1200
800
400
0
2.8
2.4
2.0
1.6
1.2
0.8
0.4
0.0
dmso 0.1%
torin1 300nM
100 uM
50 uM
25 uM
12.5 uM
6.25 uM
3.125 uM
1.562 uM
0.781 uM
0.390 uM
0.195 uM
0.097 uM
Ciliobrevin-A (µM)

Figure 5: Inhibition of endosomal trafficking translocates TFEB into the nucleus and reduces the quantity of LAMP2 positive vesicles.

Pharmacological Inhibition of Dynamin or Dynein causes nuclear translocation of TFEB

5C. Inhibition of Dynein with Ciliobrevin-A re-localizes TFEB to the nucleus. GFP-WT-TFEB was transiently transfected into HeLa cells followed by 4 hour-Ciliobrevin A treatments with the indicated concentrations. Analyses of nuclear versus cytoplasmic TFEB was carried out by confocal microscopy and quantitatively represented in the graph. Data is represented as mean ± SEM, n = 3 independent experiments.

5D.

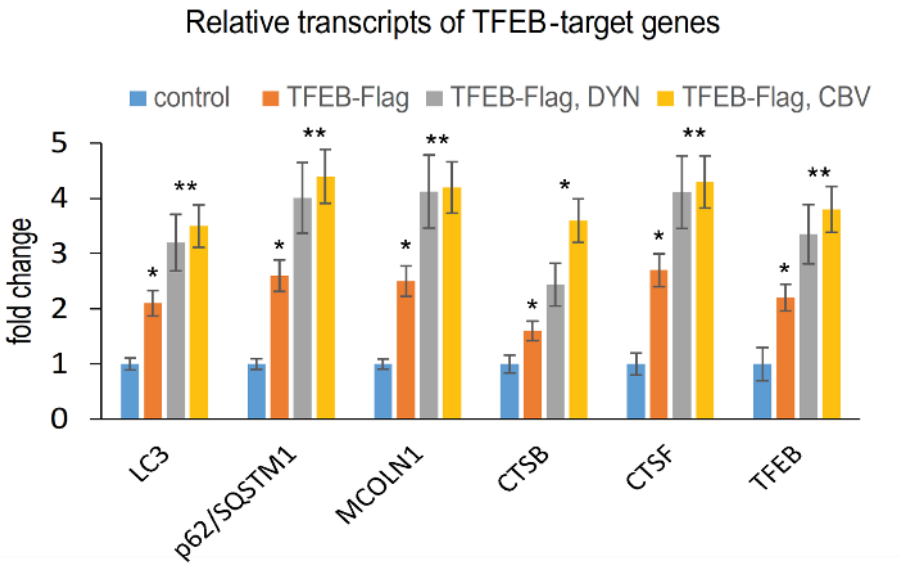
Relative transcripts of TFEB-target genes
control
TFEB-Flag
TFEB-Flag, DYN
TFEB-Flag, CBV
fold change
0
1
2
3
4
5
LC3
p62/SQSTM1
MCOLN1
CTSB
CTSF
TFEB

Figure 5: Inhibition of endosomal trafficking translocates TFEB into the nucleus and reduces the quantity of LAMP2 positive vesicles.

Pharmacological Inhibition of Dynamin or Dynein induced TFEB transcriptional activity

5D. Quantitative RT-PCR analyses of Ciliobrevin and Hydroxyl-Dynasore-treated cells showed increased transcription of TFEB target genes (LC3, p62/SQSTM1, MCOLN1, CTSB, CTSF, and TFEB) after inhibition of endocytosis with Dynasore or inhibition of retrograde trafficking with Ciliobrevin-A. Bar graphs represent fold change in mRNA levels. Data are represented as mean ± SEM, n = 3 independent experiments; *p ≤ 0.05; **p ≤ 0.01; ANOVA followed by Tukey post hoc analyses.

5E.

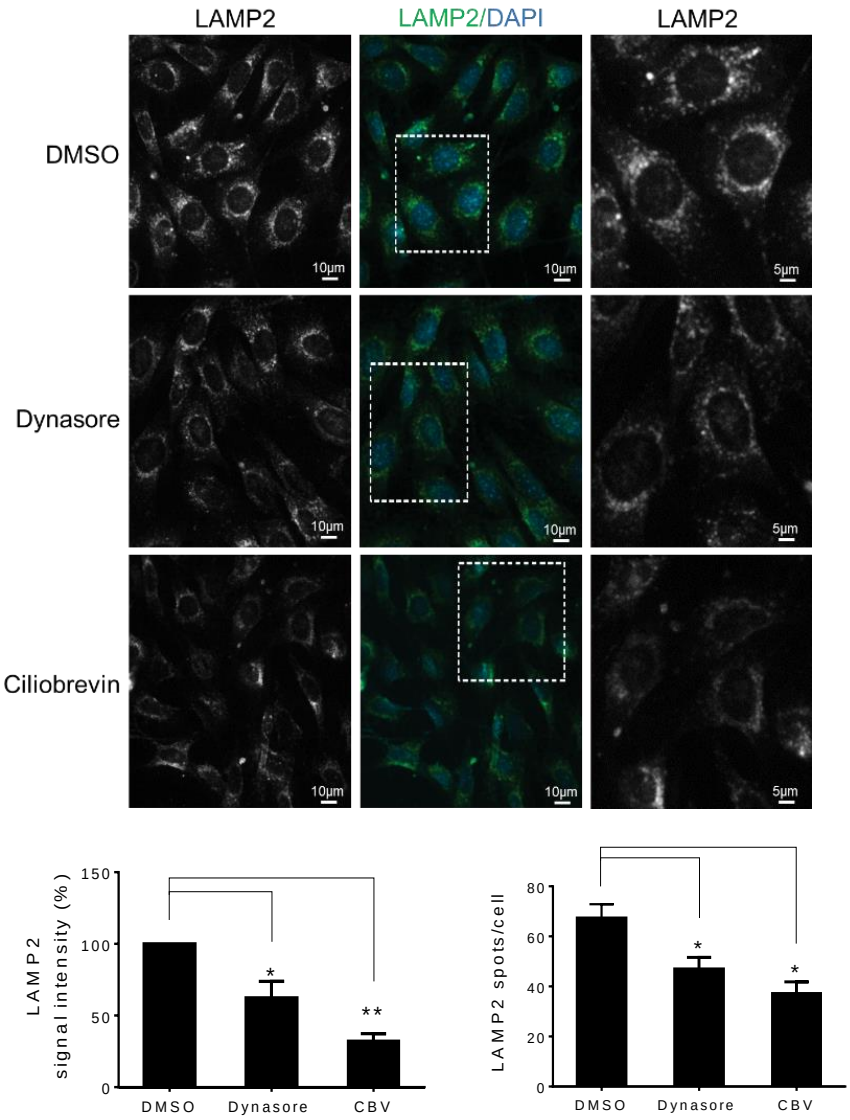
LAMP2
LAMP2/DAPI
LAMP2
DMSO
Dynasore
Ciliobrevin
10μm
5μm
LAMP2 signal intensity (%)
150
100
50
0
*
**
DMSO
Dynasore
CBV
LAMP2 spots/cell
80
60
40
20
0
*
*
DMSO
Dynasore
CBV

Figure 5: Inhibition of endosomal trafficking translocates TFEB into the nucleus and reduces the quantity of LAMP2 positive vesicles.

Pharmacological Inhibition of Dynamin or Dynein reduced the quantity of LAMP2 positive vesicles in NIH3T3 cells

5E. NIH3T3 cells treated with Dynasore or Ciliobrevin-A overnight showed a strong reduction of the intensity of LAMP2-immunoreactivity and number of LAMP2-positive spots per cell, indicative of the number of lysosomes. Right panels are magnifications of outlined areas. Bar graphs represent the quantitative analysis of the LAMP2 signal intensity and average number of LAMP2 puncta per cell in both conditions. Data are represented as mean ± SEM, n = 3 independent experiments; *p ≤ 0.05; **p ≤ 0.01; student's t-test.

9.1.5.6. Figure 6

6A.

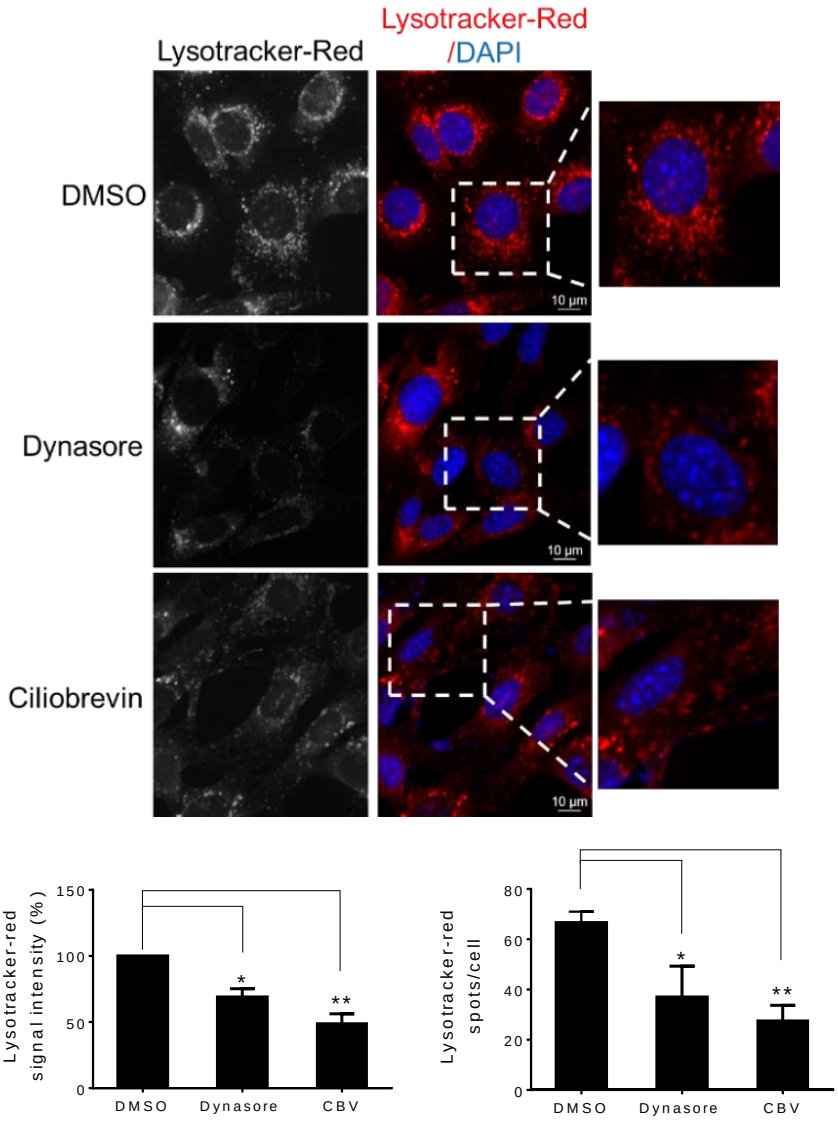

Figure 6: Inhibition of endocytic trafficking attenuates number and acidification of endolysosomes to halt autophagy flux.

Pharmacological Inhibition of Dynamin or Dynein reduced the quantity of acidic (LysoTracker-positive) vesicles in NIH3T3 cells

6A. Inhibition of endocytic trafficking in NIH3T3 fibroblasts, with either 4 hours of Dynasore or Ciliobrevin-A treatment, consequently reduces the number of acidic vesicles indicated by LysoTracker-Red fluorescence staining. Bar graphs represent the quantitative analyses of the LysoTracker-Red fluorescence intensity and average number of puncta per cell in both conditions. Data is represented as mean ± SEM, n = 3 independent experiments; *p ≤ 0.05; **p ≤ 0.01; student's t-test.

6B.

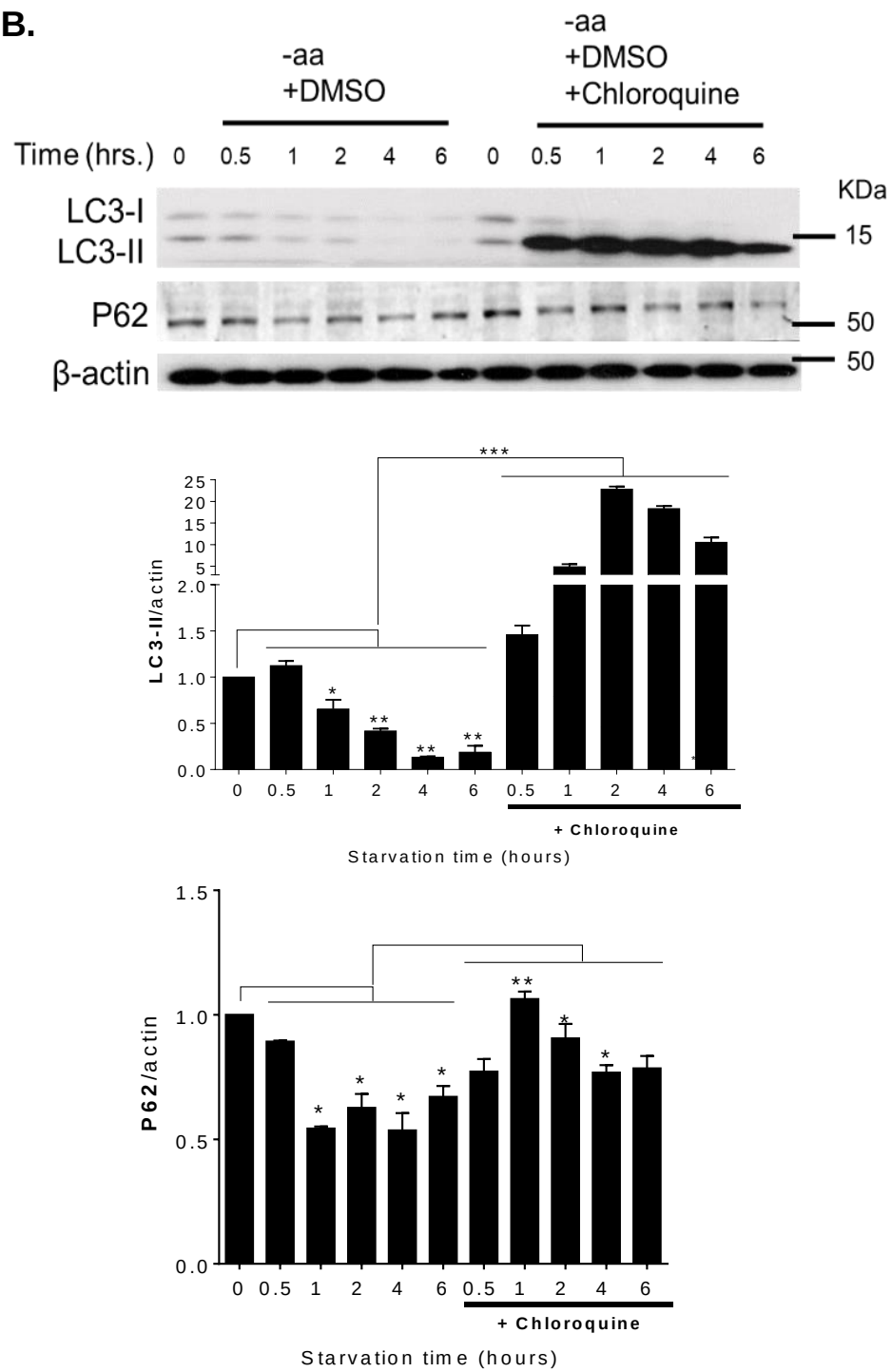
-aa
+DMSO
-aa
+DMSO
+Chloroquine
Time (hrs.) 0 0.5 1 2 4 6 0 0.5 1 2 4 6
KDa
LC3-I
LC3-II
15
P62
50
β-actin
50
LC3-II/actin
***
*
**
**
**
+ Chloroquine
Starvation time (hours)
P62/actin
**
*
*
*
*
*
*
+ Chloroquine
Starvation time (hours)

Figure 6: Inhibition of endocytic trafficking attenuates number and acidification of endolysosomes to halt autophagy flux.

Inhibition of endocytic trafficking negatively affects autophagy flux

6B. Autophagy flux assay of HEK-293T cells treated with DMSO and starved from amino acids for the indicated time points. Normal autophagy flux is indicated by the gradual decrease in the levels of LC3-II/P62 during starvation and their accumulation when lysosomal function is inhibited by chloroquine. Bar graphs represent quantitative analysis of the relative P62 and LC3 protein levels during starvation. Data are represented as mean ± SEM, n = 3 independent experiments; *p ≤ 0.05; **p ≤ 0.01; ***p ≤ 0.001; ANOVA followed by Scheffe post hoc analyses.

6C.

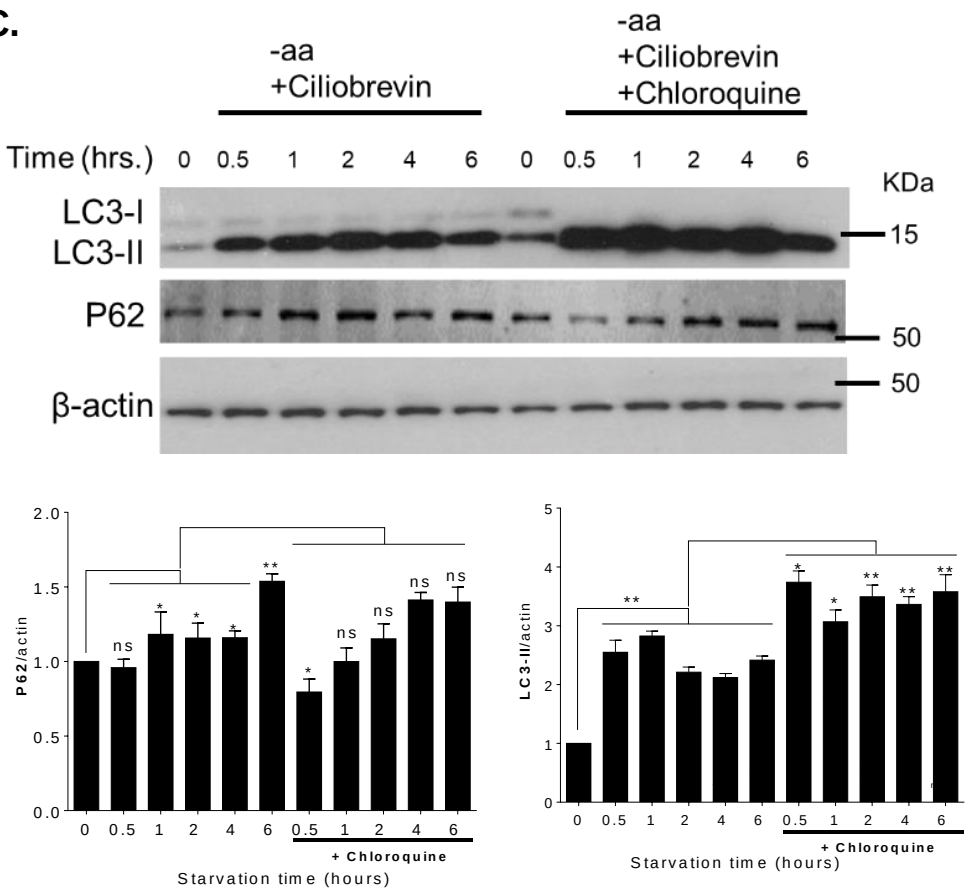
-aa
+Ciliobrevin
-aa
+Ciliobrevin
+Chloroquine
Time (hrs.) 0 0.5 1 2 4 6 0 0.5 1 2 4 6
KDa
LC3-I
LC3-II
15
P62
50
β-actin
50
P62/actin
LC3-II/actin
+ Chloroquine
Starvation time (hours)

Figure 6: Inhibition of endocytic trafficking attenuates number and acidification of endolysosomes to halt autophagy flux.

Inhibition of endocytic trafficking negatively affects autophagy flux

6C. Autophagy flux was impaired in cells treated with either Ciliobrevin-A. HEK-293T Cells were pre-incubated with Ciliobrevin-A for 2 hours prior to amino acid starvation for indicated time points. Compared to controls (figure 6C), LC3-II protein levels did not decrease, but rather increased over time indicating an impaired autophagy flux due to lysosomal inhibition. Bar graphs represent quantitative analysis of the relative P62 and LC3 protein levels during starvation. Data are represented as mean ± SEM, n = 3 independent experiments; ns denotes no significant difference *$p \leq 0.05$; **$p \leq 0.01$; ANOVA followed by Scheffe post hoc analyses.

6D.

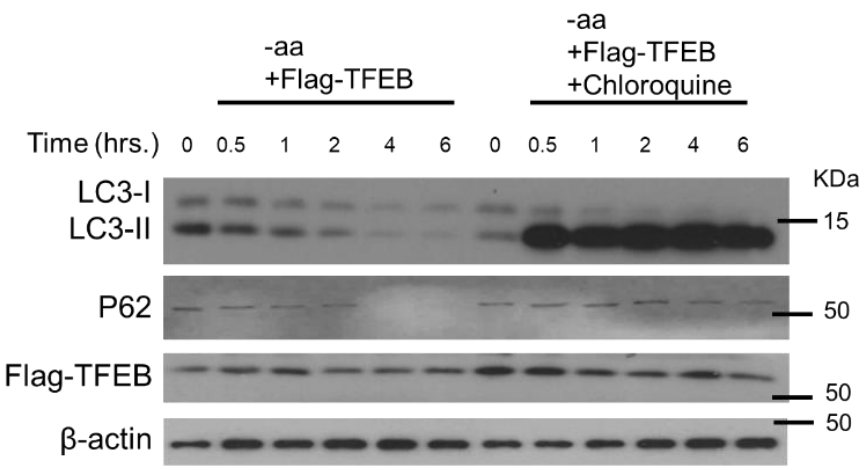
-aa
+Flag-TFEB
-aa
+Flag-TFEB
+Chloroquine
Time (hrs.) 0 0.5 1 2 4 6 0 0.5 1 2 4 6
KDa
LC3-I
LC3-II
15
P62
50
Flag-TFEB
50
β-actin
50

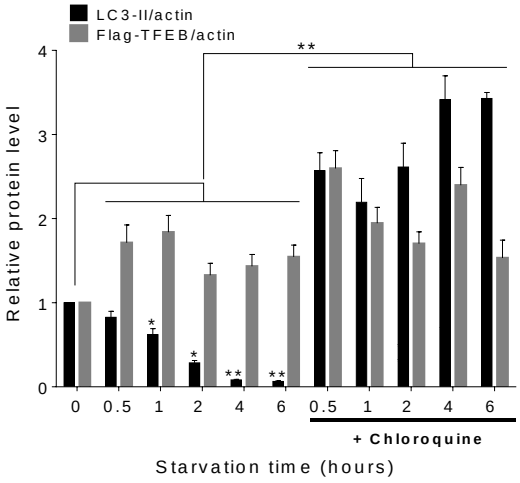
LC3-II/actin
Flag-TFEB/actin
Relative protein level
Starvation time (hours)
+ Chloroquine

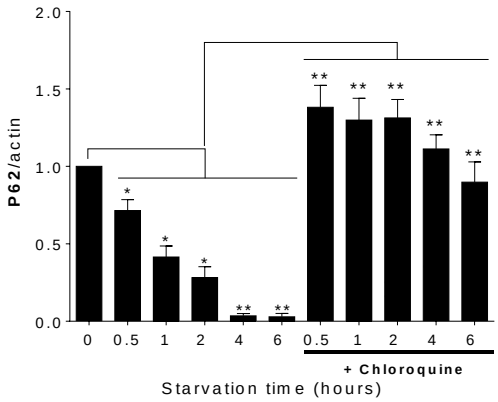
P62/actin
Starvation time (hours)
+ Chloroquine

Figure 6: Inhibition of endocytic trafficking attenuates number and acidification of endolysosomes to halt autophagy flux.

Autophagy flux is increased in TFEB overexpressing cells in an endocytosis-dependent manner

6D. Autophagy flux was increased in HEK293T cells transiently overexpressing FLAG-TFEB 48 hours. Bar graphs represent quantitative analyses of the relative P62, LC3 and FLAG-TFEB protein levels during starvation. Data are represented as mean ± SEM, n = 3 independent experiments; ns denotes no significant difference *p ≤ 0.05; **p ≤ 0.01; ANOVA followed by Scheffe post hoc analyses.

6E.

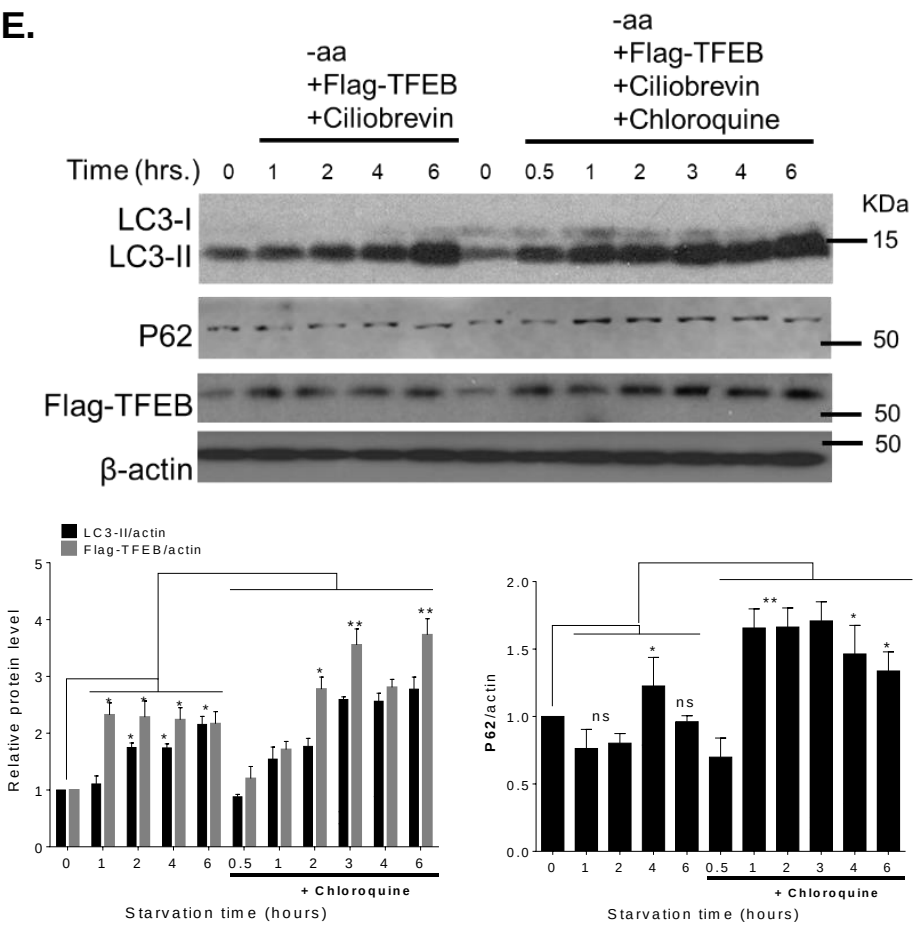
-aa
+Flag-TFEB
+Ciliobrevin
-aa
+Flag-TFEB
+Ciliobrevin
+Chloroquine
Time (hrs.) 0 1 2 4 6 0 0.5 1 2 3 4 6
KDa
LC3-I
LC3-II
15
P62
50
Flag-TFEB
50
β-actin
50
LC3-II/actin
Flag-TFEB/actin
Relative protein level
+ Chloroquine
Starvation time (hours)
P62/actin
ns
ns
+ Chloroquine
Starvation time (hours)

Figure 6: Inhibition of endocytic trafficking attenuates number and acidification of endolysosomes to halt autophagy flux.

Autophagy flux is increased in TFEB overexpressing cells in an endocytosis-dependent manner

6E. Autophagy flux was increased in cells transiently overexpressing FLAG-TFEB in an endocytic trafficking-dependent manner. Inhibition of Dynein-dependent trafficking with Ciliobrevin-A impairs autophagy flux indicating attenuated lysosomal function. Bar graphs represent quantitative analysis of the relative P62, LC3 and FLAG-TFEB protein levels during starvation. Data are represented as mean ± SEM, n = 3 independent experiments; ns denotes no significant difference *p ≤ 0.05; **p ≤ 0.01; ANOVA followed by Scheffe post hoc analyses.

6F.

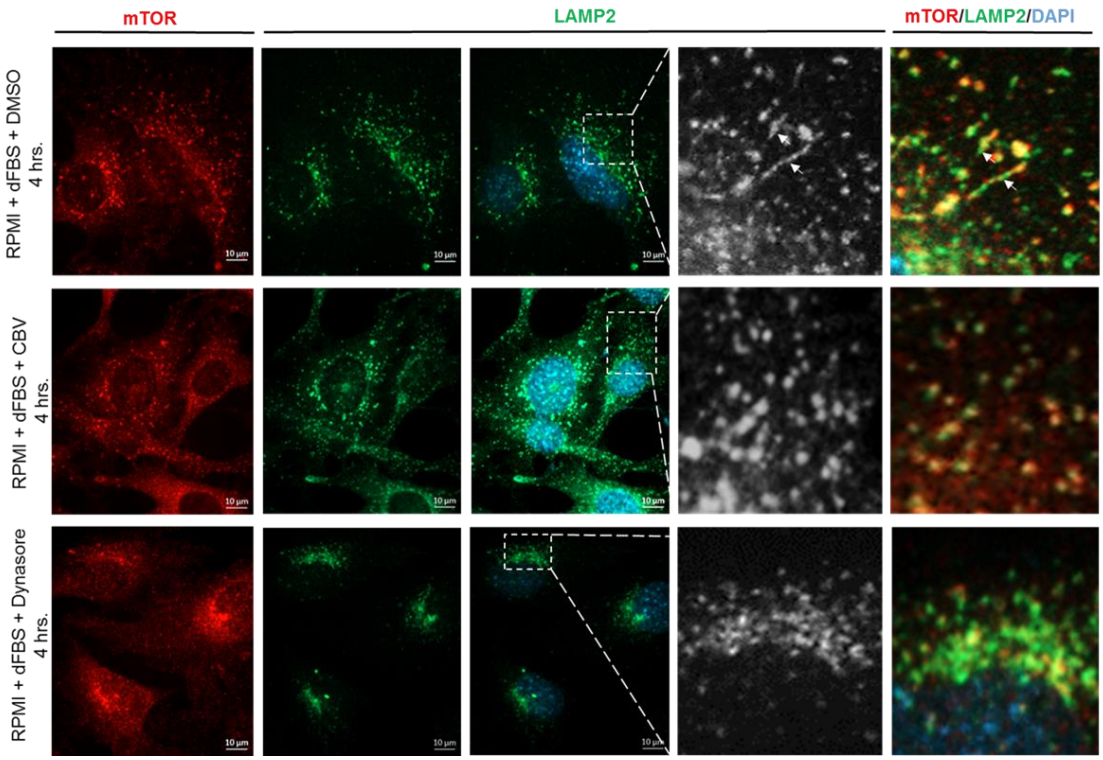
mTOR
LAMP2
mTOR/LAMP2/DAPI
RPMI + dFBS + DMSO
4 hrs.
RPMI + dFBS + CBV
4 hrs.
RPMI + dFBS + Dynasore
4 hrs.
10 µm

Figure 6: Inhibition of endocytic trafficking attenuates number and acidification of endolysosomes to halt autophagy flux.

Dynasore and Ciliobrevin treatments reduced the quantity of tubular lysosomes in amino acid-starved cells

6F. NIH-3T3 fibroblasts were incubated in amino acid-free medium containing 10% dialyzed FBS with either Dynasore or Ciliobrevin-A for 4 hours and the quantity of tubular lysosomes in each condition were analyzed by LAMP2 immunofluorescence. Bar graph represents quantitative analyses of cells with tubular lysosomes. Data are represented as mean ± SEM, n = 3 independent experiments; **p ≤ 0.01; ANOVA followed by Scheffe post hoc analyses.

10.1.5.7 Figure 7

7.

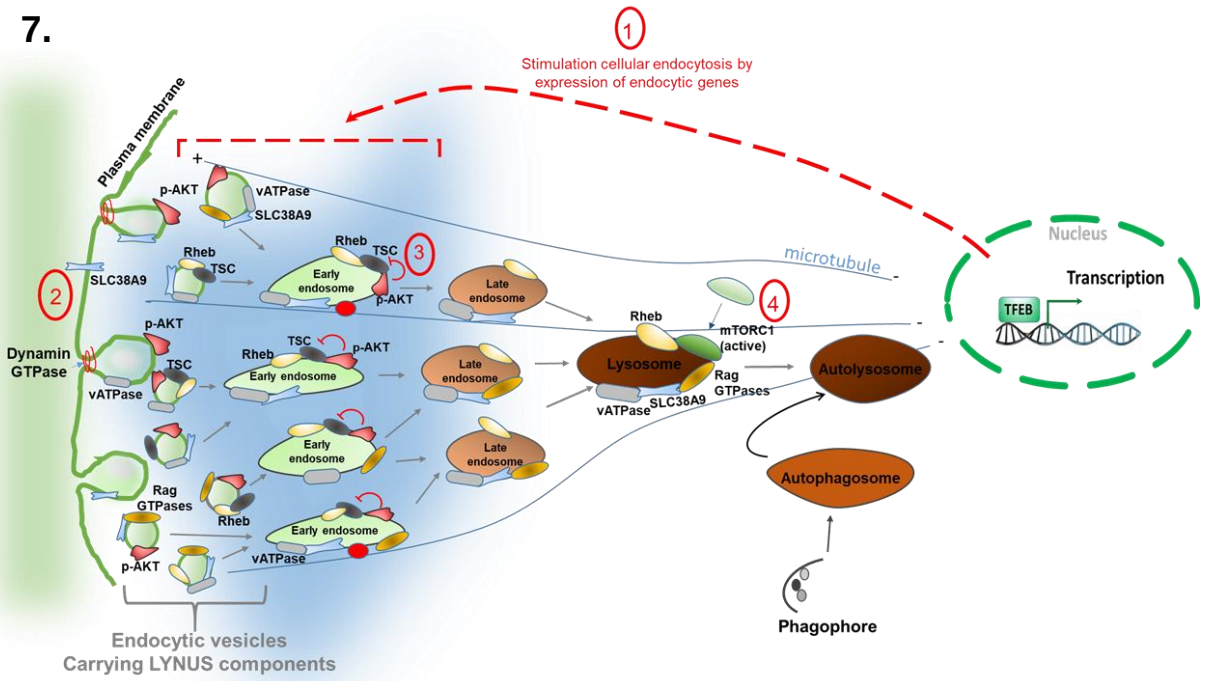

Figure 7: TFEB-mediated endocytosis activates mTORC1 by coordinating the sorting of LYNUS components on endosomal membranes.

Starvation-induced inhibition of mTORC1 promotes nuclear TFEB (**1**) activity that triggers expression of endocytic genes required for random formation of Dynamin-driven signaling endosomes that shuttle LYNUS components including active phospho-Akt and Rag GTPases (**2**), en route to lysosomes in a Dynein-dependent manner to inhibit TSC2 (**3**), tether mTORC1 (**4**) and eventually promote autophagy flux.

11. Chapter Four

11.1. Discussion and future directions

The role of cellular endocytosis during autophagy is of great importance and as such, it has been studied extensively (Barth, 2014). Endocytic trafficking is necessary for efficient autophagy flux because endosomes direct the delivery of lysosomal hydrolases such as proteases, glucosidases and lipases, to lysosomes and acidify and mature lysosomes through trafficking of the vacuolar-ATPase (vATPase) proton pump (Huotari and Helenius, 2011; Lamb et al., 2012; Luzio et al., 2007; Singh and Cuervo, 2011). However, the molecular cues that initiate these endosomal processes upon induction of autophagy still remains incompletely understood. It's still unclear how lysosomal biogenesis (reformation) is regulated after autolysosomal degradation. Some studies, however, have identified mTORC1 and core endocytic genes such as Clathrin (Chen and Yu, 2013) and the sugar transporter Spinster (Rong et al., 2011) to contribute to lysosomal reformation post-autophagy. Also in many human diseases, including lipid storage disorders, cancer and neurodegenerative diseases, in which autophagy and mTORC1 signaling are dysfunctional, endocytosis have been found deregulated (Nixon, 2005; Rosner et al., 2008). Despite the high importance of these observations, this systematic decline in the endo- and autolysosomal systems have remained incompletely understood.

Essential to these aforementioned processes is the regulatory activity of TFEB. As a master regulator of autophagy, TFEB controls the expression of autophagosome and lysosomal genes in nutrient-deprived conditions (in which

mTORC1 is inhibited) to initiate autophagy and promote lysosomal biogenesis. Preliminary studies in Dobrowolski lab and recent findings by Ballabio's research team suggested that TFEB, in a feedback mechanism, coordinates the reactivation of mTORC1 in nutrient-deprived conditions (Di Malta et al., 2017). Also TFEB transcriptome analysis carried out by Sardiello et al. (2009) revealed that TFEB may also control cellular endocytosis during starvation. I therefore sought to investigate whether TFEB plays a central role to coordinate all three cellular processes: cellular endocytosis, autophagy and reactivation of mTORC1 during starvation, and to determine the limiting factor of this signaling network.

Among the genes upregulated in mammalian cells overexpressing TFEB in fed and nutrient-deprived conditions were core endocytic genes including Caveolin, Clathrin, EEA-1, Rab5, and others (Figure 10.1.5.**1A-1D**, Table 1 and Appendix Table 2). This TFEB-mediated increase in expression of endocytic genes was further supported by results from endocytosis assays which indicated increased endocytic rates in cells transiently overexpressing TFEB in either fed or amino acid-starved conditions (Figure 10.1.5.**1E-1J**). In endosomal cell fractionation assays, the quantity of Rab5 early endosomal marker increased in endosomal fractions of cells overexpressing TFEB (Figure 10.1.5.**2A** vs. Figure 10.1.5.**2B**). These Rab5-positive endosomal fractions contained increased levels of phospho-Akt (thr308), RagD and phospho-PDK1 (Ser241) proteins required for activating mTORC1. Also, the number of less dense endocytic fractions in the 15%, 20% and 30% optiprep gradients increased, thus indicating the presence of smaller endocytic vesicles carrying varying cargos as a result of increased

endocytic flux (Figure 10.1.5.**2C**) (compare fractions 1 to 9 in Figure 10.1.5.**2A** vs. Figure 10.1.5.**2B**). Interestingly, the protein levels of the mTORC1 negative regulator TSC2 decreased in these Rab5-positive endosomal fractions of TFEB-overexpressing cells, suggesting that these endosomes may be carrying active Akt which phosphorylates TSC2 and promotes its relocalization to the cytosol. TSC2 levels also decreased dramatically in the 10% input of pre-fractionated lysates of TFEB-overexpressing cells suggesting that the cytosolic TSC2 was degraded over time (Figure 10.1.5.**2D**). In a follow-up immunofluorescence study, Rab5 colocalized with RagD (Figure 10.1.5.**2F,** lower panels), mTOR (Figure 10.1.5.**2F,** upper panels), and the Akt-PH-GFP bioprobe in mammalian cells transiently overexpressing TFEB in fed conditions (Figure 10.1.5.**2E**). These results together indicate that stimulation of cellular endocytosis and initiation of autophagy are two intertwined cellular processes coordinated by TFEB signaling.

Previous studies reported that Dynamin 2-dependent endocytosis critical for T-cell receptor-mediated activation of T-lymphocytes and maintenance of key metabolic pathways including mTORC1 to promote T-lymphocyte metabolism (Willinger et al., 2015). Subsequent studies further demonstrated that Dynamin regulates autophagy indirectly by regulating lysosomal functions in *Drosophila* (Fang et al., 2016). These findings and the results collected from the TFEB-driven endocytosis assays motivated me to investigate whether mTORC1 signaling and autophagy are generally controlled by endocytosis and accompanying intracellular retrograde trafficking. In immunocytochemical and Western blot analyses of mTORC1 signaling in cells deficient of Dynamin GTPase and Dynein motor protein

activities, mTORC1 activity was attenuated, thus revealing that cellular endocytosis is required to initiate and sustain mTORC1 signaling in mammalian cells under fed conditions (Figure 10.1.5.**3**). Importantly, mTOR relocalized to the cytosol while its negative regulator TSC2 relocalized to lysosomal membranes in cells treated with either Dynasore or Ciliobrevin (Figure 10.1.5.**3A-3B**, **3D-3E**). This suggests that Dynamin-mediated endocytosis not only controls the growth-factor signaling axis that stimulates mTORC1 kinase activity, but also controls the amino acid-dependent recruitment of mTORC1 to endolysosomal membranes. In addition, Akt phosphorylation on threonine 308 by PDK1, which renders Akt active and promotes mTORC1 activation, was unperturbed in cells deficient of Dynamin GTPase activity and mTORC1 signaling (Figure 10.1.5.**3C**). Therefore it seems that activated Akt needs to be trafficked to endolysosomal compartments harboring the TSC complex, which is then phosphorylated by the endosomal Akt and removed from endolysosomal membranes to allow Rheb to stimulate mTORC1 kinase activity. Additionally, mTORC1 signaling was also attenuated in cells overexpressing dominant negative mutant of Rab5 (Figure 10.1.5.**3F**), further confirming the indispensable role of cellular endocytosis in the mTORC1 signaling pathway.

Previous studies demonstrated that reactivation of mTORC1 during prolonged periods of starvation is carried out in an autophagy and TFEB-dependent manner, and requires the degradation of autolysosomal contents (Yu et al., 2010; Di Malta et al., 2017). In these studies, increased mTORC1 activity under starvation attenuated autophagy, stimulated generation of proto-lysosomal

tubules that extruded from autolysosomes, and further promoted maturation of proto-lysosomes into functional lysosomes, thereby replenishing the full repertoire of lysosomes in the cell in a process later described as autophagic lysosomal reformation (ALR) (Yu et al., 2010). However, these studies insufficiently explained how mTORC1 is reactivated during starvation. In my studies, the inhibition of Dynamin or Dynein proteins dramatically suppressed TFEB-mediated reactivation of mTORC1 signaling throughout the duration of amino acid starvation (Figure 10.1.5.**4**), and also inhibited the extrusion (tubulation) of autolysosomal membranes (Figure 10.1.5.**6F**), thus identifying Dynamin-mediated endocytosis as a crucial factor required for reactivation of mTORC1 and induction of ALR. Together these data suggest that nuclear TFEB signaling stimulates endocytosis and retrograde trafficking of nutrient sensing components including amino acid transporters, RagD and active Akt, which are all required to activate mTORC1. Although these are significant findings, further studies are needed in order to elucidate the specific endocytic events upstream of Dynamin and early endosomal biogenesis that are triggered by TFEB. For example, lipid rafts and membrane curvature are two important cellular processes upstream of Dynamin that are required for initiating formation and internalization of endocytic vesicles (Ewers and Helenius, 2011). It will be an addition to our knowledge of this signaling pathway to see whether TFEB signaling induces any changes in the quantity of phospholipid and sterols of the plasma membrane and intracellular compartments that are necessary for forming lipid rafts and membrane curvatures (Parton 1994; Pichler and Riezman, 2004; Sonnino et al., 2006, 2007; Ewers and Helenius, 2011).

Intracellular position of lysosomes has been shown to regulate mTORC1 signaling which in turn influences autophagosome formation (Korolchuk et al., 2011). Lysosome positioning determines many physiological processes including cholesterol homeostasis, cellular adaptation to nutrient availability, rate of autophagosome-lysosome fusion, and controls autophagic flux by acting at both the initiation and termination stages of the process (Korolchuk et al., 2011). During starvation, mTORC1 activity is repressed and lysosomes predominantly cluster at microtubule-organizing center (MTOC) of the perinuclear regions to facilitate autolysosomal biogenesis (Luzio et al., 2007; Korolchuk et al., 2011). Upon nutrient replenishment, which restores mTORC1 signaling, lysosomes scatter across the cytoplasm (Korolchuk et al., 2011). Some studies have shown that TFEB promotes perinuclear-lysosomal positioning by modulating the expression and recruitment of lysosomal proteins, TMEM55B and Dynein adaptor JIP4 (Willett et al., 2017) to lysosomal membranes. Studies in Dobrowolski lab and other labs also identified Mucolipin1, a lysosomal calcium efflux channel, as a regulator of lysosome positioning (Vergarajauregui et al., 2009; Li et al., 2016). In my studies, lysosomes remained clustered in the perinuclear regions of cells treated with a Dynamin inhibitor (Figure 10.1.5.**6**), thus suggesting that Dynamin-mediated endocytosis plays a role in regulating lysosomal positioning. Further studies are required to decipher the underlying mechanisms facilitating Dynamin-mediated lysosomal positioning and importantly to determine whether perinuclear positioning of lysosomes is maintained when mTORC1 is reactivated and autophagic lysosomal reformation is induced.

In a follow-up study, amino acid-starvation induced phagocytosis of Dextran-TMR in a TFEB-dependent manner (Figure 10.1.5.**1E-1F**). In the case of receptor-mediated endocytosis of EGF-TMR, amino acid starvation increased the quantity of intracellular EGF-TMR (Figure 10.1.5.**1G**). These data indicate that TFEB selectively stimulates a specific endocytic pathway during starvation. Moreover, growth factor receptors including insulin-like growth factor receptors (IGFR), fibroblast growth factor receptor (FGFR) and epidermal growth factor receptor (EGFR) were among the list of target genes identified in the TFEB ChIP-seq analyses. Interestingly, deregulated growth factor signaling upstream of TFEB have been implicated in neurodegeneration and cancer (Lowery and Yu, 2012; Buch, 2014; Reddy et al., 2016; Di Malta et al., 2017). Additionally, TFEB-mediated CLEAR network activity has been found attenuated in neurodegenerative disease models (Reddy et al., 2016) and upregulated in cells and tissues of patients and murine models of cancers such as renal cell carcinoma, pancreatic ductal adenocarcinoma and melanomas harboring defective growth factor signaling (Di Malta et al. 2016). Therefore more studies are needed in order to determine the role of TFEB in these signaling pathways.

Endocytosis mediates lysosomal degradation of extracellular materials and plays a key role in the acidification and maturation of lysosomes. Given these metabolic roles of endocytosis, I sought to see whether endocytosis and accompanying molecular trafficking are necessary for autophagy flux. Autophagy flux is described as the measure of autophagic degradation activity and is detected by observing accumulation and subsequent degradation of autophagosome

markers such as the phosphatidylethanolamine-conjugated form of microtubule-associated protein 1A/1B-light chain 3 (LC3-II) in lysosomes (Medina et al., 2011; Munson et al., 2015). In cells deficient of Dynamin GTPase or Dynein motor protein activity, TFEB relocalized to the nucleus (Figure 10.1.5.**5A-5D**) and was able turn on transcription of target genes including Mucolipin1, autophagosome markers LC3 and P62/SQSTM1 (Figure 10.1.5.**5D**). Although TFEB translocated to the nucleus and turned on gene expression under Dynasore or Ciliobrevin drug treatments, mTORC1 remained inactive, further supporting the role of endocytosis and retrograde trafficking in the TFEB-mediated reactivation of mTORC1 signaling. Inhibition of Dynamin or Dynein resulted in the accumulation of autophagosomes within 6 hours of amino acid starvation, indicating an inhibition of TFEB-mediated autophagy flux (Figure 10.1.5.**6**). Subsequent immunofluorescence analyses revealed that both Dynamin and Dynein inhibition caused a depletion in the quantity of lysosomes (Figures 10.1.5.**5E** and **6A**). Although more studies are required in order to fully understand the intricate roles of endocytic trafficking during autophagy flux, this reduction in lysosomal quantity could be as a result of inhibiting upstream endocytic trafficking of lysosomal hydrolases and components of the vATPase proton pump to lysosomes, all of which are required for lysosomal acidification and maturation of endosomes into lysosomes.

Lastly, there are mTORC1-independent mechanisms that regulate TFEB activity. These pathways include the direct phosphorylation of TFEB on Ser467 and Ser142 by Akt and ERK respectively (Settembre et al., 2011; Palmieri et al.,

2017). Both kinases activate mTORC1 through phosphorylation and inhibition of the TSC complex in response to growth factors (Laplante and Sabatini, 2012). Akt, is a member of the AGC serine/threonine family of protein kinases that plays a crucial role in the regulation of cell survival and apoptosis (Engelman et al., 2017). Recent studies now show that selective inhibition of Akt with a non-reducing disaccharide of glucose, trehalose, enhances autophagic clearance of proteolipid aggregates, reduces neuropathology and subsequently prolongs survival of mouse models of neurodegenerative diseases harboring defective lysosomal signaling (Palmieri et al., 2017). In my endosomal cell fractionation experiments in which TFEB was overexpressed in CAD cells and endosomal fractions of these cells analyzed via immunoblots, the concentration of active Akt (Thr308) increased in less dense optiprep fractions containing early endosome marker Rab5. Further analyses confirmed that TFEB overexpression promotes formation of endosomes carrying active Akt. These findings, along with Palmieri's data suggest a feedback mechanism in which active TFEB stimulates endocytosis of activated Akt to restore mTORC1 activity during amino acid starvation in order to promote ALR, the Akt-TFEB/ERK-TFEB pathways could be serving as alternative mechanism induced during starvation to further suppress autophagy and enhance lysosomal reformation. Further studies are still needed to determine the isoform or intracellular pool of Akt that is responsible for repressing TFEB nuclear translocation because Akt2, the alternatively spliced isoform of Akt have been reported as the only isoform to localize to endosomal membranes (Walz et al., 2010). Also the role of ERK in the reactivation of mTORC1 during amino acid

starvation should be further investigated. ERK activates mTORC1 through phosphorylation of TSC2 and further represses autophagy induction by phosphorylating TFEB to repress its nuclear localization. ERK have been found to localize to endosomal membranes (Teis et al., 2002), and as such it will be interesting to see whether TFEB-overexpression would stimulate synthesis of signaling endosomes carrying active ERK. If proven true, it will further confirm that starvation stimulates endocytosis in a TFEB-dependent manner to reactivate mTORC1 and promote lysosomal biogenesis.

11.2. Bibliography

Alers, S., Löffler, A.S., Wesselborg, S., and Stork, B. (2012). Role of AMPK-mTOR-Ulk1/2 in the regulation of autophagy: cross talk, shortcuts, and feedbacks. Mol. Cell. Biol. *32*, 2–11.

Andrews, N.W. (2000). Regulated secretion of conventional lysosomes. Trends Cell Biol. *10*, 316–321.

Andrews, N.W. (2005). Membrane repair and immunological danger. EMBO Rep. *6*, 826–830.

Barth, J.M.I., and Köhler, K. (2014). How to take autophagy and endocytosis up a notch. Biomed Res. Int. 2014, 960803.

Bejarano, E., and Cuervo, A.M. (2010). Chaperone-mediated autophagy. Proc. Am. Thorac. Soc. *7*, 29–39.

Betz, C., and Hall, M.N. (2013). Where is mTOR and what is it doing there? J. Cell Biol. *203*, 563–574.

Bosch, M., Marí, M., Herms, A., Fernández, A., Fajardo, A., Kassan, A., Giralt, A., Colell, A., Balgoma, D., Barbero, E., et al. (2011). Caveolin-1 deficiency causes cholesterol-dependent mitochondrial dysfunction and apoptotic susceptibility. Curr. Biol. 21, 681–686.

Bossi, G., and Griffiths, G.M. (2005). CTL secretory lysosomes: biogenesis and secretion of a harmful organelle. Semin. Immunol. *17*, 87–94.

Buch, S. (2014). Growth factor signaling: implications for disease & therapeutics. J. Neuroimmune Pharmacol. 9, 65–68.

Boucrot, E., Ferreira, A.P.A., Almeida-Souza, L., Debard, S., Vallis, Y., Howard, G., Bertot, L., Sauvonnet, N., and McMahon, H.T. (2015). Endophilin marks and controls a clathrin-independent endocytic pathway. Nature 517, 460–465.

Budanov, A. V., and Karin, M. (2008). p53 Target Genes Sestrin1 and Sestrin2 Connect Genotoxic Stress and mTOR Signaling. Cell *134*, 451–460.

Chauhan, S., Goodwin, J.G., Chauhan, S., Manyam, G., Wang, J., Kamat, A.M., and Boyd, D.D. (2013). ZKSCAN3 Is a Master Transcriptional Repressor of Autophagy. Mol. Cell *50*, 16–28.

Chen, Y., and Yu, L. (2013). Autophagic lysosome reformation. Exp. Cell Res. *319*, 142–146.

Codogno, P., Mehrpour, M., and Proikas-Cezanne, T. (2012). Canonical and non-canonical autophagy: Variations on a common theme of self-eating? Nat. Rev. Mol. Cell Biol. *13*, 7–12.

Cuervo, A.M. (2010). Chaperone-mediated autophagy: selectivity pays off. Trends

Endocrinol. Metab. *21*, 142–150.

Ewers, H., and Helenius, A. (2011). Lipid-mediated endocytosis. Cold Spring Harb. Perspect. Biol. 3, a004721.

Decressac, M., Mattsson, B., Weikop, P., Lundblad, M., Jakobsson, J., and Bjorklund, A. (2013). TFEB-mediated autophagy rescues midbrain dopamine neurons from -synuclein toxicity. Proc. Natl. Acad. Sci. *110*, E1817–E1826.

Degerman Gunnarsson, M., Lannfelt, L., Ingelsson, M., Basun, H., and Kilander, L. (2014). High tau levels in cerebrospinal fluid predict rapid decline and increased dementia mortality in Alzheimer's disease. Dement. Geriatr. Cogn. Disord. 37, 196–206.

Dehay, B., Bové, J., Rodríguez-Muela, N., Perier, C., Recasens, A., Boya, P., and Vila, M. (2010). Pathogenic lysosomal depletion in Parkinson's disease. J. Neurosci. *30*, 12535–12544.

Dibble, C.C., and Cantley, L.C. (2015). Regulation of mTORC1 by PI3K signaling. Trends Cell Biol. *25*, 1–11.

Dibble, C.C., and Manning, B.D. (2013). Signal integration by mTORC1 coordinates nutrient input with biosynthetic output. Nat. Cell Biol. *15*, 555–564.

Dice, J.F. (2007). Chaperone-mediated autophagy. Autophagy *3*, 295–299.

Dobrowolski, R., and De Robertis, E.M. (2012). Endocytic control of growth factor signaling: multivesicular bodies as signaling organelles. Nat. Rev. Mol. Cell Biol. *13*, 53–60.

Doherty, G.J., and McMahon, H.T. (2009). Mechanisms of endocytosis. Annu. Rev. Biochem. *78*, 857–902.

Fang, X., Zhou, J., Liu, W., Duan, X., Gala, U., Sandoval, H., Jaiswal, M., and Tong, C. (2016). Dynamin Regulates Autophagy by Modulating Lysosomal Function. J. Genet. Genomics 43, 77–86.

Feng, D., Liu, L., Zhu, Y., and Chen, Q. (2013). Molecular signaling toward mitophagy and its physiological significance. Exp. Cell Res. *319*, 1697–1705.

Ferron, M., Settembre, C., Shimazu, J., Lacombe, J., Kato, S., Rawlings, D.J., Ballabio, A., and Karsenty, G. (2013). A RANKL-PKC -TFEB signaling cascade is necessary for lysosomal biogenesis in osteoclasts. Genes Dev. *27*, 955–969.

Flinn, R.J., Yan, Y., Goswami, S., Parker, P.J., and Backer, J.M. (2010). The late endosome is essential for mTORC1 signaling. Mol. Biol. Cell 21, 833–841.

Frank, P.G., Cheung, M.W.-C., Pavlides, S., Llaverias, G., Park, D.S., and Lisanti, M.P. (2006). Caveolin-1 and regulation of cellular cholesterol homeostasis. Am. J. Physiol. Heart Circ. Physiol. 291, H677-86.

Fruscio, G. Di, Schulz, A., Cegli, R. De, Savarese, M., Mutarelli, M., Parenti, G., Ban, S., Braulke, T., Nigro, V., and Ballabio, A. (2015). Lysoplex : An efficient

toolkit to detect DNA sequence variations in the autophagy-lysosomal pathway. *11*.

Gatto, F., Rossi, B., Tarallo, A., Polishchuk, E., Polishchuk, R., Carrella, A., Nusco, E., Alvino, F.G., Iacobellis, F., De Leonibus, E., et al. (2017). AAV-mediated transcription factor EB (TFEB) gene delivery ameliorates muscle pathology and function in the murine model of Pompe Disease. Sci. Rep. *7*, 15089.

Giatromanolaki, A., Kalamida, D., Sivridis, E., Karagounis, I. V., Gatter, K.C., Harris, A.L., and Koukourakis, M.I. (2015). Increased expression of transcription factor EB (TFEB) is associated with autophagy, migratory phenotype and poor prognosis in non-small cell lung cancer. Lung Cancer *90*, 98–105.

Hinshaw, J.E. (2000). Dynamin and Its Role in Membrane Fission. Annu. Rev. Cell Dev. Biol. 16, 483–519.

Huotari, J., and Helenius, A. (2011). Endosome maturation. EMBO J. 30, 3481–3500.

Vander Haar, E., Lee, S.-I., Bandhakavi, S., Griffin, T.J., and Kim, D.-H. (2007). Insulin signaling to mTOR mediated by the Akt/PKB substrate PRAS40. Nat. Cell Biol. *9*, 316–323.

Hallsson, J.H., Haflidadóttir, B.S., Stivers, C., Odenwald, W., Arnheiter, H., Pignoni, F., and Steingrímsson, E. (2004). The basic helix-loop-helix leucine zipper transcription factor Mitf is conserved in Drosophila and functions in eye development. Genetics *167*, 233–241.

Hamasaki, M., Furuta, N., Matsuda, A., Nezu, A., Yamamoto, A., Fujita, N., Oomori, H., Noda, T., Haraguchi, T., Hiraoka, Y., et al. (2013). Autophagosomes form at ER-mitochondria contact sites. Nature *495*, 389–393.

Hara, K., Maruki, Y., Long, X., Yoshino, K., Oshiro, N., Hidayat, S., Tokunaga, C., Avruch, J., and Yonezawa, K. (2002). Raptor, a Binding Partner of Target of Rapamycin (TOR), Mediates TOR Action. Cell *110*, 177–189.

Hershey, C.L., and Fisher, D.E. (2004). Mitf and Tfe3: Members of a b-HLH-ZIP transcription factor family essential for osteoclast development and function. Bone *34*, 689–696.

Jacinto, E., Loewith, R., Schmidt, A., Lin, S., Rüegg, M.A., Hall, A., and Hall, M.N. (2004). Mammalian TOR complex 2 controls the actin cytoskeleton and is rapamycin insensitive. Nat. Cell Biol. *6*.

Jaiswal, J.K., Andrews, N.W., and Simon, S.M. (2002). Membrane proximal lysosomes are the major vesicles responsible for calcium-dependent exocytosis in nonsecretory cells. J. Cell Biol. *159*, 625–635.

Jiang, P., and Mizushima, N. (2014). Autophagy and human diseases. Cell Res. *24*, 69–79.

Kaizuka, T., Hara, T., Oshiro, N., Kikkawa, U., Yonezawa, K., Takehana, K.,

Iemura, S.-I., Natsume, T., and Mizushima, N. (2010). Tti1 and Tel2 are critical factors in mammalian target of rapamycin complex assembly. J. Biol. Chem. *285*, 20109–20116.

Kang, S.W., Wahl, M.I., Chu, J., Kitaura, J., Kawakami, Y., Kato, R.M., Tabuchi, R., Tarakhovsky, A., Kawakami, T., Turck, C.W., et al. (2001). PKCbeta modulates antigen receptor signaling via regulation of Btk membrane localization. EMBO J. *20*, 5692–5702.

Kaur, J., and Debnath, J. (2015). Autophagy at the crossroads of catabolism and anabolism. Nat. Rev. Mol. Cell Biol. *16*, 461–472.

Khayati, K., Antikainen, H., Bonder, E.M., Weber, G.F., Kruger, W.D., Jakubowski, H., and Dobrowolski, R. (2016). The amino acid metabolite homocysteine activates mTORC1 to inhibit autophagy and form abnormal proteins in human neurons and mice. FASEB J. fj.201600915R.

Kim, D.-H., Sarbassov, D.D., Ali, S.M., Latek, R.R., Guntur, K.V.., Erdjument-Bromage, H., Tempst, P., and Sabatini, D.M. (2003). GβL, a Positive Regulator of the Rapamycin-Sensitive Pathway Required for the Nutrient-Sensitive Interaction between Raptor and mTOR. Mol. Cell *11*, 895–904.

Komatsu, M., Waguri, S., Chiba, T., Murata, S., Iwata, J., Tanida, I., Ueno, T., Koike, M., Uchiyama, Y., Kominami, E., et al. (2006). Loss of autophagy in the central nervous system causes neurodegeneration in mice. Nature *441*, 880–884.

Kon, M., and Cuervo, A.M. (2010). Chaperone-mediated autophagy in health and disease. FEBS Lett. *584*, 1399–1404.

Korolchuk, V.I., Saiki, S., Lichtenberg, M., Siddiqi, F.H., Roberts, E.A., Imarisio, S., Jahreiss, L., Sarkar, S., Futter, M., Menzies, F.M., et al. (2011). Lysosomal positioning coordinates cellular nutrient responses. Nat. Cell Biol. *13*, 453–460.

Kroemer, G., Mariño, G., and Levine, B. (2010). Autophagy and the integrated stress response. Mol. Cell *40*, 280–293.

Lamb, C.A., Dooley, H.C., and Tooze, S.A. (2013). Endocytosis and autophagy: Shared machinery for degradation. BioEssays 35, 34–45.

Laplante, M., and Sabatini, D.M. (2012). mTOR signaling in growth control and disease. Cell *149*, 274–293.

Levine, B., and Klionsky, D.J. (2004). Development by self-digestion: Molecular mechanisms and biological functions of autophagy. Dev. Cell *6*, 463–477.

Lie, D.-C., Colamarino, S.A., Song, H.-J., Désiré, L., Mira, H., Consiglio, A., Lein, E.S., Jessberger, S., Lansford, H., Dearie, A.R., et al. (2005). Wnt signaling regulates adult hippocampal neurogenesis. Nature 437, 1370–1375.

Li, X., Rydzewski, N., Hider, A., Zhang, X., Yang, J., Wang, W., Gao, Q., Cheng, X., and Xu, H. (2016). A molecular mechanism to regulate lysosome motility for lysosome positioning and tubulation. Nat. Cell Biol. 18, 404–417.

Lipinski, M.M., Zheng, B., Lu, T., Yan, Z., Py, B.F., Ng, A., Xavier, R.J., Li, C., Yankner, B.A., Scherzer, C.R., et al. (2010). Genome-wide analysis reveals mechanisms modulating autophagy in normal brain aging and in Alzheimer's disease. Proc. Natl. Acad. Sci. U. S. A. *107*, 14164–14169.

Luzio, J.P., Pryor, P.R., and Bright, N.A. (2007). Lysosomes: Fusion and function. Nat. Rev. Mol. Cell Biol. 8, 622–632.

Luzio, J.P., Hackmann, Y., Dieckmann, N.M.G., and Griffiths, G.M. (2014). The biogenesis of lysosomes and lysosome-related organelles. Cold Spring Harb. Perspect. Biol. *6*, a016840.

Di Malta, C., Siciliano, D., Calcagni, A., Monfregola, J., Pastore, N., Eastes, A.N., Davis, O., Cegli, R. De, Giovannantonio, L.G. Di, Nusco, E., et al. (2017). TRANSCRIPTIONAL REGULATION OF RAGD GTPASE CONTROLS mTORC1 ACTIVITY. Science (80-.). *in press*, 1–8.

Marchand, B., Arsenault, D., Raymond-Fleury, A., Boisvert, F.-M., and Boucher, M.-J. (2015). Glycogen Synthase Kinase-3 (GSK3) Inhibition Induces Prosurvival Autophagic Signals in Human Pancreatic Cancer Cells. J. Biol. Chem. *290*, 5592–5605.

Martina, J.A., Chen, Y., Gucek, M., and Puertollano, R. (2012). MTORC1 functions as a transcriptional regulator of autophagy by preventing nuclear transport of TFEB. Autophagy *8*, 903–914.

Martina, J.A., Diab, H.I., Brady, O.A., and Puertollano, R. (2016). TFEB and TFE3 are novel components of the integrated stress response. EMBO J. *35*, 479–495.

Medina, D.L., Fraldi, A., Bouche, V., Annunziata, F., Mansueto, G., Spampanato, C., Puri, C., Pignata, A., Martina, J.A., Sardiello, M., et al. (2011). Transcriptional activation of lysosomal exocytosis promotes cellular clearance. Dev. Cell *21*, 421–430.

Medina, D.L., Di Paola, S., Peluso, I., Armani, A., De Stefani, D., Venditti, R., Montefusco, S., Scotto-Rosato, A., Prezioso, C., Forrester, A., et al. (2015). Lysosomal calcium signalling regulates autophagy through calcineurin and TFEB. Nat. Cell Biol. *17*, 288–299.

Menon, S., Dibble, C.C., Talbott, G., Hoxhaj, G., Valvezan, A.J., Takahashi, H., Cantley, L.C., and Manning, B.D. (2014). Spatial control of the TSC complex integrates insulin and nutrient regulation of mTORC1 at the lysosome. Cell *156*, 771–785.

Menzies, F.M., Fleming, A., and Rubinsztein, D.C. (2015). Compromised autophagy and neurodegenerative diseases. Nat. Rev. Neurosci. *16*, 345–357.

Mizushima, N., Yoshimori, T., and Levine, B. (2010). Methods in Mammalian Autophagy Research. Cell *140*, 313–326.

Mora, R., Bonilha, V.L., Marmorstein, A., Scherer, P.E., Brown, D., Lisanti, M.P., and Rodriguez-Boulan, E. (1999). Caveolin-2 localizes to the Golgi complex but

redistributes to plasma membrane, caveolae, and rafts when co-expressed with caveolin-1. J. Biol. Chem. 274, 25708–25717.

Motyckova, G., Weilbaecher, K.N., Horstmann, M., Rieman, D.J., Fisher, D.Z.E., and Fisher, D.Z.E. (2001). Linking osteopetrosis and pycnodysostosis: regulation of cathepsin K expression by the microphthalmia transcription factor family. Proc. Natl. Acad. Sci. U. S. A. *98*, 5798–5803.

Mukherjee, S., Ghosh, R.N., and Maxfield, F.R. (1997). Endocytosis. Physiol. Rev. *77*, 759–803.

Munson, M.J., Allen, G.F., Toth, R., Campbell, D.G., Lucocq, J.M., and Ganley, I.G. (2015). mTOR activates the VPS34-UVRAG complex to regulate autolysosomal tubulation and cell survival. EMBO J. 34, 2272–2290.

Nada, S., Hondo, A., Kasai, A., Koike, M., Saito, K., Uchiyama, Y., and Okada, M. (2009). The novel lipid raft adaptor p18 controls endosome dynamics by anchoring the MEK–ERK pathway to late endosomes. EMBO J. *28*, 477–489.

Napolitano, G., and Ballabio, A. (2016). TFEB at a glance. J. Cell Sci. *129*, 2475–2481.

Neefjes, J., and van der Kant, R. (2014). Stuck in traffic: an emerging theme in diseases of the nervous system. Trends Neurosci. *37*, 66–76.

Nezich, C.L., Wang, C., Fogel, A.I., and Youle, R.J. (2015). MiT/TFE transcription factors are activated during mitophagy downstream of Parkin and Atg5. J. Cell Biol. *210*, 435–450.

Nixon, R. (2013). The role of autophagy in neurodegenerative disease. Nat. Med. *19*, 983–997.

Nixon, R.A. (2005). Endosome function and dysfunction in Alzheimer's disease and other neurodegenerative diseases. Neurobiol. Aging *26*, 373–382.

Nnah, I.C., Khayati, K., and Dobrowolski, R. (2015). Cellular metabolism and lysosomal mTOR signaling. Cell Death Ther. *1*.

Nojima, H., Tokunaga, C., Eguchi, S., Oshiro, N., Hidayat, S., Yoshino, K., Hara, K., Tanaka, N., Avruch, J., and Yonezawa, K. (2003). The mammalian target of rapamycin (mTOR) partner, raptor, binds the mTOR substrates p70 S6 kinase and 4E-BP1 through their TOR signaling (TOS) motif. J. Biol. Chem. *278*, 15461–15464.

Palmieri, M., Impey, S., Kang, H., di Ronza, A., Pelz, C., Sardiello, M., and Ballabio, A. (2011). Characterization of the CLEAR network reveals an integrated control of cellular clearance pathways. Hum. Mol. Genet. *20*, 3852–3866.

Palmieri, M., Pal, R., Nelvagal, H.R., Lotfi, P., Stinnett, G.R., Seymour, M.L., Chaudhury, A., Bajaj, L., Bondar, V. V., Bremner, L., et al. (2017). mTORC1-independent TFEB activation via Akt inhibition promotes cellular clearance in neurodegenerative storage diseases. Nat. Commun. *8*, 14338.

Parenti, G., Andria, G., and Ballabio, A. (2015). Lysosomal Storage Diseases: From Pathophysiology to Therapy. Annu. Rev. Med. *66*, 471–486.

Pearce, L.R., Huang, X., Boudeau, J., Pawłowski, R., Wullschleger, S., Deak, M., Ibrahim, A.F.M., Gourlay, R., Magnuson, M.A., and Alessi, D.R. (2007). Identification of Proctor as a novel Rictor-binding component of mTOR complex-2. Biochem. J. *405*.

Peña-Llopis, S., Vega-Rubin-de-Celis, S., Schwartz, J.C., Wolff, N.C., Tran, T.A.T., Zou, L., Xie, X.-J., Corey, D.R., and Brugarolas, J. (2011). Regulation of TFEB and V-ATPases by mTORC1. EMBO J. *30*, 3242–3258.

Peterson, T.R., Laplante, M., Thoreen, C.C., Sancak, Y., Kang, S.A., Kuehl, W.M., Gray, N.S., and Sabatini, D.M. (2009). DEPTOR Is an mTOR Inhibitor Frequently Overexpressed in Multiple Myeloma Cells and Required for Their Survival. Cell *137*, 873–886.

Platta, H.W., and Stenmark, H. (2011). Endocytosis and signaling. Curr. Opin. Cell Biol. *23*, 393–403.

Pichler, H., and Riezman, H. (2004). Where sterols are required for endocytosis. Biochim. Biophys. Acta - Biomembr. 1666, 51–61.

Puertollano, R. (2014). mTOR and lysosome regulation. F1000Prime Rep. *6*.

Raben, N., and Puertollano, R. (2016). TFEB and TFE3: Linking Lysosomes to Cellular Adaptation to Stress*. Annu. Rev. Cell Dev. Biol. *32*, 255–278.

Reddy, K., Cusack, C.L., Nnah, I.C., Khayati, K., Saqcena, C., Huynh, T.B., Noggle, S.A., Ballabio, A., and Dobrowolski, R. (2016). Dysregulation of Nutrient Sensing and CLEARance in Presenilin Deficiency. Cell Rep. *14*, 2166–2179.

Rehli, M., Elzen, N. Den, Cassady, A.I., Ostrowski, M.C., Hume, D.A., and Den Elzen, N. (1999). Cloning and characterization of the murine genes for bHLH-ZIP transcription factors TFEC and TFEB reveal a common gene organization for all MiT subfamily members. Genomics *3*, 111–120.

Rong, Y., McPhee, C.K., Deng, S., Huang, L., Chen, L., Liu, M., Tracy, K., Baehrecke, E.H., Yu, L., and Lenardo, M.J. (2011). Spinster is required for autophagic lysosome reformation and mTOR reactivation following starvation. Proc Natl Acad Sci U S A *108*, 7826–7831.

Rong, Y., Liu, M., Ma, L., Du, W., Zhang, H., Tian, Y., Cao, Z., Li, Y., Ren, H., Zhang, C., et al. (2012). Clathrin and phosphatidylinositol-4,5-bisphosphate regulate autophagic lysosome reformation. Nat Cell Biol *14*, 924–934.

Rothberg, K.G., Heuser, J.E., Donzell, W.C., Ying, Y.-S., Glenney, J.R., and Anderson, R.G.W. (1992). Caveolin, a protein component of caveolae membrane coats. Cell 68, 673–682.

Sancak, Y., Thoreen, C.C., Peterson, T.R., Lindquist, R.A., Kang, S.A., Spooner, E., Carr, S.A., and Sabatini, D.M. (2007). PRAS40 Is an Insulin-Regulated Inhibitor

of the mTORC1 Protein Kinase. Mol. Cell *25*, 903–915.

Sancak, Y., Bar-Peled, L., Zoncu, R., Markhard, A.L., Nada, S., and Sabatini, D.M. (2010). Ragulator-rag complex targets mTORC1 to the lysosomal surface and is necessary for its activation by amino acids. Cell *141*, 290–303.

Sarbassov, D.D., Ali, S.M., Sengupta, S., Sheen, J.-H., Hsu, P.P., Bagley, A.F., Markhard, A.L., and Sabatini, D.M. (2006). Prolonged Rapamycin Treatment Inhibits mTORC2 Assembly and Akt/PKB. Mol. Cell *22*, 159–168.

Sardiello, M. (2016). Transcription factor EB: from master coordinator of lysosomal pathways to candidate therapeutic target in degenerative storage diseases. Ann. N. Y. Acad. Sci. *1371*, 3–14.

Sardiello, M., Palmieri, M., di Ronza, A., Medina, D.L., Valenza, M., Gennarino, V.A., Di Malta, C., Donaudy, F., Embrione, V., Polishchuk, R.S., et al. (2009). A gene network regulating lysosomal biogenesis and function. Science *325*, 473–477.

Saxton, R.A., and Sabatini, D.M. (2017). mTOR Signaling in Growth, Metabolism, and Disease. Cell *168*, 960–976.

Schalm, S.S., Fingar, D.C., Sabatini, D.M., and Blenis, J. (2003). TOS Motif-Mediated Raptor Binding Regulates 4E-BP1 Multisite Phosphorylation and Function. Curr. Biol. *13*, 797–806.

Schulze, R.J., Weller, S.G., Schroeder, B., Krueger, E.W., Chi, S., Casey, C.A., and McNiven, M.A. (2013). Lipid droplet breakdown requires Dynamin 2 for vesiculation of autolysosomal tubules in hepatocytes. J. Cell Biol. 203, 315–326.

Settembre, C., Di Malta, C., Polito, V.A., Garcia Arencibia, M., Vetrini, F., Erdin, S., Erdin, S.U., Huynh, T., Medina, D., Colella, P., et al. (2011). TFEB links autophagy to lysosomal biogenesis. Science *332*, 1429–1433.

Settembre, C., Fraldi, A., Medina, D.L., and Ballabio, A. (2013). Signals from the lysosome: a control center for cellular clearance and energy metabolism. Nat. Rev. Mol. Cell Biol. *14*, 283–296.

Shintani, T., and Klionsky, D.J. (2004). Autophagy in health and disease: a double-edged sword. Science *306*, 990–995.

Sidransky, E., Nalls, M.A., Aasly, J.O., Aharon-Peretz, J., Annesi, G., Barbosa, E.R., Bar-Shira, A., Berg, D., Bras, J., Brice, A., et al. (2009). Multicenter Analysis of Glucocerebrosidase Mutations in Parkinson's Disease. N. Engl. J. Med. *361*, 1651–1661.

Sandro Sonnino, *, Alessandro Prinetti, Laura Mauri, Vanna Chigorno, and, and Tettamanti, G. (2006). Dynamic and Structural Properties of Sphingolipids as Driving Forces for the Formation of Membrane Domains.

Sonnino, S., Mauri, L., Chigorno, V., and Prinetti, A. (2007). Gangliosides as components of lipid membrane domains. Glycobiology 17, 1R–13R.

Sorkin, A., and von Zastrow, M. (2009). Endocytosis and signaling: intertwining molecular networks. Nat. Rev. Mol. Cell Biol. *10*, 609–622.

Stenmark, H., Parton, R.G., Steele-Mortimer, O., Lütcke, A., Gruenberg, J., and Zerial, M. (1994). Inhibition of rab5 GTPase activity stimulates membrane fusion in endocytosis. EMBO J. 13, 1287–1296.

Teis, D., Wunderlich, W., and Huber, L.A. (2002). Localization of the MP1-MAPK scaffold complex to endosomes is mediated by p14 and required for signal transduction. Dev. Cell 3, 803–814.

Thorn, H., Stenkula, K.G., Karlsson, M., Ortegren, U., Nystrom, F.H., Gustavsson, J., and Stralfors, P. (2003). Cell surface orifices of caveolae and localization of caveolin to the necks of caveolae in adipocytes. Mol. Biol. Cell 14, 3967–3976.

Tucker, W.C. (2004). Reconstitution of Ca2+-Regulated Membrane Fusion by Synaptotagmin and SNAREs. Science (80-.). *304*, 435–438.

Urrutia, R. (2003). KRAB-containing zinc-finger repressor proteins. Genome Biol. *4*, 231.

Vergarajauregui, S., Martina, J.A., and Puertollano, R. (2009). Identification of the penta-EF-hand protein ALG-2 as a Ca2+-dependent interactor of Mucolipin-1. J. Biol. Chem. 284, 36357–36366.

Vieira, A. V., Lamaze, C., and Schmid, S.L. (1996). Control of EGF Receptor Signaling by Clathrin-Mediated Endocytosis. Science (80-.). 274, 2086–2089.

Vomastek, T., Iwanicki, M.P., Burack, W.R., Tiwari, D., Kumar, D., Parsons, J.T., Weber, M.J., and Nandicoori, V.K. (2008). Extracellular signal-regulated kinase 2 (ERK2) phosphorylation sites and docking domain on the nuclear pore complex protein Tpr cooperatively regulate ERK2-Tpr interaction. Mol. Cell. Biol. *28*, 6954–6966.

Walz, H.A., Shi, X., Chouinard, M., Bue, C.A., Navaroli, D.M., Hayakawa, A., Zhou, Q.L., Nadler, J., Leonard, D.M., and Corvera, S. (2010). Isoform-specific regulation of Akt signaling by the endosomal protein WDFY2. J. Biol. Chem. 285, 14101–14108.

Wang, L., Harris, T.E., Roth, R.A., and Lawrence, J.C. (2007). PRAS40 regulates mTORC1 kinase activity by functioning as a direct inhibitor of substrate binding. J. Biol. Chem. *282*, 20036–20044.

Way, M., and Parton, R.G. (1996). M-caveolin, a muscle-specific caveolin-related protein. FEBS Lett. 378, 108–112.

Wedaman, K.P., Reinke, A., Anderson, S., Yates, J., McCaffery, J.M., and Powers, T. (2003). Tor kinases are in distinct membrane-associated protein complexes in Saccharomyces cerevisiae. Mol. Biol. Cell 14, 1204–1220.

Willett, R., Martina, J.A., Zewe, J.P., Wills, R., Hammond, G.R. V., and Puertollano, R. (2017). TFEB regulates lysosomal positioning by modulating TMEM55B

expression and JIP4 recruitment to lysosomes. Nat. Commun. 8, 1580.

Wolfson, R.L., Chantranupong, L., Wyant, G.A., Gu, X., Orozco, J.M., Shen, K., Condon, K.J., Petri, S., Kedir, J., Scaria, S.M., et al. (2017). KICSTOR recruits GATOR1 to the lysosome and is necessary for nutrients to regulate mTORC1. Nature *543*, 438–442.

Wu, F., and Yao, P.J. (2009). Clathrin-mediated endocytosis and Alzheimer's disease: An update. Ageing Res. Rev. *8*, 147–149.

Wullschleger, S., Loewith, R., and Hall, M.N. (2006). TOR signaling in growth and metabolism. Cell *124*, 471–484.

Yamamoto, H., Komekado, H., and Kikuchi, A. (2006). Caveolin Is Necessary for Wnt-3a-Dependent Internalization of LRP6 and Accumulation of β-Catenin. Dev. Cell 11, 213–223.

Yamasaki, T., Takahashi, A., Pan, J., Yamaguchi, N., and Yokoyama, K.K. (2009). Phosphorylation of Activation Transcription Factor-2 at Serine 121 by Protein Kinase C Controls c-Jun-mediated Activation of Transcription. J. Biol. Chem. *284*, 8567–8581.

Yang, Z., and Klionsky, D.J. (2010). Mammalian autophagy: core molecular machinery and signaling regulation. Curr. Opin. Cell Biol. *22*, 124–131.

Yonezawa, K., Tokunaga, C., Oshiro, N., and Yoshino, K. (2004). Raptor, a binding partner of target of rapamycin. Biochem. Biophys. Res. Commun. *313*, 437–441.

Yu, L., McPhee, C.K., Zheng, L., Mardones, G.A., Rong, Y., Peng, J., Mi, N., Zhao, Y., Liu, Z., Wan, F., et al. (2010). Termination of autophagy and reformation of lysosomes regulated by mTOR. Nature *465*, 942–946.

Zhang, J., Zhou, W., Lin, J., Wei, P., Zhang, Y., Jin, P., Chen, M., Man, N., and Wen, L. (2016). Autophagic-lysosomal reformation depends on mTOR reactivation in H2O2-induced autophagy. Int. J. Biochem. Cell Biol. *70*, 76–81.

Zhao, Y., Xiong, X., and Sun, Y. (2011). DEPTOR, an mTOR Inhibitor, Is a Physiological Substrate of SCFβTrCP E3 Ubiquitin Ligase and Regulates Survival and Autophagy. Mol. Cell *44*, 304–316.

11.3. Appendices

Table 2: Set of all 623 endocytic genes regulated by TFEB

The shown 623-endocytic genes were regulated by overexpression of TFEB as previously described (Di Fruscio et al., 2015)

	Biological function; Biological process_NCBI	Bionformatics Tools	Genes
cytoplasm	protein transport		**AAGAB**
clathrin-coated vesicle	endocytosis		**AAK1**
endocytic vesicle	endosomal transport		**ABCA1**
lysosomal membrane	transmembrane transport		**ABCA2**
ATP-binding cassette (ABC) transporter complex	transmembrane transport		**ABCA7**
lysosomal membrane	transmembrane transport		**ABCB9**
cytoplasm	autophagy	amiGO	**ABL1**
cytoplasm	regulation of autophagy	amiGO	**ABL2**
recycling endosome membrane	protein transport		**ACAP1**
endosome membrane	protein localization to endosome		**ACAP2**
cellular_component	regulation of ARF GTPase activity		**ACAP3**
cytoplasm	regulation of ARF GTPase activity		**ADAP1**
early endosome	epinephrine binding		**ADRB1**
lysosome	endosome to lysosome transport	AmiGO and UniProt	**ADRB2**
integral component of plasma membrane	adrenergic receptor signaling pathway		**ADRB3**

cytoplasm	G-protein coupled acetylcholine receptor signaling pathway		**ADRBK1**
cytoplasm	desensitization of G-protein coupled receptor protein signaling pathway		**ADRBK2**
lysosome	protein deglycosylation		**AGA**
cytoplasm	small GTPase mediated signal transduction		**AGAP1**
nucleus	small GTPase mediated signal transduction		**AGAP2**
positive regulation of phagocytosis	endocytosis		**AHSG**
synaptic vesicle membrane	endocytosis		**AMPH**
endosome	vesicle targeting, trans-Golgi to endosome		**AP1AR**
trans-Golgi network membrane	post-Golgi vesicle-mediated transport		**AP1B1**
lysosomal membrane	post-Golgi vesicle-mediated transport		**AP1G1**
trans-Golgi network	vesicle-mediated transport		**AP1G2**
trans-Golgi network	endosome to melanosome transport		**AP1M1**
trans-Golgi network	vesicle targeting		**AP1M2**
trans-Golgi network membrane	receptor-mediated endocytosis		**AP1S1**
trans-Golgi network membrane	post-Golgi vesicle-mediated transport	Netview and AmiGO	**AP1S2**
trans-Golgi network membrane	post-Golgi vesicle-mediated transport		**AP1S3**
clathrin coat of trans-Golgi network vesicle	endocytosis		**AP2A1**
endocytic vesicle membrane	endocytosis		**AP2A2**

endocytic vesicle membrane	endocytosis		**AP2B1**
endocytic vesicle membrane	endocytosis		**AP2M1**
endocytic vesicle membrane	endocytosis		**AP2S1**
lysosomal membrane	protein targeting to lysosome		**AP3B1**
clathrin-coated vesicle membrane	post-Golgi vesicle-mediated transport		**AP3B2**
Golgi apparatus	transport of lysosomal membrane proteins		**AP3D1**
lysosome	protein targeting to lysosome	AmiGO and UniProt	**AP3M1**
Golgi apparatus	protein trafficking to lysosomes and specialized organelles		**AP3M2**
AP-3 adaptor complex	Endocytosis		**AP3S1**
AP-3 adaptor complex	Endocytosis		**AP3S2**
trans-Golgi network	vesicle-mediated transport		**AP4B1**
trans-Golgi network	vesicle-mediated transport		**AP4E1**
trans-Golgi network	Golgi to endosome transport		**AP4M1**
Golgi apparatus	vesicle-mediated transport		**AP4S1**
AP-type membrane coat adaptor complex	endosomal transport		**AP5B1**
AP-type membrane coat adaptor complex	endosomal transport		**AP5M1**
AP-type membrane coat adaptor complex	endosomal transport		**AP5S1**
AP-type membrane coat adaptor complex	endosomal transport		**AP5Z1**
endocytic vesicle	cholesterol transport		**APOA1**

early endosome	high-density lipoprotein particle clearance		**APOE**
integral component of plasma membrane	endocytosis		**APP**
trans-Golgi network	small GTPase mediated signal transduction		**ARAP1**
cytoplasm	small GTPase mediated signal transduction		**ARAP2**
cytoplasm	vesicle-mediated transport		**ARAP3**
Golgi membrane	post-Golgi vesicle-mediated transport		**ARF1**
Golgi apparatus	vesicle-mediated transport		**ARF5**
endocytic vesicle	vesicle-mediated transport		**ARF6**
Golgi-associated vesicle membrane	retrograde vesicle-mediated transport, Golgi to ER		**ARFGAP1**
Golgi apparatus	vesicle-mediated transport		**ARFGAP2**
Golgi apparatus	vesicle-mediated transport		**ARFGAP3**
trans-Golgi network	intracellular vesicular trafficking		**ARFGEF1**
trans-Golgi network	intracellular vesicular trafficking		**ARFGEF2**
Golgi membrane	intracellular protein transport		**ARFIP1**
trans-Golgi network	small GTPase mediated signal transduction		**ARFIP2**
trans-Golgi network	retrograde transport, endosome to Golgi		**ARFRP1**
membrane	receptor-mediated endocytosis		**ARHGAP27**
cytoplasm	protein transport		**ARHGAP33**
trans-Golgi network	Golgi to plasma membrane protein transport		**ARL1**
intracellular	small GTPase mediated signal transduction		**ARL10**

intracellular	small GTPase mediated signal transduction		**ARL11**
intracellular	small GTPase mediated signal transduction		**ARL13A**
cytoplasmic membrane-bounded vesicle	small GTPase mediated signal transduction		**ARL13B**
cytoplasmic membrane-bounded vesicle	small GTPase mediated signal transduction		**ARL14**
cytoplasm	biological_process		**ARL14EP**
cellular_component	biological_process		**ARL14EPL**
extracellular vesicular exosome	small GTPase mediated signal transduction		**ARL15**
Golgi apparatus	small GTPase mediated signal transduction		**ARL17A**
Golgi apparatus	small GTPase mediated signal transduction		**ARL17B**
mitochondrial intermembrane space	small GTPase mediated signal transduction		**ARL2**
mitochondrial intermembrane space	small GTPase mediated signal transduction		**ARL2BP**
Golgi apparatus	post-Golgi vesicle-mediated transport		**ARL3**
trans-Golgi network	small GTPase mediated signal transduction		**ARL4A**
trans-Golgi network	endocytic recycling		**ARL4C**
trans-Golgi network	small GTPase mediated signal transduction		**ARL4D**
intracellular	small GTPase mediated signal transduction		**ARL5A**
intracellular	small GTPase mediated signal transduction		**ARL5B**
intracellular	small GTPase mediated signal transduction		**ARL5C**

integral component of membrane	regulates actin dynamics and peripheral vesicular trafficking		**ARL6IP6**
intracellular	small GTPase mediated signal transduction		**ARL9**
cytoplasm	post-Golgi vesicle-mediated transport		**ARRB1**
endocytic vesicle	G-protein coupled receptor internalization		**ARRB2**
lysosome	autophagy		**ARSA**
lysosome	lysosome organization		**ARSB**
lysosomal lumen	ceramide metabolic process		**ASAH1**
cytoplasm	regulation of ARF GTPase activity		**ASAP1**
Golgi cisterna membrane	regulation of ARF GTPase activity		**ASAP2**
cytoplasm	positive regulation of ARF GTPase activity		**ASAP3**
integral component of plasma membrane	receptor-mediated endocytosis		**ASGR1**
integral component of membrane	lysosomal intracellular trafficking		**ATP6AP1**
integral component of membrane	cellular protein metabolic process		**ATP6AP2**
lysosomal membrane	transmembrane transport		**ATP6V0A2**
lysosomal membrane	transmembrane transport		**ATP6V0A4**
endosome membrane	transmembrane transport		**ATP6V0B**
lysosomal membrane	transmembrane transport		**ATP6V0C**
lysosomal membrane	transmembrane transport		**ATP6V0D1**
endosome membrane	transmembrane transport		**ATP6V0D2**
endosome membrane	transmembrane transport		**ATP6V0E1**
endosome membrane	transmembrane transport		**ATP6V0E2**

vacuolar proton-transporting V-type ATPase complex	transmembrane transport		**ATP6V1A**
vacuolar proton-transporting V-type ATPase complex	transmembrane transport		**ATP6V1B1**
vacuolar proton-transporting V-type ATPase complex	transmembrane transport		**ATP6V1B2**
vacuolar proton-transporting V-type ATPase complex	transmembrane transport		**ATP6V1C1**
vacuolar proton-transporting V-type ATPase complex	transmembrane transport		**ATP6V1C2**
vacuolar proton-transporting V-type ATPase complex	transmembrane transport		**ATP6V1D**
vacuolar proton-transporting V-type ATPase complex	transmembrane transport		**ATP6V1E1**
cytoplasm	transmembrane transport		**ATP6V1E2**
vacuolar proton-transporting V-type ATPase complex	transmembrane transport		**ATP6V1F**
vacuolar proton-transporting V-type ATPase complex	transmembrane transport		**ATP6V1G1**
vacuolar proton-transporting V-type ATPase complex	transmembrane transport		**ATP6V1G2**
vacuolar proton-transporting V-type ATPase complex	transmembrane transport		**ATP6V1G3**
vacuolar proton-transporting V-type ATPase complex	transmembrane transport		**ATP6V1H**

Azurophil granules, specialized lysosomes of the neutrophil	positive regulation of phagocytosis		**AZU1**
cytoplasm	endocytosis		**BIN1**
transport vesicle	secretion of lysosomal enzymes		**BLOC1S3**
BLOC-1 complex	intracellular vesicular trafficking		**BLOC1S4**
BLOC-1 complex	endosome to melanosome transport		**BLOC1S5**
BLOC-1 complex	intracellular vesicular trafficking; secretion of lysosomal enzymes		**BLOC1S6**
endocytic vesicle membrane	caveolin-mediated endocytosis		**CAV1**
integral component of plasma membrane	vesicle organization		**CAV2**
plasma membrane	endocytosis		**CAV3**
plasma membrane	positive regulation of receptor-mediated endocytosis		**CBL**
plasma membrane	signal transduction		**CBLB**
nucleus	cell surface receptor signaling pathway		**CBLC**
endosome	chemokine-mediated signaling pathway		**CCR5**
endocytic vesicle	defense response to virus		**CD207**
endocytic vesicle	regulation of receptor-mediated endocytosis		**CD2AP**
cytoplasm	endocytosis		**CDC42**
external side of plasma membrane	regulation of endocytosis		**CDH13**
early endosome	transmembrane transport		**CFTR**

Rab-protein geranylgeranyltransferase complex	vesicular trafficking, exocytosis		**CHM**
Rab-protein geranylgeranyltransferase complex	intracellular protein transport		**CHML**
late endosome membrane	protein transport		**CHMP1B**
late endosome membrane	endosomal transport		**CHMP2A**
late endosome membrane	endosomal transport		**CHMP2B**
late endosome membrane	endosomal transport		**CHMP3**
late endosome membrane	endosomal transport		**CHMP4A**
late endosome membrane	endosomal transport		**CHMP4B**
late endosome membrane	endosomal transport		**CHMP4C**
endosome membrane	endosome to lysosome transport		**CHMP5**
late endosome membrane	endosomal transport		**CHMP6**
chloride channel complex	transmembrane transport		**CLCN1**
chloride channel complex	transmembrane transport		**CLCN2**
plasma membranes and in intracellular vesicles	transmembrane transport		**CLCN3**
endosome membrane	transmembrane transport		**CLCN4**
lysosomal membrane	endocytosis		**CLCN5**
lysosomal membrane	transmembrane transport		**CLCN6**
lysosomal membrane	chloride transmembrane transport		**CLCN7**
chloride channel complex	transport		**CLCNKA**
chloride channel complex	transport		**CLCNKB**
Golgi apparatus	post-Golgi vesicle-mediated transport		**CLINT1**
Golgi apparatus	macroautophagy		**CLN3**

clathrin-coated endocytic vesicle membrane	endocytosis		**CLTA**
clathrin coat of trans-Golgi network vesicle	vesicle-mediated transport		**CLTB**
clathrin coat of trans-Golgi network vesicle	receptor-mediated endocytosis		**CLTC**
clathrin coat of trans-Golgi network vesicle	intracellular protein transport		**CLTCL1**
plasma membrane	positive regulation of cell proliferation		**CSF1R**
lysosomal membrane	L-cystine transport		**CTNS**
lysosome	intracellular protein transport		**CTSA**
lysosome	proteolysis		**CTSC**
lysosome	proteolysis		**CTSD**
endolysosome lumen	proteolysis		**CTSK**
trans-Golgi network	receptor-mediated endocytosis		**CTTN**
endocytic vesicle	receptor-mediated endocytosis	AmiGO and UniProt	**CUBN**
plasma membrane	chemokine-mediated signaling pathway		**CXCR1**
integral component of plasma membrane	chemokine-mediated signaling pathway		**CXCR2**
cytoplasmic membrane-bounded vesicle	chemokine-mediated signaling pathway		**CXCR4**
plasma membrane	endocytosis		**CYTH2**
lysosomal membrane	positive regulation of clathrin-mediated endocytosis		**DAB2**
cytoplasm	ER-to-Golgi transport		**DCTN1**
phagocytic vesicle membrane	protein transport		**DMBT1**
cytoplasm	post-Golgi vesicle-mediated transport		**DNAJC6**

membrane coat	endocytosis		**DNM1**
peroxisome	endocytosis		**DNM1L**
microtubule	endocytosis		**DNM2**
perinuclear region of cytoplasm	endocytosis		**DNM3**
lysosome	execution phase of apoptosis	AmiGO and UniProt	**DRAM2**
BLOC-1 complex	post-Golgi vesicle-mediated transport		**DTNBP1**
cytoplasmic dynein complex	post-Golgi vesicle trafficking		**DYNC1H1**
early endosome	early endosome to late endosome transport		**EEA1**
lysosomal membrane	negative regulation of secretion		**EGF**
transmembrane glycoprotein	cell surface receptor signaling pathway		**EGFR**
early endosome membrane	endocytic recycling		**EHD1**
recycling endosome membrane	regulation of endocytosis		**EHD2**
recycling endosome membrane	endocytic recycling		**EHD3**
recycling endosome membrane	regulation of endocytosis		**EHD4**
cytoplasm	endocytosis		**EPN1**
clathrin-coated vesicle	endocytosis		**EPN2**
clathrin-coated vesicle	biological_process		**EPN3**
plasma membrane	endocytosis		**EPS15**
plasma membrane	endocytosis		**EPS15L1**
endosome membrane	cell surface receptor signaling pathway		**ERBB2**

plasma membrane	negative regulation of signal transduction		**ERBB3**
basolateral plasma membrane	negative regulation of cell proliferation		**ERBB4**
cytoplasm	negative regulation of epidermal growth factor receptor signaling pathway		**ERRFI1**
integral component of plasma membrane	connective tissue replacement involved in inflammatory response wound healing		**F2R**
late endosome membrane	protein transport		**FAM125A**
endosome	protein transport		**FAM125B**
Golgi apparatus	ER to Golgi ceramide transport		**FAPP2 (PLEKHA8)**
Golgi apparatus	small GTPase mediated signal transduction		**FGD1**
early endosome membrane	small GTPase mediated signal transduction		**FGD2**
actin cytoskeleton	regulation of cell shape		**FGD4**
integral component of membrane	epidermal growth factor receptor signaling pathway		**FGFR2**
integral component of membrane	fibroblast growth factor receptor signaling pathway		**FGFR3**
integral component of membrane	fibroblast growth factor receptor signaling pathway		**FGFR4**
endosome membrane	vacuole organization		**FIG4**
integral component of membrane	transmembrane receptor protein tyrosine kinase signaling pathway		**FLT1**
lysosome	endocytosis	AmiGO and UniProt	**FNBP1**
plasma membrane	receptor-mediated endocytosis		**FOLR1**

lysosome	glycosaminoglycan catabolic process		**FUCA1**
lysosome	galactosylceramide catabolic process		**GALC**
lysosomal lumen	keratan sulfate catabolic process		**GALNS**
nucleus	positive regulation of angiogenesis		**GATA2**
Golgi apparatus	regulate the trafficking of proteins between the trans-Golgi network and the lysosome		**GGA1**
trans-Golgi network	intracellular protein transport		**GGA2**
trans-Golgi network	intracellular protein transport		**GGA3**
cytoplasm	regulation of ARF GTPase activity		**GIT1**
nucleoplasm	regulation of ARF GTPase activity		**GIT2**
lysosome	glycosphingolipid catabolic process		**GLA**
lysosomal lumen	glycosaminoglycan catabolic process		**GLB1**
lysosomal lumen	ganglioside catabolic process		**GM2A**
cis-Golgi network	transport		**GOLIM4**
photoreceptor disc membrane	regulation of G-protein coupled receptor protein signaling pathway		**GRK1**
cytoplasm	regulation of G-protein coupled receptor protein signaling pathway		**GRK4**
cytoplasm	regulation of G-protein coupled receptor protein signaling pathway		**GRK5**

membrane	regulation of G-protein coupled receptor protein signaling pathway		**GRK6**
membrane	termination of G-protein coupled receptor signaling pathway		**GRK7**
lysosomal lumen	hyaluronan catabolic process		**GUSB**
lysosome	regulation of podosome assembly	Netview and AmiGO	**HCK**
cytoplasm	negative regulation of autophagy		**HERC1**
lysosomal lumen	glycosaminoglycan metabolic process		**HEXA**
lysosomal lumen	glycosaminoglycan metabolic process		**HEXB**
recycling endosome	iron ion import into cell		**HFE**
endosome	endosomal transport		**HGS**
lysosomal membrane	lysosomal transport		**HGSNAT**
clathrin-coated vesicle	positive regulation of receptor-mediated endocytosis		**HIP1**
clathrin-coated vesicle	receptor-mediated endocytosis		**HIP1R**
integral component of plasma membrane	immune response		**HLA-A**
integral component of plasma membrane	immune response		**HLA-B**
integral component of plasma membrane	immune response		**HLA-C**
ER to Golgi transport vesicle membrane	innate immune response		**HLA-E**
ER to Golgi transport vesicle membrane	regulation of immune response		**HLA-F**
ER to Golgi transport vesicle membrane	cellular defense response		**HLA-G**

Golgi apparatus	endocytosis		**HRAS**
cytoplasm	endocytosis		**HSPA1A**
cytoplasm	endocytosis		**HSPA1B**
colocalizes_with COP9 signalosome	response to unfolded protein		**HSPA1L**
cell surface	response to unfolded protein		**HSPA2**
colocalizes_with COP9 signalosome	response to unfolded protein		**HSPA6**
cytoplasm	response to unfolded protein		**HSPA8**
cytoplasm	negative regulation of autophagy	amiGO	**HTR2B**
lysosome	hyaluronan catabolic process		**HYAL1**
lysosomal lumen	glycosaminoglycan metabolic process		**IDS**
lysosome	lysosome organization		**IDUA**
intraciliary transport particle B	small GTPase mediated signal transduction		**IFT27**
integral component of plasma membrane	insulin-like growth factor receptor signaling pathway		**IGF1R**
trans-Golgi network transport vesicle	receptor-mediated endocytosis	Netview and AmiGO	**IGF2R**
integral component of membrane	cell surface receptor signaling pathway		**IL2RA**
integral component of plasma membrane	interleukin-2-mediated signaling pathway		**IL2RB**
integral component of plasma membrane	interleukin-2-mediated signaling pathway		**IL2RG**
cytosol	membrane trafficking		**INPP1**
cytosol	membrane trafficking		**INPP4A**
Golgi apparatus	regulation of nucleocytoplasmic transport		**INPP4B**

plasma membrane	phosphatidylinositol dephosphorylation		**INPP5A**
endoplasmic reticulum-Golgi intermediate compartment	phosphatidylinositol dephosphorylation		**INPP5B**
membrane	signal transduction		**INPP5D**
Golgi cisterna membrane	regulate Golgi-vesicular trafficking		**INPP5E**
intracellular	phosphatidylinositol-mediated signaling		**INPP5F**
cytosol	phosphatidylinositol dephosphorylation		**INPP5J**
trans-Golgi network	membrane trafficking		**INPP5K**
cytoplasm	endocytosis		**INPPL1**
intracellular membrane-bounded organelle	regulation of ARF protein signal transduction		**IQSEC1**
cytoplasm	regulation of ARF protein signal transduction		**IQSEC2**
cytoplasm	regulation of ARF protein signal transduction		**IQSEC3**
plasma membrane	ubiquitin-dependent protein catabolic process		**ITCH**
endocytic vesicle	synaptic vesicle endocytosis		**ITSN1**
cytoplasm	clathrin-mediated endocytosis		**ITSN2**
integral component of plasma membrane	angiogenesis		**KDR**
lysosome	negative regulation of autophagy	amiGO	**KIAA0226**
early endosome membrane	intracellular trafficking		**KIF16B**
integral component of membrane	Kit signaling pathway		**KIT**
lysosomal membrane	platelet activation		**LAMP2**

Golgi apparatus	transport		**LAPTM4A**
endomembrane system	transport		**LAPTM4B**
lysosome	transport		**LAPTM5**
lysosome	low-density lipoprotein particle clearance	AmiGO and UniProt	**LDLR**
recycling endosome	receptor-mediated endocytosis		**LDLRAP1**
lysosome	lipid catabolic process		**LIPA**
integral component of plasma membrane	receptor-mediated endocytosis		**LRP1B**
lysosome	endocytosis	AmiGO and UniProt	**LRP2**
integral component of plasma membrane	receptor-mediated endocytosis		**LRP3**
microtubule cytoskeleton	endosome to lysosome transport via multivesicular body sorting pathway		**LYST**
endosome	endosome to lysosome transport		**M6PR**
lysosome	mannose metabolic process		**MAN2B1**
lysosome	mannan catabolic process		**MANBA**
lysosomal membrane	transmembrane transport		**MCOLN1**
integral component of membrane	starvation-induced autophagy.		**MCOLN3**
endocytic vesicle membrane	negative regulation of DNA damage response, signal transduction by p53 class mediator		**MDM2**
integral component of plasma membrane	signal transduction		**MET**
integral component of membrane	transmembrane transport		**MFSD1**
lysosomal membrane	transmembrane transport		**MFSD8**

microtubule organizing center	melanocyte differentiation		**MLPH**
endosome membrane	receptor-mediated endocytosis		**MRC1**
endocytic vesicle membrane	receptor-mediated endocytosis		**MSR1**
late endosome	endosome to lysosome transport		**MTM1**
plasma membrane	phosphatidylinositol biosynthetic process		**MTMR1**
cellular_component	phosphoinositides (PIs)-metabolising enzyme		**MTMR10**
cytoplasm	phosphoinositides (PIs)-metabolising enzyme		**MTMR12**
perinuclear region of cytoplasm	phosphatidylinositol biosynthetic process		**MTMR14**
early endosome membrane	positive regulation of early endosome to late endosome transport		**MTMR2**
membrane	phosphatidylinositol dephosphorylation		**MTMR3**
early endosome membrane	peptidyl-tyrosine dephosphorylation		**MTMR4**
cytoplasm	phosphatidylinositol biosynthetic process		**MTMR6**
cytosol	peptidyl-tyrosine dephosphorylation		**MTMR7**
nuclear envelope	peptidyl-tyrosine dephosphorylation		**MTMR8**
cytosol	peptidyl-tyrosine dephosphorylation		**MTMR9**
endocytic vesicle	endocytosis		**MTSS1**
cytoplasm	intracellular vesicle transport to the plasma membrane		**MYO1C**

cytoplasm	cytoplasmic vesicle transport and anchorage		**MYO5A**
cytoplasmic vesicle membrane	vesicle-mediated transport		**MYO5B**
colocalizes_with clathrin-coated endocytic vesicle	endocytosis		**MYO6**
lysosomal membrane	lysosome organization	AmiGO and UniProt	**MYO7A**
lysosome	glycolipid catabolic process		**NAGA**
clathrin vesicle coat	endocytosis		**NECAP1**
clathrin vesicle coat	endocytosis		**NECAP2**
Golgi apparatus	protein targeting to lysosome		**NEDD4**
cytosol	positive regulation of endocytosis		**NEDD4L**
lysosomal membrane	autophagy		**NPC1**
lysosome	transport of cholesterol through the late endosomal/lysosomal system		**NPC2**
integral component of plasma membrane	peptidyl-tyrosine phosphorylation		**NTRK1**
early endosome	endocytic adaptor		**NUMB**
cytoplasm	endocytosis		**NUMBL**
trans-Golgi network	positive regulation of Rac GTPase activity		**OCRL**
nucleus	lipid transport (is believed to transport sterols from lysosomes to the nucleus)		**OSBP**
late endosome	vesicle-mediated transport		**OSBPL1A**
lysosomal membrane	transmembrane transport		**OSTM1**
cytoplasm	endocytosis		**PACSIN3**
cytosol	establishment or maintenance of cell polarity		**PARD3**

cytosol	cell-cell junction maintenance		**PARD6A**
plasma membrane	establishment or maintenance of cell polarity		**PARD6B**
cytoplasm	cell division		**PARD6G**
lysosome	lysosomal transport	AmiGO and UniProt	**PCSK9**
cytoplasm	binds to endophilins, proteins that regulate membrane shape during endocytosis		**PDCD6IP**
integral component of plasma membrane	negative regulation of platelet activation		**PDGFRA**
cytoplasm	receptor-mediated endocytosis		**PDLIM7**
lysosomal membrane	phosphatidylinositol phosphorylation		**PI4K2A**
cytoplasm	phosphatidylinositol biosynthetic process		**PI4K2B**
Golgi-associated vesicle membrane	phosphatidylinositol-mediated signaling		**PI4KA**
endosome	receptor-mediated endocytosis		**PI4KB**
colocalizes_with clathrin coat of coated pit	receptor-mediated endocytosis		**PICALM**
extracellular vesicular exosome	exocytosis		**PIK3C2A**
phosphatidylinositol 3-kinase complex	intracellular protein trafficking		**PIK3C2B**
phosphatidylinositol 3-kinase complex	intracellular protein trafficking		**PIK3C2G**
plasma membrane	phosphatidylinositol-3-phosphate biosynthetic process		**PIK3CA**
cytoplasm	positive regulation of autophagy	amiGO	**PIK3CB**
cytoplasm	endocytosis		**PIK3CG**

plasma membrane	phosphatidylinositol 3-kinase signaling		**PIK3R1**
phosphatidylinositol 3-kinase complex	phosphatidylinositol-3-phosphate biosynthetic process		**PIK3R2**
early endosome membrane	retrograde transport, endosome to Golgi		**PIKFYVE**
plasma membrane	phosphatidylinositol phosphorylation		**PIP4K2A**
endoplasmic reticulum membrane	phosphatidylinositol phosphorylation		**PIP4K2B**
extracellular vesicular exosome	phosphatidylinositol metabolic process		**PIP4K2C**
nucleus	phagocytosis		**PIP5K1A**
endomembrane system	phosphatidylinositol phosphorylation		**PIP5K1B**
focal adhesion	clathrin-mediated endocytosis		**PIP5K1C**
cytoplasm	phosphatidylinositol phosphorylation		**PIPSL**
cytoplasm	phosphatidylinositol transporter activity		**PITPNA**
endoplasmic reticulum membrane	retrograde vesicle-mediated transport, Golgi to ER		**PITPNB**
cytosol	phosphatidylinositol transporter activity		**PITPNC1**
Golgi cisterna membrane	protein transport		**PITPNM1**
endomembrane system	phosphatidylinositol metabolic process		**PITPNM3**
membrane	positive regulation of exocytosis		**PLA2G6**
cytoplasm	inositol phosphate metabolic process		**PLCB1**
plasma membrane	signal transduction		**PLCG1**

plasma membrane	phosphatidylinositol biosynthetic process		**PLCG2**
lysosomal membrane	small GTPase mediated signal transduction		**PLD1**
endoplasmic reticulum membrane	small GTPase mediated signal transduction		**PLD2**
late endosomes/lysosomes	receptor-mediated endocytosis		**PPT1**
cytosol	protein targeting to membrane		**PRKCI**
membrane	negative regulation of protein complex assembly		**PRKCZ**
integral component of plasma membrane	lipid transport		**PSAP**
plasma membrane	signal transduction		**PSD**
endosome	phosphatidylcholine biosynthetic process		**PSD2**
postsynaptic membrane	regulation of ARF protein signal transduction		**PSD3**
plasma membrane	regulation of ARF protein signal transduction		**PSD4**
phagosome	phosphoinositides(PIs)-metabolising enzymes		**PTEN**
recycling endosome	intracellular vesicle trafficking		**RAB10**
trans-Golgi network	plasma membrane to endosome transport		**RAB11A**
recycling endosome	retrograde transport, endosome to plasma membrane		**RAB11B**
recycling endosome	protein transport		**RAB11FIP1**
endosome	protein transport		**RAB11FIP2**
endosome	endocytic recycling		**RAB11FIP3**
recycling endosome membrane	transport		**RAB11FIP4**

recycling endosome membrane	protein transport		**RAB11FIP5**
autophagosomes	endosome to lysosome transport		**RAB12**
trans-Golgi network	endosomal transport		**RAB13**
lysosomal membrane	Golgi to endosome transport	AmiGO and UniProt	**RAB14**
endosome membrane	protein transport		**RAB15**
recycling endosome	membrane trafficking		**RAB17**
plasma membrane	protein transport		**RAB18**
extracellular vesicular exosome	protein transport		**RAB19**
early endosome	autophagy		**RAB1A**
Golgi apparatus	endoplasmic reticulum (ER) to Golgi transport		**RAB1B**
phagocytic vesicle membrane	phagosome-lysosome fusion		**RAB20**
endosome	protein transport		**RAB21**
early endosome	endocytosis		**RAB22A**
extracellular vesicular exosome	protein transport		**RAB25**
transport vesicle membrane	regulation of exocytosis		**RAB26**
lysosome	exocytosis	Netview and AmiGO	**RAB27A**
trans-Golgi network transport vesicle	positive regulation of exocytosis		**RAB27B**
plasma membrane	small GTPase mediated signal transduction		**RAB28**
endoplasmic reticulum-Golgi intermediate compartment membrane	small GTPase mediated signal transduction		**RAB2A**

endoplasmic reticulum membrane	small GTPase mediated signal transduction		**RAB2B**
trans-Golgi network	small GTPase mediated signal transduction		**RAB30**
early endosome	Golgi to plasma membrane protein transport		**RAB31**
phagocytic vesicle membrane	small GTPase mediated signal transduction		**RAB32**
plasma membrane	small GTPase mediated signal transduction		**RAB33A**
Golgi apparatus	lysosome localization		**RAB34**
clathrin-coated endocytic vesicle	endosomal transport		**RAB35**
Golgi apparatus	small GTPase mediated signal transduction		**RAB36**
endoplasmic reticulum-Golgi intermediate compartment	small GTPase mediated signal transduction		**RAB37**
phagocytic vesicle membrane	small GTPase mediated signal transduction		**RAB38**
phagocytic vesicle membrane	phagosome-lysosome fusion		**RAB39A**
Golgi apparatus	small GTPase mediated signal transduction		**RAB39B**
acrosomal vesicle	synaptic vesicle exocytosis		**RAB3A**
perinuclear region of cytoplasm	regulation of exocytosis		**RAB3B**
perinuclear region of cytoplasm	regulation of exocytosis		**RAB3C**
extracellular vesicular exosome	exocytosis		**RAB3D**
cytosol	Golgi to plasma membrane transport		**RAB3IP**
plasma membrane	protein transport		**RAB40A**

plasma membrane	protein transport		**RAB40AL**
plasma membrane	protein transport		**RAB40B**
plasma membrane	protein transport		**RAB40C**
cytoplasm	protein transport		**RAB41**
membrane	small GTPase mediated signal transduction		**RAB42**
Golgi apparatus	retrograde transport, plasma membrane to Golgi		**RAB43**
plasma membrane	protein transport		**RAB44**
endosome	regulation of endocytosis		**RAB4A**
recycling endosome	protein transport		**RAB4B**
early endosome	endocytosis		**RAB5A**
endosome	regulation of endocytosis		**RAB5B**
lysosomal membrane	regulation of endocytosis		**RAB5C**
Golgi apparatus	retrograde vesicle-mediated transport, Golgi to ER		**RAB6A**
Golgi apparatus	retrograde vesicle-mediated transport, Golgi to ER		**RAB6B**
cytoplasm	small GTPase mediated signal transduction		**RAB6C**
lysosome	endosome to lysosome transport	AmiGO and UniProt	**RAB7A**
extracellular vesicular exosome	small GTPase mediated signal transduction		**RAB7L1**
recycling endosome membrane	vesicle docking involved in exocytosis		**RAB8A**
lysosome	positive regulation of exocytosis	AmiGO and UniProt	**RAB9A**
phagocytic vesicle	endosome-to-Golgi transport		**RAB9B**
endocytic vesicle	endocytosis		**RABEP1**
early endosome	endocytosis		**RABEP2**

endosome	vesicle docking involved in exocytosis		**RABEPK**
recycling endosome	endocytosis		**RABGEF1**
cellular component	small GTPase mediated signal transduction		**RABIF**
intraciliary transport particle	small GTPase mediated signal transduction		**RABL2A**
cellular component	small GTPase mediated signal transduction		**RABL2B**
cellular component	small GTPase mediated signal transduction		**RABL3**
cytoplasm	small GTPase mediated signal transduction		**RABL6**
trans-Golgi network	actin cytoskeleton organization		**RAC1**
lysosome	protein transport	AmiGO and UniProt	**RAMP2**
lysosome	positive regulation of receptor recycling	AmiGO and UniProt	**RAMP3**
perinuclear region of cytoplasm	protein transport		**RASEF**
endosome membrane	peptidyl-tyrosine phosphorylation		**RET**
lysosomal membrane	endosome to lysosome transport	AmiGO and UniProt	**RILP**
presynaptic membrane	synaptic vesicle exocytosis		**RIMS1**
presynaptic membrane	regulation of exocytosis		**RIMS2**
plasma membrane	endocytosis		**RIN1**
cytoplasm	endocytosis		**RIN2**
early endosome	endocytosis		**RIN3**
cytosol	negative regulation of cell proliferation		**RNF41**
membrane	intracellular protein transport		**RPH3A**

early endosome membrane	regulation of endocytosis		**RUFY1**
integral component of membrane	regulation of Rab GTPase activity		**SBF1**
membrane	regulation of Rab GTPase activity		**SBF2**
recycling endosome membrane	post-Golgi vesicle-mediated transport		**SCAMP2**
endocytic vesicle membrane	receptor-mediated endocytosis		**SCARF1**
integral component of membrane	Golgi to plasma membrane protein transport		**SEC14L3**
integral component of membrane	Golgi to plasma membrane protein transport		**SEC14L4**
lysosome	receptor-mediated endocytosis	AmiGO and UniProt	**SFTPD**
clathrin-coated vesicle	positive regulation of receptor-mediated endocytosis		**SGIP1**
lysosomal lumen	proteoglycan metabolic process		**SGSH**
early endosome membrane	endocytosis		**SH3GL1**
clathrin-coated endocytic vesicle membrane	synaptic vesicle endocytosis		**SH3GL2**
early endosome membrane	endocytosis		**SH3GL3**
mitochondrial outer membrane	positive regulation of protein oligomerization		**SH3GLB1**
cytoplasm	biological_process		**SH3GLB2**
cytoplasmic vesicle membrane	endocytosis		**SH3KBP1**
plasma membrane	regulation of intracellular protein transport		**SH3TC2**
endoplasmic reticulum	intracellular protein transport		**SIL1**
lysosomal membrane	transmembrane transport		**SLC11A2**

lysosomal membrane	transmembrane transport	Netview and AmiGO	**SLC15A3**
lysosomal membrane	sialic acid transport		**SLC17A5**
lysosomal membrane	transmembrane transport		**SLC29A3**
lysosomal membrane	transmembrane transport		**SLC36A1**
integral component of membrane	transmembrane transport		**SLC37A3**
plasma membrane	regulation of clathrin-mediated endocytosis		**SMAP1**
cytoplasm	regulation of ARF GTPase activity		**SMAP2**
lysosomal lumen	sphingomyelin metabolic process		**SMPD1**
plasma membrane	protein localization to cell surface		**SMURF1**
ubiquitin ligase complex	ubiquitin-dependent SMAD protein catabolic process		**SMURF2**
SNARE complex	synaptic vesicle docking involved in exocytosis		**SNAP25**
plasma membrane	autophagic vacuole fusion		**SNAP29**
plasma membrane	protein transport		**SNAP91**
BLOC-1 complex	synaptic vesicle exocytosis		**SNAPIN**
plasma membrane	negative regulation of exocytosis		**SNCA**
late endosome membrane	endosomal transport		**SNF8**
early endosome membrane	endocytosis		**SNX1 (sorting nexin)**
extrinsic component of endosome membrane	endosome organization		**SNX10**
endosome	intracellular endosomal trafficking pathways		**SNX11**

membrane	protein transport		**SNX12**
early endosome membrane	intracellular trafficking		**SNX13**
integral component of membrane	protein transport		**SNX14**
cytoplasm	intracellular protein transport		**SNX15**
late endosome/ lysosome	endosome to lysosome transport	AmiGO and UniProt	**SNX16**
early endosome	regulation of endocytosis		**SNX17**
endosome membrane	endocytosis		**SNX18**
cytoplasmic vesicle membrane	protein transport		**SNX19**
endosome membrane	endocytosis		**SNX2**
endosome membrane	protein transport		**SNX20**
cytoplasmic vesicle membrane	protein transport		**SNX21**
cytoplasmic vesicle membrane	protein transport		**SNX22**
cytoplasmic vesicle membrane	protein transport		**SNX24**
endosome membrane	SNX25 negatively regulates TGF-Beta signaling by enhancing the receptor degradation through lysosome pathway.		**SNX25**
early endosome membrane	endosome to lysosome transport		**SNX27**
cellular component	phosphatidylinositol binding		**SNX29**
early endosome	endocytosis	Netview	**SNX3**
cytoplasm	protein transport		**SNX30**
protein complex	protein transport		**SNX31**
cellular component	protein transport		**SNX32**

cytoplasmic membrane-bounded vesicle	endocytosis		**SNX33**
early endosome membrane	endocytosis		**SNX4**
colocalizes_with early endosome membrane	pinocytosis		**SNX5**
early endosome membrane	retrograde transport, endosome to Golgi		**SNX6**
cytoplasmic vesicle membrane	protein transport		**SNX7**
early endosome membrane	early endosome to Golgi transport		**SNX8**
trans-Golgi network	receptor-mediated endocytosis		**SNX9**
endosome	receptor-mediated endocytosis		**SORL1**
lysosome	positive regulation of phagocytosis		**SPACA3**
mitochondrial outer membrane	regulating endosomal trafficking		**SPG20**
lysosome	intracellular signal transduction		**SRC**
integral component of plasma membrane	receptor-mediated endocytosis		**STAB1**
integral component of plasma membrane	receptor-mediated endocytosis		**STAB2**
early endosome membrane	endosomal transport		**STAM**
early endosome membrane	endosomal transport		**STAM2**
early endosome	positive regulation of cell proliferation		**STAMBP**
endosome membrane	transmembrane transport		**STEAP3**
clathrin adaptor complex	regulation of endocytosis		**STON1**
clathrin adaptor complex	regulation of endocytosis		**STON2**
Golgi membrane	retrograde transport, endosome to Golgi		**STX10 (syntaxin)**

Golgi apparatus	regulate protein transport among late endosomes and the trans-Golgi network		**STX11**
phagocytic vesicle	synaptic vesicle exocytosis		**STX12**
Golgi apparatus	retrograde transport, endosome to Golgi		**STX16**
Golgi membrane	ER to Golgi vesicle-mediated transport		**STX18**
integral component of membrane	vesicle-mediated transport		**STX19**
SNARE complex	synaptic vesicle docking involved in exocytosis		**STX1A**
integral component of plasma membrane	regulation of exocytosis		**STX1B**
intracellular membrane-bounded organelle	intracellular protein transport		**STX2**
extracellular vesicular exosome	exocytosis		**STX3**
SNARE complex	post-Golgi vesicle-mediated transport		**STX4**
endoplasmic reticulum-Golgi intermediate compartment membrane	retrograde transport, endosome to Golgi		**STX5**
trans-Golgi network membrane	retrograde transport, endosome to Golgi		**STX6**
lysosomal membrane	post-Golgi vesicle-mediated transport		**STX7**
late endosome membrane	endosome to lysosome transport		**STX8**
plasma membrane	vesicle docking involved in exocytosis		**STXBP1**
cytosol	protein transport		**STXBP2**

cytoplasmic vesicle membrane	exocytosis		**STXBP5**
integral component of membrane	exocytosis		**STXBP5L**
integral component of membrane	vesicle-mediated transport		**STXBP6**
cytosol	synaptic vesicle endocytosis		**SYNJ1**
membrane	endocytosis		**SYNJ2**
cytoplasm	intracellular protein transport		**SYNRG**
integral component of synaptic vesicle membrane	endocytosis		**SYP**
endocytic vesicle membrane	regulation of exocytosis		**SYT1**
exocytic vesicle	vesicle docking involved in exocytosis		**SYTL2**
lysosomal membrane	transmembrane transport		**TCIRG1**
recycling endosome	transmembrane transport		**TF**
cytoplasm	negative regulation of transcription by competitive promoter binding		**TFAP2A (AP-2alpha)**
endosome	receptor-mediated endocytosis		**TFRC**
lysosomal membrane	transport		**TMEM9**
endosome	endocytosis		**TOM1**
lysosomal membrane	transmembrane transport		**TPCN1**
lysosomal membrane	transmembrane transport		**TPCN2**
lysosome	proteolysis		**TPP1**
cytoplasm	endocytosis		**TRAF6**
lysosomal membrane and Golgi membrane	small GTPase mediated signal transduction		**TRIM23**
early endosome	endosomal transport		**TSG101**

Golgi-associated vesicle	eye pigment biosynthetic process		**TYR**
endosome membrane	melanosome organization		**TYRP1**
autophagic vacuole	positive regulation of autophagy	amiGO	**ULK1**
early endosome	endosome organization		**USP8**
lysosome	regulation of Golgi to plasma membrane protein transport	AmiGO and UniProt	**VAMP4**
early endosome	regulation of endocytosis		**VAMP8**
lysosomal membrane	intracellular protein transport	AmiGO and UniProt	**VPS16**
endosome membrane	endosomal transport		**VPS25**
endosome	endosomal transport		**VPS28**
lysosomal membrane	retrograde transport, endosome to Golgi		**VPS35**
lysosome	endosomal transport	AmiGO and UniProt	**VPS36**
endosome membrane	endosomal transport		**VPS37A**
endosome membrane	endosomal transport		**VPS37B**
endosome membrane	endosomal transport		**VPS37C**
endosome membrane	endosomal transport		**VPS37D**
endosome membrane	intracellular protein transport		**VPS45**
extracellular vesicular exosome	endosomal transport		**VPS4A**
lysosome	endosome to lysosome transport via multivesicular body sorting pathway	AmiGO and UniProt	**VPS4B**
endosome membrane	endosomal transport		**VTA1**
endocytic vesicle membrane	positive regulation of clathrin-mediated endocytosis		**WASL**
ubiquitin ligase complex	transmembrane transport		**WWP1**

early endosome	regulation of endocytosis		**ZFYVE16**
endosome	endosomal transport		**ZFYVE20**
early endosome membrane	endocytosis		**ZFYVE9**

11.4. Curriculum Vitae

Israel Chukwudi Nnah

4404 Furman Avenue, Apt. #1 • Bronx, New York 10466 • (347) 740-1940
Israel.nnah@rutgers.edu

EDUCATION

Rutgers University, Department of Biological Sciences, Newark, NJ

- PhD in Cellular and Molecular Biology **2012 – 2017**

City College of New York, City University of New York (CUNY), Department of Biology, New York, NY

- M.A. in Biology, Neurogenetics **2010 – 2012**
- B.Sc. in Biology **2003 – 2009**

EMPLOYMENT

ACTIVITY/ OCCUPATION	START DATE (mm/yy)	END DATE (mm/yy)	FIELD	INSTITUTION/ COMPANY	SUPERVISOR/ EMPLOYER
Biologist/Sales Representative	11/2011	08/2012	Biotechnology	Snova Biotechnologies	Nancy Quan, MD
Research Assistant	08/2009	05/2012	Biology	City College of NY	T. Venkatesh, PhD
Lab Technician	06/2008	12/2009	Education	City College of NY	Doris Grasserbauer
Office Assistant	09/2005	06/2008	Biomedicine	City College of NY	Meyer Fisher, PhD
Workshop leader/Tutor	08/2004	05/2006	Chemistry	City College of NY	A. E. Dreyfuss

CONTRIBUTION TO SCIENCE

As a Ph.D. candidate at Rutgers-Newark University, my thesis project in Dr. Dobrowolski's laboratory focuses on understanding the cellular and molecular mechanisms that contribute to onset of neurodegeneration. The emphasis is put on deciphering the role of endolysosomal trafficking in metabolic control of proteostasis and regulation of catabolic pathways involved in the onset of Alzheimer's disease (AD). My work has suggested that cellular endocytosis and accompanying molecular trafficking control the activation of mechanistic target of Rapamycin complex 1 (mTORC1), a key kinase that is deregulated in many human diseases including cancer and neurodegeneration. For this project, I utilize living human neurons and mouse cell lines as experimental models to learn a new stem cell-based system used to model AD. This, in turn, offers a great advantage to my research such as avoiding overexpression of

aggregation-prone proteins and studying clearance of these supposedly neurotoxic human proteins at many different genetic backgrounds.

As a master's student at City College of New York, I spent two years of research in Venkatesh laboratory studying the mechanistic role of glial cell malfunction in the onset of neurodegeneration. My studies mainly focused on understanding how the Rap/Fzr gene, a regulatory component of the ubiquitin ligase, Anaphase-promoting complex, regulates gliogenesis during the development of Drosophila melanogaster central nervous system. Results from this study suggest that hyperactive Rap/Fzr induces morphological changes in developing D. melanogaster brains and drives neurodegeneration of the medulla region of adult fly brains.

Amongst the main goals for my postdoctoral training, I envision to learn advanced molecular cell biological techniques, and conduct research in a most efficient way, which will result in a number of contributions to the growth of our scientific field. Following my postdoctoral training, I plan to seek a career in academia to further extend my expertise in cellular neuroscience, commitment to hard work and high quality.

PUBLICATIONS

- **Nnah, I.C.**, Antikainen, H., Yang, Y., Xu, H., Dobrowolski, R. *Activation of the Calcium Efflux Channel Mucolipin1 Promotes Autolysosomal Clearance of Amyloid and Restores Memory in a Mouse Model for Alzheimer's Disease.* (in preparation).

- **Nnah, I. C.,** Wang, B., Saqcena, C., Bagley, D., De Cegli, R., Napolitano, G., Medina, L. D., Ballabio, A. & Dobrowolski, R. *TFEB-driven endocytosis coordinates mTORC1 signaling, lysosomal biogenesis, and autophagy*. (under peer-review)

- Saqcena, C., **Nnah, I. C.**, Wang, B., Antikainen, H., Avcu, P., Fortress, A. M., Bonder, E. M., Pang, K. C. H. & Dobrowolski, R. *Autophagy induction drives neuroprotection by inhibiting the TFEB/ATF4-mediated integrated stress response after traumatic brain injury*. (under peer-review)

- Kim, B. H., Clausi, G. M., **Nnah, I. C**., Saqcena, C., Dobrowolski, R. & Levison, S. W. (2016). *Age-dependent effects of ALK5 inhibition and mechanism of neuroprotection in neonatal hypoxic-ischemic brain injury*. Developmental Neuroscience, 2017; 39 (1-4): 338-351

- Reddy, K., Cusack, C.L., **Nnah, I. C**, Khayati, K., Huynh, T.B., Noggle, S., Ballabio, A. & Dobrowolski, R. (2015). *Dysregulation of Nutrient Sensing and CLEARance in Presenilin Deficiency*. Cell Reports, 2016; 14 (9): 2166-2179

- **Nnah, I. C.**, Khayati, K. & Dobrowolski, R. (2015). *Cellular metabolism and lysosomal mTOR signaling*. Cell Death in Therapy, DeGruyterOpen, 2015; 1:11-22.

RESEARCH PROJECTS

Rutgers University-Newark, Department of Biological Sciences, Newark, NJ
Pre-doctoral Fellow in Cell & Molecular biology; Advisor: Radek Dobrowolski, PhD
(2013 – 2017)

- **Thesis project**: *Regulation of mTORC1-TFEB cellular signaling pathway by endosomal trafficking*
  - This study is considered the main project of my PhD thesis and identified TFEB-mediated endocytosis as a critical process that drives the assembly of mTORC1-containing nutrient sensing complex.
  - I investigated the role of the transcription factor EB (TFEB), a master regulator of lysosomal biogenesis and autophagy, in the regulation of mechanistic target of Rapamycin complex 1 (mTORC1) activity during starvation in mammalian cells.
  - I found that TFEB mediates formation of endosomes carrying proteins such as phospho-Akt (pT308-Akt), RagD, and the amino acid transporter SLC38A9. These TFEB-induced signaling endosomes en route to lysosomes are required to dissociate the mTORC1 inhibitor TSC2, re-tether and activate mTORC1 on endolysosomal membranes during prolonged starvation to efficiently drive autophagy.

- **Collaborative project 1**: *Elucidating the role of TFEB-MCOLN1-mediated vesicular trafficking in Alzheimer's disease*
  - I contributed to the evaluation of the role of, Mucolipin1 (MCOLN1), an endolysosomal calcium efflux channel and a transcriptional target of TFEB. This study showed that activation of the TFEB-MCOLN1 signaling pathway in AD restores molecular trafficking.
  - In my analyses, I have shown that re-activation of MCOLN1 channels promotes autolysosomal clearance of Amyloid beta and phospho-Tau deposits in Familial Alzheimer's disease (FAD) mice models and cultured cells

- **Collaborative project 2**: *Age-dependent effects of ALK5 inhibition and mechanism of neuroprotection in neonatal hypoxic-ischemic brain injury*
  - In collaboration with Dr. Steven W. Levison's laboratory, we found that inhibition of the activin-like kinase 5 (ALK5) TGF-β receptor reduced neuronal death in the rat models of hypoxic-ischemic brain injury.
  - I contributed to the further evaluation of the therapeutic efficacy of SB505124, a small molecule that acts as an antagonist for ALK5, in a rat model of moderate perinatal hypoxic-ischemic brain injury.

- **Collaborative project 3**: *Dysregulation of Nutrient sensing and clearance in presenilin deficiency*
  - This study was the first to identify a dysregulation of the amino acid-sensing function of mTORC1 in cells deficient of the AD-associated presenilin proteins leading to constitutively active mTORC1 and inhibition of TFEB-mediated molecular clearance, cumulatively leading to the onset of AD-like pathophysiology.
  - I contributed to the evaluation of the role of Sestrin 2, now known to be a cellular leucine sensor, in amino acid sensing of mTORC1 in wild-type and presenilin-deficient cells.

- During the course of this project, I have learned to culture and differentiate human induced pluripotent stem cells (iPSCs), human neuronal stem cells (NSCs), as well as handle, genotype and dissect transgenic mice.

- **Collaborative Project 4:** *Autophagy induction drives neuroprotection by inhibiting the TFEB/ATF4-mediated integrated stress response after traumatic brain injury.*
  - In collaboration with Dr. Saqcena and co. we sought out to understand the role of autophagy in TBI-related neuronal cell death.
  - In turn, we observed that the pro-autophagy protein, Beclin-1, induces autophagy that counteracts lysosomal inhibition and increases autophagic flux by temporarily sequestering lysosomal substrates and reducing lysosomal load after traumatic brain injury.

Rutgers University-Newark, Department of Biological Sciences, Newark, NJ
Pre-doctoral Rotation Student in Cell & Molecular biology; Advisor: Nan Gao, PhD
(**2012 – 2013)**

- **Rotation Project**: *Regulation of primary ciliogenesis by Rab8a*
  - Employed a repertoire of experimental techniques that included modern DNA recombination techniques, protein biochemistry, and immunocytochemical assays to determine the role of Rab8a protein in the formation of primary cilia in mammalian cells

City College of New York, CUNY, Department of Biology, New York, NY
Masters Student in Biology (Neurogenetics); Advisor: Tadmiri Venkatesh, PhD
(**2009 – 2011)**

- **Thesis Project**: *Elucidating the role of Rap/Fzr protein during CNS development in Drosophila melanogaster*
  - I studied the impact of Rap/Fzr gene overexpression, a regulatory component of the Anaphase-promoting complex (APC), on the development and morphology of the *D. melanogaster* central nervous system.
  - In a series of gain-of-function experiments, I observed that the overexpression of rap/fzr caused abnormal development of brain tissues in *D. melanogaster*

TEACHING EXPERIENCE

Rutgers University, Department of Biological Sciences, Newark, NJ

- Teaching Assistant for the following courses:

Foundations of Cell & Molecular Biology	Fall 2017
General Microbiology	Summer 2017
Foundations of Cell & Molecular Biology	Spring 2017
Foundations of Cell & Molecular Biology	Fall 2016
Foundations of Cell & Molecular Biology	Spring 2016
Foundations of Cell & Molecular Biology	Fall 2015
Introductory General Biology	Fall 2014

RESEARCH SKILLS & TECHNIQUES

- Mammalian cell culture and cell fractionation
- Human induced pluripotent stem cell (iPSC) culture
- Human neural stem cell (NSC) and embryoid body/hanging drop culture and differentiation
- DNA transformation and Isolation from competent bacterial cells
- DNA Plasmid transfection
- DNA cloning
- Fluorescence confocal microscopy (Zeiss spinning disc and LSM 510)
- Transmission electron microscopy
- Southern and Western blotting
- Genotyping and Polymerase Chain Reaction (PCR)
- Immunocytochemistry and Immunohistochemistry
- Protein biochemistry
- Handling of transgenic mice
- Dissection and tissue sample collection from transgenic mice
- Statistical analyses (t-test, ANOVA, posthoc analyses) of biological data

ABSTRACTS

- **Nnah, I.C.**, Dobrowolski, R. *TFEB Regulates Endocytic Trafficking of Essential Lysosomal Nutrient Sensing Complex Components to Mediate mTORC1 Signaling and Autophagy Flux.* American Society for Cell Biology (ASCB), Philadelphia, Pennsylvania, 2017

- **Nnah, I. C,** Reddy, K., Saqcena, C., and Dobrowolski, R. *mTORC1-TFEB, Master Regulator of Autophagy & Lysosomal Signaling, Modulates Cellular Endocytosis.* Abstract for poster presentation at the ABRCMS, San Antonio, Texas, 2014

- **Nnah, I. C,** Saqcena, C., Reddy, K., and Dobrowolski, R. *The Role of TFEB and mTORC1, Master Regulators of Autophagy and Lysosomal signaling in Caveolin-mediated Endocytosis.* Abstract for poster presentation at the ABRCMS, Nashville, Tennessee, 2013

- **Nnah I. C,** Braun A., and Venkatesh T. *Morphological and Neuroanatomical Changes Associated with Glia Targeted Expression of Cdh1/Rap/Fzr in the Drosophila Central Nervous System*. Abstract for poster presentation at the ABRCMS, St Louis, Missouri, 2011

ACADEMIC HONORS

- Academic Honors & Fellowships
  - Peter F. Vallone Scholar, City College of NY, New York
    2003 – 2005
  - Research Initiative for Scientific Enhancement (RISE) Fellow
    2010 – 2012
  - Minority Biomedical Research Support (MBRS) Fellow
    2012 – 2015
  - Bridges Scholar, Compact for Faculty Diversity's Institute on Teaching and Mentoring 2014 – 2016
  - Rutgers University, Graduate Student Scholarship Award *(monetary award)* 2017

- Invitations to Professional Conferences
  - Annual Biomedical Research Conference for Minority Students (ABRCMS)
    2009 – 2014
  - Genetics Society of American Conferences (GSA), 49th & 50th Annual Drosophila Research Conferences

    2008 – 2009
  - American Society for Cell Biology (ASCB) conference
    2014
  - Annual Conference of the Institute on Teaching and Mentoring
    2014 – 2016

- **Professional Presentations**
  - Poster presentations at the Annual Biomedical Research Conference for Minority Students (ABRCMS)

    2009 – 2011
  - Biological Colloquium, Rutgers University, Newark, New Jersey
    2012
  - Poster presentations at the Annual Biomedical Research Conference for Minority Students (ABRCMS)

    2013 – 2014
  - Poster Presentation at the Rutgers Brain Health Institute Symposium
    2014 – 2015
  - Seminar to Dr. Wessling-Resnick lab group at Harvard University T.H Chan School of Public Health
    2017

- Professional Memberships
  - Member of the American Society for Cell Biology (ASCB)
    2013 – Present
  - Member of the American Association for Cancer Research (AACR)
    2013 – 2015